Terrestrial plant productivity and soil moisture constraints

Tiexi Chen

Cover page: Photograph of West peak of Mount Hua in Shanxi Province of China by SUN Jiayi.

Terrestrial plant productivity and soil moisture constraints
(Ph.D. thesis, VU University Amsterdam)
In Dutch: Plant productiviteit op land en relaties met bodemvocht
(Academisch Proefschrift, Vrije Universiteit Amsterdam)

This study was funded through European Union Grants FP7-226701 (Project CARBO-EXTREME), FP7-244240 (Project CLIMAFRICA), ESA Climate Change Initiative Soil Moisture Programme (Project ESA CCI Soil Moisture # 4000104814), and the State Scholarship Fund of China Scholarship Council (CSC).

The publishing of this thesis was financed by National Natural Science Foundation of China (Grant No.91337108 and 41375099).

ISBN： 978 90 5383 077 2
NUR-code: 934
Subject headings:
Soil Moisture / drought index / GPP / NPP / light use efficiency / eddy flux / croplands

VRIJE UNIVERSITEIT

Terrestrial plant productivity and soil moisture constraints

ACADEMISCH PROEFSCHRIFT

ter verkrijging van de graad Doctor aan
de Vrije Universiteit Amsterdam,
op gezag van de rector magnificus
prof.dr. F.A. van der Duyn Schouten,
in het openbaar te verdedigen
ten overstaan van de promotiecommissie
van de Faculteit der Aard- en Levenswetenschappen
op vrijdag 2 mei 2014 om 13.45 uur
in de aula van de universiteit,
De Boelelaan 1105

door

Tiexi Chen

geboren te Heilongjiang, China

promotor: prof.dr. A.J. Dolman
copromotor: dr. G.R. van der Werf

reading committee: prof. dr. J.W. Erisman
dr. R.A.M. de Jeu
dr. E.J. Moors
prof. dr. W. Peters
prof. dr. P. Verburg

Acknowledgement

It was an honor to pursue a PhD at the VU University. Such an experience has changed the trajectory of my life. After the Spring Festival 2008, I met this opportunity which was a total surprise to me, so I made my decision to accept it immediately. I think this is one of the best decisions I have made in my life. Here towards the end of my PhD, I would like to show my gratitude to the people who gave me lots of support during these years.

First and foremost, I want to thank my supervisor, Prof. Han Dolman, for offering me not only a patient and precious supervision but also financial support to be able to reunite with my family. I really appreciate the freedom he gave me that I could have time and confidence to develop my own ideas under his guide. I would also like to thank my daily supervisor, Dr. Guido van der Werf. What I have benefited from him most are the academic ethics and regulations that a rigorous scientist should have. High tribute shall be paid to Dr. Richard de Jeu, whose support solved many essential problems. Special thanks should go to WANG Guojie, who picked me up at the airport when I first arrived and took care of me like an older brother afterwards. Thanks to Yvonne van Sligtenhorst, I felt like home at the VU because of her help with many daily trifles.

I must thank my master supervisor, Prof. CHEN Xing, and my university counselor, Mr. LUO Xiaochun. Without their help, I would not have been able to seize this opportunity to study abroad. I am also deeply grateful for the help from the diplomats of the Educational Section of the Embassy of the People's Republic of China in the Kingdom of the Netherlands: XIA Lei, FANG Qingchao and ZHANG Xiaodong and those from Nanjing University: WU Xiaoman, QIU Pengfei.

I would also like to thank my colleagues in the department. I'm really happy to have shared time with the lunch team which is already becoming fond memories, although I did not talk a lot. Thus I should express my gratitude to the members: Yanjiao, Lintao, Marjan, Jun, Angela, Artem, Katrin, Luca, Hylke. My sincere thanks also go to Ko, Maarten, Sampurno, Thijs, Robert, Antoon, Berny, Roxana, Dimmie, Lieselotte, Diego and many other colleagues, who are very nice and friendly. Besides, I really learned a lot from LIU Yi about how to become an efficient young researcher.

I'm so happy I could meet many Chinese friends here who brought me a memorable life. I had really an unforgettable time with these friends: WU Gang, LIU Tie, CHEN Chengfeng, ZHAO Jing, TAO Jianping, GONG cheng, GUO Baoluo, LIU Fangbin, SHAN Ling. I'm glad we had a young parents group to share our experience: LIU Xiaolong & LIANG Yu, LI Peng & JIANG Leimeng, WANG Hongliang & ZHOU Jia, YIN Si & ZHOU Fujin, ZHANG Kai & AI Qing, and LV Chao's family. Badminton gave a necessary rest to my mind. Great thanks to my team, LI Lintao, ZHU Jialu, HONG Kunbin, ZHANG Kai, Lydia, Joanna, FAN Zhenzhen, WANG Zhiling, WANG Junwei, ZHANG Lu, MA Lisong, JIN Xin, ZHENG Shuwei and others. We have won the third place twice in the ACSSNL tournaments. Hope that they can beat

the Delft team in the future. I also want to thank other friends in the sports center at the beginning of my study here: LIU Xiaolong, ZHANG Jinhua, XIAO Zhengxia, ZHUO Qiquan, JIN Kaikai, and HU Hai. We are old close friends now. In addition, deep gratitude goes to Mr. PAN Xiulong's family who treated me as a family member. I also want to thank SUN Jiayi, LIU Xuan, SHEN Hong, YAN Peifeng, ZHAO Yongjing, ZHANG Qingyuan, ZHAO Maosheng, ZENG Fanwei, John, SU Shenjian, ZHANG Feng, Ben and LI Zhengpeng for their support during my hard time.

I am indebted to my beloved parents and my older brother for their love and support to aspire to my dream freely. It is not easy for a rural family. I want to thank my grandparents for their strength in adversity. I hope I can bring glory to them and our clan. Heartfelt gratitude goes to my parents in law for their help to take care when we were extremely busy. At last, I whole-heartedly appreciate the devotion of my wife to our family.

谨以此文献给可爱的女儿陈颀颀，祝你健康、快乐的成长！

Contents

Chapter 1 General Introduction

1.1 Research Background

1.1.1 Climate change and carbon cycle

The global surface temperature has risen over the past century, both on land and over the oceans. The growth rate of land surface temperature (LST) is larger than that of sea surface temperature (SST), particular after 1979 when LST increased about twice as fast as the surface temperature of the ocean (Trenberth et al., 2007). Greenhouse gases are generally considered as the main cause of the observed global warming through increased radiative forcing.

Several studies have demonstrated that climate may be very sensitive to the atmospheric CO_2 concentration, both in the past and at present (Pagani et al., 2010; Schneider and Schneider, 2010). The atmospheric carbon dioxide (CO_2) concentration was around 260-280 ppm (parts per million by volume) from the end of the last ice age about 10,000 years ago until the beginning of the industrial revolution (Indermuhle et al., 1999). It has increased to about 400 ppm nowadays (Dlugokencky and Tans, 2013). Based on ice core records, current atmospheric CO_2 concentrations are at their highest level since at least the 800 kyr (Luthi et al.,2008; Sigman et al., 2010). Over that period, the atmospheric CO_2 concentration typically varied within a range between 180 and 280ppm with a well-known periodicity associated with the Pleistocene glacial cycles.

The concentration of atmospheric CO_2 reflects the balance between carbon emissions (sources) and carbon sinks. It is clear that the growth of atmospheric CO_2 during the industrial Era is caused by human activities, primarily from fossil fuel burning and land use change (LUC). Between 1751 and 2009, human activities have emitted about 360 Pg C (petagram of carbon) into atmosphere from fossil fuel combustion (Boden et al., 2012). Although the CO_2 emissions from fossil fuel increased monotonously at decadal time scales, recent estimates (Friedlingstein et al., 2010) suggest lower CO_2 emissions from LUC during the last decade (1.1±0.7 Pg C yr^{-1}) than during the 1990s (1.5±0.7 Pg C yr^{-1}).

Almost half of the anthropogenic carbon has been taken up by ocean and land sinks (Le Quéré et al., 2009), maintaining on average a stable airborne fraction (the percentage of carbon from the anthropogenic emissions that remains in the atmosphere) of about 45%. However, using 11 C^4MIP models, Friedlingstein et al. (2006) predicted a decline of carbon uptake by carbon sinks in the future. The behaviour of the airborne fraction is still subject to controversy. Both Canadell et al. (2007) and Le Quéré et al. (2009) suggest that the airborne fraction has increased during the past 50 years, indicating a potential saturation of the carbon sinks. However, Knorr (2009) and Ballantyne et al. (2012) find that global carbon sinks have not significantly decreased their sink ability.

Due to the uptake of anthropogenic CO_2 from the atmosphere, the pH value of the ocean has decreased significantly (Caldeira and Wickett, 2003), known as ocean acidification. The rate of ocean CO_2 absorption is mainly determined by the CO_2 partial pressure (pCO_2) difference between the atmosphere and the sea surface and the wind speed. A faster pCO_2 increase in the ocean than in the atmosphere will slow the CO_2 flux into the ocean (Lenton et al., 2009; Takahashi et al., 2009). Several studies have demonstrated weaker ocean sinks compared with carbon emissions (Le Quéré et al., 2013; McKinley et al., 2011; Schuster and Watson, 2007).

Sinks on land probably exhibit a larger potential to keep moderating the growth rate of atmospheric CO_2 concentration (Le Quéré et al., 2013; Sarmiento et al., 2010). For instance, Northern forests are suggested to be a large carbon sink (Myneni et al., 2001). A recent study demonstrated a large and persistent carbon sink of 2.4±0.4 Pg C yr^{-1} in the global forests during 1990-2007 (Pan et al.,2011). Land carbon sinks also tend to exhibit much more interannual variation than ocean sinks (Le Quéré et al., 2013; Sarmiento et al., 2010).

1.1.2 Terrestrial NPP and GPP estimates

Gross primary production (GPP) is the production of organic compounds, mainly through photosynthesis, directly fixing atmospheric CO_2 into ecosystems. GPP is the largest flux in the terrestrial biological carbon cycle. Net primary production (NPP) equals GPP minus autotrophic respiration (R_a). Both GPP and NPP are key input variables required to obtain any other flux in the terrestrial carbon cycle. Therefore, improving GPP and NPP estimates is very important to advance the understanding of all components of the terrestrial carbon cycle.

Although the knowledge of photosynthetic processes at the levels of plant cell, leaf and canopy have been well established, the estimates of large-scale GPP or NPP still have substantial uncertainties. Due to spatial diversity of global ecosystems, there are no direct global measurements of GPP and NPP data available. Recently, Beer et al. (2010) provided an observationally constrained estimate of global GPP of 123±8 Pg C yr^{-1} using eddy covariance flux data and diagnostic models, which is considered somewhat as a standard value (e.g. Bonan et al., 2011; Chen et al., 2012). However, this value was questioned by Welp et al. (2011) who suggested a much larger 150-175 Pg C yr^{-1} of global GPP based on the isotope ratios of oxygen ($^{18}O/^{16}O$) of atmospheric CO_2. Therefore, there are still large uncertainties in GPP and NPP estimates. It should be noted that the isotope method of Welp et al. (2011) could only be used to calculate global average values. And due to the limitations of the number of flux towers and their data record length, high-resolution estimates and long term observational data are still unavailable.

Traditionally, there are two widely used approaches to estimate GPP and NPP from site level to global scale. The light use efficiency (LUE) approach is an empirical method, originally developed by Monteith (Monteith,1972; Monteith and Moss, 1977). The LUE approach assumes that the growth in plant biomass is directly proportional to the amount of absorbed solar radiation. Another method is a physically based way to

estimate the carboxylation rate in the reactions of photosynthesis, i.e. the plants absorb CO_2 in the atmosphere by combining CO_2 with a five-carbon sugar (RuBP) or with the three-carbon molecule phosphoenolpyruvate (PEP; Collatz et al., 1991; Collatz et al., 1992).

In practice, the LUE approach is easier to apply, especially when using remotely sensed vegetation indices as input in the satellite era. During the early stages, the LUE method was applied in field studies to evaluate the relationship between radiation and changes in dry matter (Cannell et al., 1987) which could be linked to NPP. Numerous field studies have been applied by measuring above ground dry matter or total dry matter (including roots) and canopy intercepted (or absorbed) solar radiation. Then the light use efficiency was calculated as the linear ratio between light energy and dry matter. The light use efficiency has been investigated across various plant types but with a strong focus on crops (e.g. Sinclair and Horie, 1989; Kiniry et al., 1989).

In-situ spectrometer data demonstrated the connection between vegetation indices and vegetation build-up (Tucker, 1979). NDVI (Normalized Difference Vegetation Index) was found to be related to photosynthesis when plants are not subject to environmental stress (Sellers, 1985). The relationship between vegetation index and plant absorbed photosynthetically active radiation (PAR) was well demonstrated by Asrar et al., (1984). Therefore, combined with the work of Monteith (1972) and Monteith and Moss (1977), the connections among biomass, PAR and vegetation index were established. As a logical follow-up, models combining remotely sensed vegetation index and the LUE method were created to estimate large scale NPP estimates (Field et al., 1995; Knorr and Heimann, 1995; Potter et al., 1993; Ruimy et al., 1994). Model performance could be evaluated by comparing modelled NPP and that based on measurements (Potter et al., 2003). Later, the LUE approach was extended to estimate GPP, the direct outcome of plant photosynthesis using sunlight because the LUE method is more likely to be fundamentally related to GPP (Landsberg et al., 1997; Prince and Goward, 1995; Ruimy et al., 1996; Running et al., 2000). Roughly, half of the GPP is used for plant maintenance processes, generally referred to as autotrophic respiration (R_a), and the remainder is available for plant growth as NPP. Therefore, using the LUE method to estimate NPP has a default assumption that R_a is proportional to GPP. The LUE method is still under development but is one of the most efficient methods to estimate GPP and NPP from site level to large scales and is used in several modelling frameworks (Goerner et al., 2011; van der Werf et al., 2010; Xiao et al., 2005; Yuan et al., 2010; Zhao and Running, 2010).

The LUE method is an empirical approach, and therefore, models based on LUE require a number of biome or ecosystem specific parameters to specify the diversity of the global ecosystems as detailed as possible. For this, a look-up table is created with required parameters. The key parameter of the LUE approach, maximum light use efficiency (ε^*), is widely evaluated to improve model performance. For example, Zhao and Running (2010) modified the ε^* look-up table of MODIS GPP products compared to a previous version (Heinsch et al., 2003). The data sets used to constrain ε^* are increasing in number and length, mostly from flux towers using eddy covariance methods (Baldocchi et al., 2001; Reichstein et al., 2005), and several studies have provided updated

constraints (Zhang et al., 2008; Connolly et al., 2009). On the other hand, once the vegetation index is updated or changed, ε* also has to be re-evaluated to fit field measurements. For example, Potter et al., (2007) used enhanced vegetation index (EVI) in the CASA model instead of fraction of photosynthetically active radiation (fPAR) to estimate NPP estimations, changing ε* from 0.39 g C MJ^{-1} with fPAR to 0.55 g C MJ^{-1} with MODIS EVI.

One particular issue in LUE model development is the difference between ε* as used in models and that constrained by field measurements (e.g. Lobell et al., 2002). Usually, ε* values based on field measurements in croplands are much higher than those used in models, sometimes more than 2-4 times. In the early stage, many ε (actual light use efficiency involving environmental stresses) values were estimated by measuring plant dry matter at site level. More and more data have become available, especially from flux towers using eddy covariance methods which offer reliable GPP records with known uncertainties (Baldocchi et al., 2001; Reichstein et al., 2005). Hence, efforts are needed to re-evaluate ε* using these new records to improve the LUE model performance.

1.1.3 The impact of water availability on the terrestrial carbon cycle

The response of vegetation to climate change is crucial in understanding ecosystem dynamics and in quantifying terrestrial carbon cycle behaviour. Water availability, solar radiation and temperature are the three main constraints that determine the spatial distribution of ecosystems and plant growth (Churkina and Running, 1998; Heimann and Reichstein, 2008; Nemani et al., 2003). Due to the lengthening of the growing season, plant growth has already been observed to increase in high latitudes (Myneni et al., 1997). Based on flux tower measurements in Canada, Chen et al. (2006) found that boreal ecosystems absorbed more carbon in warmer years. Warmer springs will tend to lead to more CO_2 uptake by the northern hemisphere ecosystems but this enhancement could be cancelled by drier summers (Angert et al., 2005). In addition, autumn warming could also lead to net CO_2 losses in northern ecosystems (Piao et al., 2008; Parmentier et al., 2011). Both from theoretical and observational points of view, increased diffuse radiation such as arising from atmospheric aerosols will increase CO_2 uptake in forest and croplands (Niyogi et al. 2004). Mercado et al. (2009) found that the fertilization effects of enhanced diffuse radiation on vegetation had the potential to increase the global land carbon sink significantly.

Water availability is a primary constraint compared to radiation and temperature (Churkina and Running, 1998; Heimann and Reichstein, 2008; Nemani et al., 2003). The availability of water influences more than half of the primary productivity of global terrestrial ecosystems according to Heimann and Reichstein (2008). During the last decades, several studies have demonstrated that extreme droughts may impact terrestrial productivity in a significant way and reduce the sink strength at (sub) continental scale (Ciais et al., 2005; Reichstein et al., 2007a, 2013; van der Molen et al., 2011). Several recent droughts, such as those in Australia (2002-2009), Europe (2003) and Amazonia (2005, 2010) had measurable impacts on plant production (Gobron et al., 2010; Zhao and Running, 2010). Moreover, droughts can also increase deforestation and associated fire activities (van der Werf et al., 2004). Therefore, drought may have caused

considerable decreases in the carbon uptake globally (Dolman et al., 2010), which is further emphasized by Reichstein et al. (2013). Climate extremes, especially water dynamics related to drought and floods, could reduce ecosystem carbon stocks and cancel the expected enhancements of terrestrial ecosystem carbon.

Soil moisture is the key parameter for plant productivity and is directly related to soil water dynamics. Unfortunately, the precise effects of water availability on the terrestrial carbon cycle are still not well understood. Moreover, the results of drought events mentioned above were often obtained without adequate observations of soil moisture. Model based soil moisture and several drought indices that are in different ways related to actual soil moisture are often used as proxies (Hirschi et al., 2011; Lotsch et al., 2003; Nicholson et al., 1990). Observed soil moisture is arguably the best representation of the actual amount of water contained in the soil, and is key to understanding the climate-soil-vegetation system both spatially and temporally (Porporato and Rodriguez-Iturbe, 2002; Rodriguez-Iturbe, 2000). Therefore, precipitation and drought indices are still the main tools to evaluate water availability constraints. This in spite of the fact that remotely sensed soil moistures are now being developed offering large-scale and continuous observational records of the water status of the land surface globally (de Jeu et al., 2008; Dolman and de Jeu, 2010; Liu et al., 2011, 2012). Therefore, studies to improve the knowledge of water-related vegetation dynamics are applied using remote sensed soil moisture data.

1.2 Objectives and outline of this thesis

1.2.1 Cropland GPP and NPP estimations

As mentioned previously, existing studies of global GPP and NPP still show large disagreements (Beer et al., 2010; Koffi et al., 2012; Ryu et al., 2011; Zhao and Running, 2010), especially over croplands. For instance, Beer et al. (2010) reported a global cropland GPP of 14.8 Pg C yr^{-1} using flux tower records and several diagnostic models. In contrast, Saugier et al. (2001) estimated this number to be 8.2 Pg C yr^{-1}.

To improve GPP and NPP estimates using LUE methods requires both well evaluated plant type specific look-up tables of ε* and more sophisticated model structures. Chapters 2-3 mainly focus on estimating GPP and NPP of global croplands using the LUE approach. ε* values of crop types vary over a larger range compared with other vegetation classes. There were many field-based results available across different crop types because plant dry matter and solar radiation are relatively easy to measure in agricultural fields. Observation techniques are continuously improving, which bring more and more new observational records. At field level, flux towers offer net ecosystem exchange (NEE) data from hourly to annual time scales (Baldocchi et al., 2001), which can be separated into GPP and the respiration component using techniques developed for instance by Lasslop et al. (2010) and Reichstein et al. (2005). In chapter 2 we aim to improve the prediction of the maximum light efficiency (ε^*_{NPP}) using eddy flux measurements in North America and Europe and compare the ε^*_{NPP} estimates with previously reported values.

Based on observational records, ε* varies widely across crop types. However, the ε* used in LUE models is generally applicable for one major vegetation class only (Goerner et al., 2011; Potter et al., 1993; Xiao et al., 2005; Yuan et al., 2010; Zhao and Running, 2010). As a result, usually the same ε* is used for all types of croplands. Previous studies have also highlighted that ε^*_{GPP} or ε^*_{NPP} based on site measurements are much higher than that used in models for croplands. The causalities behind this discrepancy are unresolved. Because LUE is an empirical approach, using crop type specific data rather than one uniform value in the model may improve current estimates. Based on this hypothesis, in chapter 3, we used ε^*_{GPP} estimates based on field measurements directly in our improved LUE model, separating global croplands into 26 different types. We made two innovations in our model to improve these estimates of global cropland GPP. The cropland area distribution data that we used could define the cropland types by month and distinguish the growing periods. We also assigned different ε^*_{GPP} values to the 26 crop types. However, this requires a much more complex look-up table of ε^*_{GPP}. A combination of direct estimates of ε^*_{GPP} using flux tower measurements and converted ε^*_{GPP} from previous studies was conducted. The objective of this chapter is to provide a more realistic estimate of global cropland GPP than previous studies.

1.2.2 Soil moisture constraints on vegetation

Previous studies have illustrated a clear impact of drought events on plant production (Gobron et al., 2010; Zhao and Running, 2010). Drought occurrence and severity are likely to increase in the future (Dai, 2013, but see also Sheffield et al., 2012). However, the regional details of these increases and their impacts are still not very clear. In existing analyses, drought indices are often used as a proxy to study the relationship between vegetation dynamics and water availability (Hirschi et al., 2011; Lotsch et al., 2003; Nicholson et al., 1990). Over ten different drought indices have been developed during the twentieth-century (Heim 2002). These drought indices are the most widely used proxies to indicate drought intensity and are still being refined.

The study in chapter 4 investigates the relationships between a newly created drought index, the standardized precipitation-evapotranspiration index (SPEI, Vicente-Serrano et al., 2010), and NDVI. SPEI was designed to combine the advantages of PDSI (Palmer Drought Severity Index; Palmer, 1965) and SPI (standardized precipitation index; McKee et al., 1993), the two most widely used drought indices. PDSI is more physical by considering both precipitation and temperature to model soil water conditions. SPI is easy to calculate and could represent integrated effects of precipitation on multiple time scales. SPEI is calculated in a similar manner as SPI but also considers temperature effects by involving potential evapotranspiration. Our objective of this chapter is to find a way to categorize the spatial pattern of the relationships between drought and vegetation with a much stronger regional focus compared to earlier global studies.

In-situ observed soil moisture still is arguably the best representation of the actual amount of water contained in the soil. However, field measurements of soil moisture cannot offer large-scale records efficiently. Remotely sensed soil moisture provides in principle long-term and continuous data with global coverage. Considerable effort has been put into developing soil moisture based on satellite measurements. Soil moisture in

the surface layer detected from space borne passive and active microwave instruments has been shown to provide effective estimates at regional and global scales (de Jeu et al., 2008; Gao et al., 2006; McCabe et al., 2005; Njoku et al., 2002; Owe et al., 2008; Wagner et al., 2003; Wen et al., 2003). There are however some limitations in the application of remote sensing based data. For instance, the uncertainties in high-density vegetation areas are very large (Parinussa et al., 2011). In contrast, in semi-arid regions data quality is much higher. In chapter 5, we analyze the relationships between soil moisture and NDVI using three different statistical methods to more comprehensively characterize their relationships, offering an observational benchmark for coupled vegetation climate models. We chose mainland Australia as target region because the soil moisture data there have been well evaluated with ground based measurements (Draper et al., 2009). Our objective is to understand and describe the spatial and temporal pattern of these soil moisture vegetation relationships in such a typical water-limited region. The methods in this paper are useful to extend this kind of study to global scale to achieve more general conclusions in the future.

The final chapter provides a synthesis of this thesis, integrating the findings of the work in this thesis and other related studies. It also provides recommendations for further research.

Chapter 2 Evaluation of cropland maximum light use efficiency using eddy flux measurements in North America and Europe[1]

Abstract

Croplands cover 12% of the ice-free land surface and play an important role in the global carbon cycle. Light use efficiency (LUE) models have often been employed to estimate the exchange of CO_2 between croplands and the atmosphere. A key parameter in these models is the maximum light use efficiency (ε^*_{NPP}), but estimates of ε^*_{NPP} vary by at least a factor 2. Here we used 12 agricultural eddy-flux measurement sites in North America and Europe to constrain LUE models in general and ε^*_{NPP} in particular. We found that LUE models could explain on average about 70% of the variability in net ecosystem exchange (NEE) when we increased the ε^*_{NPP} from 0.5 to 0.65-2.0g C per MJ Photosynthetic Active Radiation (PAR). Our results imply that croplands are more important in the global carbon budget than often thought. In addition, inverse modelling approaches that utilize LUE model outputs as a-priori input may have to be revisited in areas where croplands are an important contributor to regional carbon fluxes.

2.1 Introduction

Globally, crop ecosystems cover about 12% of the ice-free land surface. Regionally, this fraction can increase to 33% in Europe and 20% in the United States (Ramankutty et al., 2008). Schulze et al. (2009) suggested that croplands are a net source of greenhouse gasses to the atmosphere in Europe. In contrast, croplands were identified as a sink in the United States (West et al., 2010). Smith et al. (2008) proposed that croplands could have a large potential in greenhouse gas mitigation through specific GHG-management practices, and different local management practices may be one of the reasons why croplands sometimes appear as a source and sometimes as a sink in different regions of the world.

Designed as a core infrastructure of the global terrestrial monitoring network (Running et al., 1999), the eddy covariance technique is a widely used method to observe carbon fluxes between the land surface and the atmosphere (Baldocchi et al., 2001). The data is particularly useful to study terrestrial ecosystem carbon cycle processes on time scales from hourly to yearly. Flux towers measurements using eddy covariance methods are widely used across a variety of terrestrial ecosystems, including croplands. Flux towers measure the net flux of carbon dioxide (net ecosystem exchange (NEE)), which can be

[1] This chapter is based on Chen, T, van der Werf, G. R., Dolman, A. J., and Groenendijk, M.: Evaluation of cropland maximum light use efficiency using eddy flux measurements in North America and Europe, Geophys Res Lett, 38, L14707, DOI: 10.1029/2011gl047533, 2011.

separated into an assimilation component (gross primary production (GPP)), and the respiration component (total ecosystem respiration (R_e)) using techniques developed for instance by Reichstein et al. (2005). In addition to flux measurements, additional observations are usually made including photosynthetic available radiation (PAR). This data stream offers an opportunity to study the light use efficiency of croplands.

Light use efficiency (LUE) models are widely used to diagnose terrestrial ecosystem productivity such as gross primary productivity (GPP) and net primary productivity (NPP, GPP minus autotrophic respiration) (Field et al., 1998; Running et al., 2004). NPP and GPP can be expressed as a product of absorbed photosynthetically active radiation (PAR) and a light use efficiency coefficient; ε (Monteith, 1972; Monteith and Moss, 1977). While the LUE approach has become widely accepted, the exact determination of the core parameter ε*, the potential maximum ε that may be reached when temperature and moisture are not limiting plant carbon uptake, is still problematical. Zhang et al., (2008) suggested to increase the cropland ε* in the algorithm used to derive GPP and NPP from the Moderate Resolution Imaging Spectroradiometer (MODIS) MOD17 product after calibration with flux data from a site with double-cropped winter wheat and summer maize in China. Besides the MOD17 product, remote sensing data from the MODIS instruments include the fraction of photosynthetically active radiation (fPAR) at 1 km^2 (Running et al., 1999). We evaluated ε^*_{NPP} of croplands using flux tower measurements and MODIS derived fPAR data together with the Carnegie-Ames-Stanford Approach (CASA) biogeochemical model across North America and Europe to determine whether the default value of ε^*_{NPP} is representative and if not, what it should be to capture the carbon dynamics observed by flux towers over croplands.

2.2 Methods

2.2.1 Site description

There are around thirty cropland sites in the FLUXNET database (www.fluxdata.org). Twelve of these sites had at least 2 years of data and contained also meteorological parameters such as PAR, temperature, and precipitation. We chose these twelve sites for our analysis, evenly spread over North America and Europe (Table 2.1).

2.2.2 fPAR from MODIS land products subsets

MODIS land products subsets are provided at 1km resolution for a 7*7 km box centered on the flux towers through the Oak Ridge National Laboratory Distributed Active Archive Center (Oak Ridge National Laboratory Distributed Active Archive Center (ORNL DAAC), 2010). These subsets are specifically designed for validation of models and remote sensing products, or for characterization of field sites (http://daac.ornl.gov/cgi-bin/MODIS/GR_col5_1/mod_viz.html). Following previous studies (Connolly et al., 2009; Zhang et al., 2007), we only used data from the center pixel where the tower was located.

Table 2.1. Eddy covariance site information for croplands.

Site code	Site name	Country	Latitude	Longitude	Data period	Reference
BE-Lon	Lonzee	Belgium	50.5522	4.74494	2004-2006	Aubinet et al., 2009
DE-Geb	Gebesee	Germany	51.1001	10.9143	2004-2006	Werner L. Kutsch
DE-Kli	Klingenberg	Germany	50.8929	13.5225	2005-2006	Christian Bernhofer
DK-Ris	Risbyholm	Denmark	55.5303	12.0972	2004-2005	Soegaard et al., 2003
ES-ES2	El salerSueca	Spain	39.2755	-0.31522	2004-2006	Maria-Jose Sanz
FR-Gri	Grignon	France	48.844	1.95243	2005-2006	Pierre Cellier
US-ARM	OK ARM Southern Great Plains site – Lamont	USA	36.6058	-97.4888	2003-2004	Fischer et al., 2007
US-Bo1	Bondville, IL	USA	40.0062	-88.2904	2000-2007	Meyers et al., 2006
US-IB1	IL Fermi National Accelerator Laboratory-Batavia	USA	41.8593	-88.2227	2006-2007	Roser Matamala
US-Ne1	NE - Mead - irrigated continuous maize site	USA	41.1651	-96.4766	2001-2004	Verma et al., 2005
US-Ne2	NE - Mead - irrigated maize-soybean rotation site	USA	41.1649	-96.4701	2001-2004	Verma et al., 2005
US-Ne3	NE - Mead - rain fed maize-soybean rotation site	USA	41.1797	-96.4397	2001-2004	Verma et al., 2005

2.2.3 Model and optimized method

The CASA biogeochemical model that is used here (Potter et al., 1993) is based on the LUE approach and operates with a monthly time step. The general equation of LUE models is:

$$NPP = PAR \times fPAR \times f(\varepsilon) \times \varepsilon^{*} \quad (2.1)$$

Where f(ε) accounts for the effects of environment stress including water stress and temperature effects. Empirical studies suggested that ε* for NPP calculations (here denoted as ε^*_{NPP}) varies between 1.1 and 1.4 g C MJ^{-1} for croplands (Russell et al., 1989). In the CASA version used here (van der Werf et al., 2010), ε^*_{NPP} was set to 0.5 g C MJ^{-1} globally to match global NPP values of 60 Pg C $year^{-1}$ (Beer et al., 2010). The Q_{10} value which governs the temperature response of heterotrophic respiration was set to 1.5 in the soil sub-model and CASA was spun up with the average input data for 250 years, when assimilation was equal to respiration on an annual scale. We ran CASA with meteorological data (PAR, temperature, precipitation) measured by the flux towers. We first ran CASA with the default ε^*_{NPP} (0.5 g C MJ^{-1}), and then increased ε^*_{NPP} with steps of 0.05, keeping the other input datasets - which are better constrained than ε^*_{NPP} - constant. The ε^*_{NPP} value corresponding to the lowest root mean square difference between FLUXNET observed NEE and simulated NEE from CASA was then considered optimal:

$$RMSE = [\frac{1}{N}\sum_{n=1}^{N}(NEE_{CASA} - NEE_{flux})^2]^{1/2} \quad (2.2)$$

2.3 Results

2.3.1 NPP comparisons

Most LUE-based models use the same equation to estimate GPP and NPP, the difference often lies in a different ε*. Therefore the ratio between GPP and NPP is constant in most LUE approaches, allowing us to compare the variability in CASA-derived NPP with flux towers-derived GPP. Correlation coefficients between NPP and GPP varied between 0.58 and 0.96 with an average of 0.87 (Table 2.2).

2.3.2 NEE comparisons

Modelling NEE with the default ε^*_{NPP} of 0.5 g C MJ^{-1}, and with optimized ε^*_{NPP} were both compared with flux towers measured NEE. We used Taylor diagrams (Taylor, 2001) to quantitatively depict the comparison. Since the measurement values vary between sites, the data was normalized first to plot all sites in one single diagram.

Figure 2.1 shows the Taylor diagrams (Taylor, 2001), and a time series for one site is given as an example in Figure 2.2. For the Taylor diagrams, we divided the model results and flux towers measurements by the standard deviation of the corresponding flux towers measurements. Therefore, there is only one reference point indicating the measured NEE which is located on the x-axis at unity. Thus, flux towers measurements have the same standard deviation (normalized to 1) in the Taylor diagram. We found that correlation coefficients between predicted and observed fluxes varied between 0.54 and 0.98. These values were identical for original and optimized ε^*_{NPP} because a change in ε^*_{NPP} operates linearly. Original modelled NEE with default ε^*_{NPP} compared poorly

with flux towers observations, showing a uniform underestimation of the standard deviation which only explained between 2% and 34% of the flux towers NEE variance, with an average of 13%. A significant improvement in the amplitude of NEE variations was made with our optimized ε^*_{NPP} where NEE from CASA explained flux towers NEE variance of about 29% to 94%, with an average value of 68%.

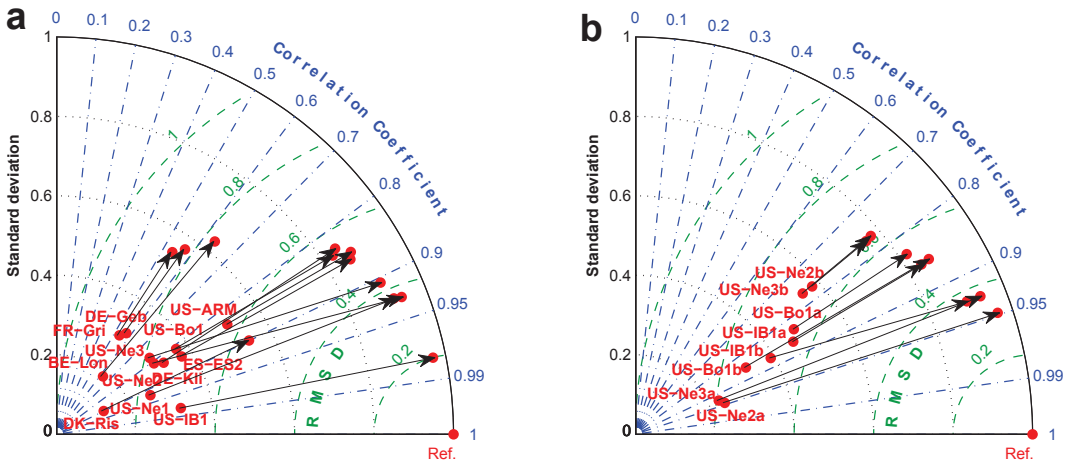

Figure 2.1. CASA modelled NEE compared with flux towers measurements in normalized pattern statistics. Site codes are described in Table 2.2. Original modelling results with ε^*_{NPP} = 0.5 g C MJ^{-1} for NEE are plotted at the tail of the arrows, and the rows point refer to revised modelled NEE with optimized ε^*_{NPP}. Ref point indicates flux towers measured NEE. a) 12 sites used in this study; b) only those sites with plant rotation information (plant type information in Table 2.2).

2.3.3 ε^*_{NPP}

Our optimized ε^*_{NPP} values for the 12 cropland sites varied between 0.65 and 2.0 g C MJ^{-1} (Table 2.2). Importantly, ε^*_{NPP} changed with crop type; the lowest values were found for wheat (0.85 g C MJ^{-1} at one site) and soybean (0.65-0.90 g C MJ^{-1} at 4 sites), while rice (1.15 g C MJ^{-1} at one sites) and maize (1.30-1.95 g C MJ^{-1} at 5 sites) had higher values. These values fall within the range compiled by Lobell et al. (2002).

2.3.4 ε^*_{GPP} MOD17 GPP comparison with flux towers

The MODIS GPP product MOD17 is also based on the LUE approach, with an ε^*_{GPP} of 0.68 g C MJ^{-1} for croplands (Heinsch et al., 2003). Here we simply calculated observed light use efficiency ε_{GPP} as the ratio between measured GPP and incident photosynthetically active radiation (PAR) at flux towers, i.e. ε_{GPP} = fPAR×f (ε) ×ε^*_{GPP}. This approach neglects potential limitations that could lower ε from its maximum value, but this effect is likely minimal in well-watered crops in the growing season when fPAR is close to unity. Crops

have in general a more pronounced growth cycle than natural ecosystems due to set planting and harvesting dates. We defined the growing season from May to August based the observed seasonality in the flux towers. We then chose the largest ε_{GPP} over these 4 months, denoted as ε (L). We found that ε (L) ranged between 1.31 and 2.91 g C MJ^{-1}, with one outlier; an ε (L) of 0.37 g C MJ^{-1} (Table 2.2).

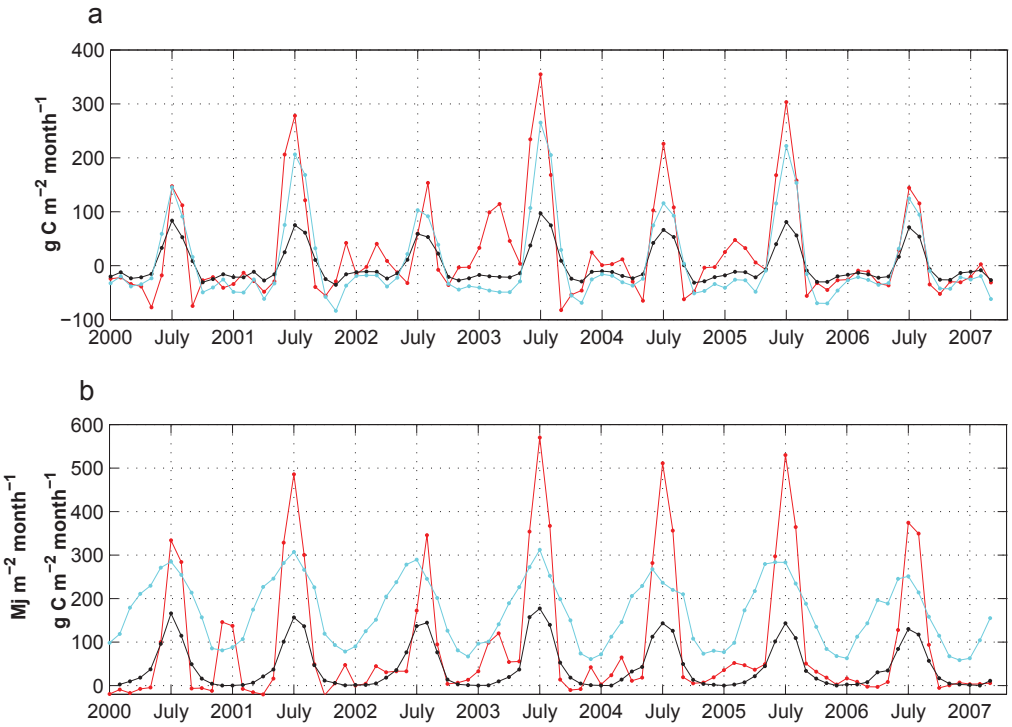

Figure 2.2. An example of time series of monthly carbon flux information, site BO Bondville, IL USA. a) CASA modelled NEE with optimized ε^*_{NPP} (cyan) and default ε^*_{NPP} = 0.5 g C MJ^{-1} (black) compare with flux towers NEE (red), rotations considered. b) Red line is flux towers measured GPP compare with MOD17 GPP (black). Cyan line indicates photosynthetically active radiation (PAR, Unit is million joules per square meter per month).

2.4 Discussion and conclusions

The LUE approach is commonly used to estimate the efficiency of radiation conversion to plant production, both for GPP (Zhao and Running, 2010) and for NPP (Field et al., 1995). By including respiration and other carbon loss processes, a biogeochemical model such as CASA could further calculate NEE, representing the net carbon flux between ecosystems and the atmosphere. NEE is also measured directly using the eddy-covariance method, allowing for a direct model – measurement comparison. When using the 'standard' ε^*_{NPP} value of 0.5 g C MJ^{-1}, CASA captured 2%-34% (range) of the temporal variability in NEE in the 12 cropland sites we investigated.

To capture the NEE magnitude, the model required a substantial increase in ε^*_{NPP} for all 12 cropland sites. On average, we found that an ε^*_{NPP} of 1.25 g C MJ^{-1} yielded the lowest RMSE when assessing the performance of all sites, with individual sites ranging from 0.65 to 2.0 g C MJ^{-1}. Although most models use a constant ε^*_{NPP} value for different crop types, our findings indicate that different crop types may have different ε^*_{NPP} values, although a larger number of sites for each individual crop type is required to gain more confidence in the exact values. For example, while we included both irrigated and non-irrigated sites in our study, we could not systematically assess the impact of irrigation on ε^*_{NPP} due to the limited number of station. Our finding of an underestimation of ε^*_{NPP} also applied to the MODIS MOD17 GPP product over crop sites.

Table 2.2. Statistics information between modelling and flux towers observation [a].

Site code	NPP ($\varepsilon^*_{0.5}$), GPP (FLUX TOWERS)		Plant type	ε^* (optimized)	NEE (ε^*_{opt}), NEE (FLUX TOWERS)		ε (L)
	r	var rate			r	var rate	
BE-Lon	0.76	0.03		1.55	0.64	0.39	1.96
DE-Geb	0.7	0.06		0.9	0.57	0.32	1.86
DE-Kli	0.95	0.05		1.25	0.83	0.71	1.61
DK-Ris	0.91	0.01		2	0.9	0.29	2.91
ES-ES2	0.95	0.04	rice	1.15	0.86	0.74	1.55
FR-Gri	0.58	0.05		0.9	0.54	0.3	1.92
US-ARM	0.92	0.2	wheat	0.85	0.85	0.76	0.37
US-Bo1	0.9	0.05			0.84	0.69	
US-Bo1a	0.88	0.06	soybean	0.85	0.83	0.67	2.16
US-Bo1b	0.94	0.05	maize	1.3	0.86	0.74	1.87
US-IB1	0.89	0.05			0.93	0.81	
US-IB1a	0.94	0.04	maize	1.45	0.98	0.94	1.96
US-IB1b	0.83	0.07	soybean	0.9	0.86	0.7	1.31
US-Ne1	0.95	0.03	maize	1.7	0.93	0.84	2.26
US-Ne2	0.89	0.03			0.93	0.88	
US-Ne2a	0.96	0.02	maize	1.9	0.95	0.93	2.22
US-Ne2b	0.87	0.07	soybean	0.65	0.77	0.57	1.66
US-Ne3	0.85	0.04			0.91	0.81	
US-Ne3a	0.92	0.02	maize	1.95	0.93	0.87	1.99
US-Ne3b	0.87	0.07	soybean	0.7	0.76	0.6	1.39

[a] Correlation and variance rate between NPP (CASA with default ε^*_{NPP} = 0 5 g C MJ^{-1}) and GPP (flux towers measurement), and between NEE (CASA with optimized ε^*_{NPP}) and NEE from flux towers measurement. ε (L) see Part 2.3.4

Our results are somewhat sensitive to the parameterization of respiration in CASA, because lower respiration fluxes could in principle explain part of the mismatch we found between modelled and measured NEE. Figure 2.3 shows that this is unlikely to explain a substantial part of the mismatch because with lower respiration fluxes

(autotrophic and / or heterotrophic) and consequently lower NPP values the NPP during the growing season would be lower than NEE, which is physically not plausible. Moors et al. (2010) suggested the ratio of NPP to NEE to be about 1.6 for croplands during the growing season. With optimized ε^*_{NPP}, our results indicated a ratio of 1.7 on average (Figure 2.3). In addition, the sensitivity of our results to changes in heterotrophic respiration is modest; by changing the Q_{10} value to a range between 1 and 2 (Table 2.3) we found that the average optimized ε* ranged between 0.98 and 1.43, instead of the value of 1.25 we derived with the standard Q_{10} value of 1.5.

Besides the limited number of cropland sites available, uncertainties exist due to the scaling of the 1 km^2 pixel located on the flux tower which may not be fully representative of the flux tower footprint. Tower measurements in general represent a horizontal range of about 500 m around the tower (Running et al., 1999), although the actual fetch will vary with wind (speed and direction) and surface roughness and other meteorological conditions (Schmid, 2002).

Table 2.3. Optimized maximum light use efficiency (ε^*_{NPP}) values for the studied sites for different Q_{10} values. Rotation information was considered, denoted as "a" or "b" in the last letter of site code.

site code	Q_{10}										
	1	1.1	1.2	1.3	1.4	1.5	1.6	1.7	1.8	1.9	2
BE-Lon	1.25	1.3	1.35	1.45	1.5	1.55	1.65	1.7	1.75	1.8	1.8
DE-Geb	0.7	0.75	0.8	0.85	0.85	0.9	0.95	1	1	1.05	1.1
DE-Kli	0.95	1	1.05	1.1	1.2	1.25	1.3	1.35	1.4	1.45	1.45
DK-Ris	2	2	2	2	2	2	2	2	2	2	2
ES-ES2	1.05	1.05	1.1	1.1	1.15	1.15	1.2	1.2	1.2	1.25	1.25
FR-Gri	0.7	0.7	0.75	0.8	0.85	0.9	0.95	0.95	1	1.05	1.05
US-ARM	0.7	0.75	0.8	0.8	0.85	0.85	0.85	0.85	0.8	0.8	0.8
US-Bo1a	0.6	0.65	0.7	0.75	0.8	0.85	0.9	0.95	1	1.05	1.1
US-Bo1b	1	1.1	1.15	1.2	1.25	1.3	1.35	1.4	1.45	1.5	1.55
US-IB1a	1.1	1.15	1.25	1.3	1.4	1.45	1.55	1.6	1.7	1.75	1.8
US-IB1b	0.65	0.7	0.75	0.8	0.85	0.9	0.95	1	1.05	1.1	1.15
US-Ne1	1.25	1.35	1.45	1.55	1.65	1.7	1.8	1.9	1.95	2	2
US-Ne2a	1.4	1.5	1.6	1.7	1.8	1.9	1.95	2	2	2	2
US-Ne2b	0.5	0.5	0.5	0.55	0.6	0.65	0.7	0.75	0.8	0.85	0.9
US-Ne3a	1.4	1.5	1.6	1.75	1.85	1.95	2	2	2	2	2
US-Ne3b	0.5	0.5	0.55	0.6	0.65	0.7	0.75	0.8	0.85	0.85	0.9
average	0.98	1.03	1.09	1.14	1.2	1.25	1.3	1.34	1.37	1.41	1.43

In addition to the MODIS data, we also used the JRC-fPAR product (Gobron et al., 2010). The comparison showed a reasonable level of agreement between the two products with no overall bias (Figure 2.4). Using the JRC-fPAR product would therefore not change our main conclusions. We did not include site-specific details on management regimes and stage in the crop rotation cycle, which may impact carbon fluxes. By including as many sites as possible (n=12) some of these factors will average out, but care should be taken with interpreting the results for individual sites.

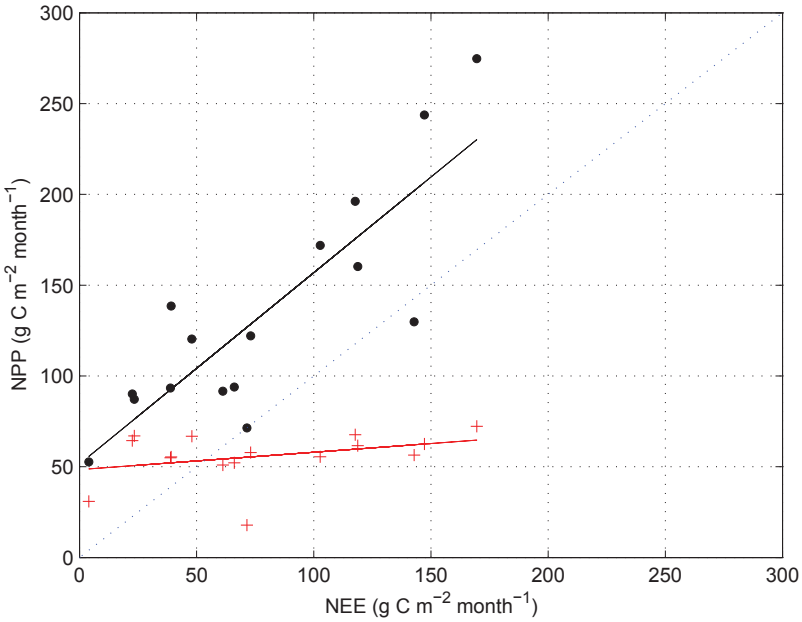

Figure 2.3. Monthly average NEE and NPP during the growing season (May to September). Black dots indicate modelled NPP with the optimized ε^*_{NPP} (Table 2.2), red plus signs indicate NPP with the "standard" ε^*_{NPP} of 0.5 g C MJ^{-1} PAR. Linear regression lines are included and the blue line indicates the 1:1 line. Since NPP cannot be smaller than NEE, boosting ε^*_{NPP} is a more plausible mechanism to explain the observed mismatch than, for example, seeking the causes of the mismatch in lower respiration fluxes.

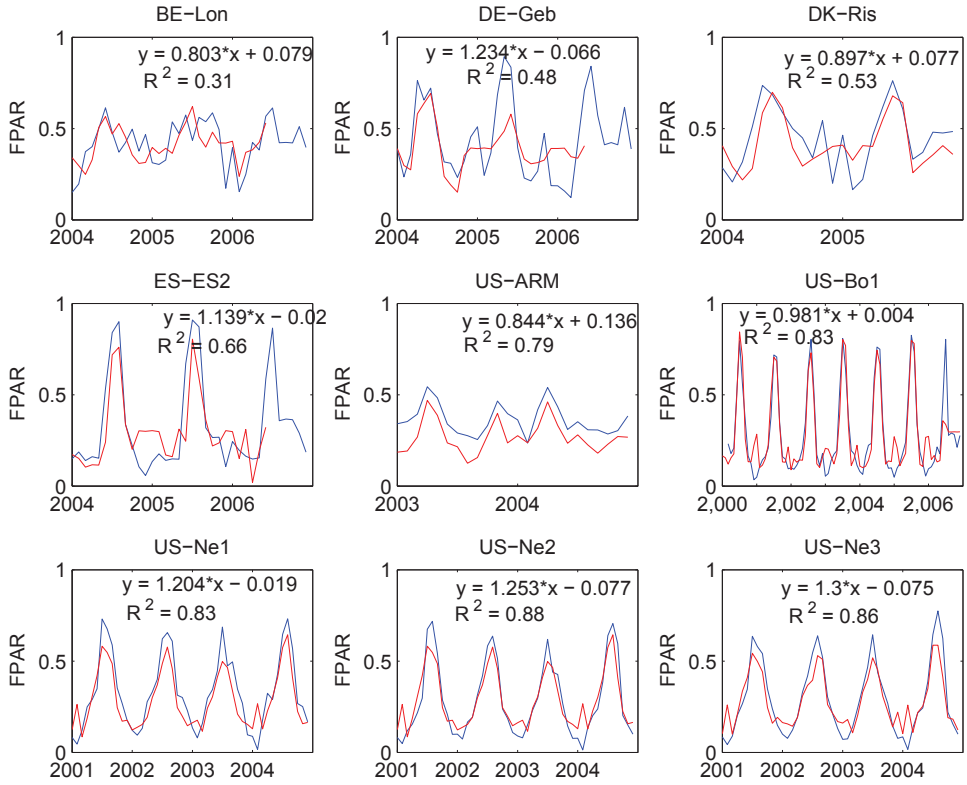

Figure 2.4. FPAR from MODIS (blue) and JRC (red) for our study sites and periods. 9 sites were chosen based on JRC data availability (two years of data at least). y indicates MODIS FPAR, x is JRC FPAR.

Chapter 3 Global cropland monthly Gross Primary Production in the year 2000[2]

Abstract

Croplands cover about 12% of the ice-free terrestrial land surface. Compared with natural ecosystems, croplands have distinct characteristics due to anthropogenic influences. Their global gross primary production (GPP) is not well constrained and estimates vary between 8.2 and 14.2 Pg C yr^{-1}. We quantified global cropland GPP using a light use efficiency (LUE) model, employing satellite observations and survey data of crop types and distribution. A novel step in our analysis was to assign a maximum light use efficiency estimate (ε^*_{GPP}) to each of the 26 different crop types, instead of taking a uniform value as done in the past. These ε^*_{GPP} values were based on flux tower CO_2 exchange measurements and a literature survey of field studies, and ranged from 1.21 g C MJ^{-1} to 2.96 g C MJ^{-1}. Global cropland GPP was estimated to be 11.05 Pg C yr^{-1} in the year 2000. Maize contributed most to this (1.55 Pg C yr^{-1}), and the continent of Asia contributed most with 38.9% of global cropland GPP. In the continental United States, annual cropland GPP (1.28 Pg C yr^{-1}) was close to values reported previously (1.24 Pg C yr^{-1}) constrained by harvest records, but our estimates of ε^*_{GPP} values were much higher. Our results are sensitive to satellite information and survey data on crop type and extent, but provide a consistent and data-driven approach to generate a look-up table of ε^*_{GPP} for the 26 crop types for potential use in other vegetation models.

3.1 Introduction

The terrestrial biosphere assimilates an estimated 120-150 Pg C yr^{-1} (Beer et al., 2010; Welp et al., 2011) as Gross Primary Production (GPP). Roughly, half of the GPP is used for plant maintenance processes and is generally referred to as autotrophic respiration (R_a). The remainder is available for plant growth as Net Primary Production (NPP), which is subsequently consumed mostly by heterotrophs (R_h) and fire.

Biochemical processes of photosynthesis at cell or leaf level are relatively well known, but accurate estimates of GPP at larger scales (regions or the globe) are still uncertain. Direct measurements of net ecosystem exchange (NEE: GPP – R_h – R_a), such as eddy covariance measurements, suffer from the large spatial heterogeneity in the exchange between plants and the atmosphere which makes upscaling difficult. Therefore, current global GPP estimates still mainly rely on model results. However, considerable differences exist between various studies (Zhao et al., 2005; Ryu et al., 2011; Koffi et al.,

[2] This chapter is based on Chen, T., van der Werf, G. R., Gobron, N., Moors, E. J., and Dolman, A. J.: Global cropland monthly Gross Primary Production in the year 2000, Biogeosciences Discuss., 11, 3465-3488, DOI:10.5194/bgd-11-3465-2014, 2014

2012; Beer et al., 2010), in particular for croplands. For example, Beer et al. (2010) reported global cropland GPP of 14.8 Pg C yr^{-1} using flux tower measurements based on eddy covariance methods and several diagnostic models. In contrast, Saugier et al. (2001) estimated this number to be 8.2 $PgCyr^{-1}$.

Croplands cover about 12% of the ice-free land surface globally (Ramankutty et al., 2008), contributing considerably to the global carbon cycle (Hicke et al., 2004). Additionally, the area occupied by croplands changes over time with consequences for global carbon stocks. For example, a large carbon sink was found in the abandoned croplands of the Soviet Union (Vuichard et al., 2008). Vice versa, deforestation is often related to the expansion of cropland (Morton et al., 2006) which leads to a decrease in above ground biomass. However, croplands may also have a large capacity for carbon sequestration (Parr and Sullivan, 2011).

The light use efficiency (LUE) approach has been widely used to estimate GPP. Monteith (1972) developed this approach assuming that the growth in plant biomass is directly proportional to absorbed solar radiation. During the early period, mostly field measurements of plant dry matter and solar radiation were applied to evaluate the LUE approach. The LUE approach was also applied to estimate net primary production (NPP) in large-scale models (Field et al., 1995; Knorr and Heimann, 1995; Potter et al., 1993; Ruimy et al., 1994, 1999). The LUE application was later extended to estimate GPP largely because LUE is more likely to be fundamentally related to GPP, the direct outcome of photosynthesis (Prince and Goward, 1995; Ruimy et al., 1996; Running et al., 2000; Landsberg et al., 1997).

In the LUE approach, NPP or GPP is assumed proportional to the absorbed photosynthetically active radiation (PAR) at an efficiency rate, ε. Because ε is affected by environmental factors, the maximum light use efficiency (ε*, Haxeltine and Prentice, 1996; Potter et al., 1993), defined as an environmentally optimized ε, is widely used in models. Numerous studies have estimated ε or ε* at site level (Table 3.1). In the parameterizations of models, ε* is more often used than ε because ε* tends to be more stable between various plant types. Besides, subsequent environmental restrictions can be calculated using local environmental inputs. The LUE approach is thus widely used to estimate GPP or NPP from site level to large scales by combining satellite-based vegetation index measurements (Goerner et al., 2011; Potter et al., 1993; Xiao et al., 2005; Yuan et al., 2010; Zhao and Running, 2010; Field et al., 1995; Knorr and Heimann, 1995; Ruimy et al., 1994, 1996, 1999; Prince and Goward, 1995). Although all these models use the LUE concept, they are often use different vegetation indices, ε* values, and may calculate environmental stresses in a different way.

Observational studies have illustrated that ε varies widely between crops even when corrected for environmental stresses and nutrient limitation (Table 3.1). The LUE method is an empirical approach, requiring look-up table of the key parameter to quantify the diversified ecosystems. However, in practice, the ε* in LUE models is identical globally

for all plant types or for major vegetation classes, such as croplands or grasslands (Goerner et al., 2011; Potter et al., 1993; Xiao et al., 2005; Yuan et al., 2010; Zhao and Running, 2010). Usually croplands have only one ε* value in models to represent the average condition, which introduce inevitable biases at local scales. This situation is largely due to two main constraints, suggesting also a strategy for improvement of the estimates. One is the paucity of land surface cover data, most of which did not offer sufficient detail to separate plant or crop types. The other is the adequate use of the large number of studies that have aimed to parameterize ε* using site level measurements.

This study aims to estimate global cropland GPP using recently developed global cropland distribution data for the year 2000 to partition global croplands into 26 crop types. To improve the parameterization of the ε^*_{GPP} model, both eddy covariance flux measurements and a survey of previous reported ε^*_{GPP} values are used to generate a look-up table of ε^*_{GPP} for these 26 crop types.

3.2 Methods and datasets

3.2.1 Introduction

We used a biogeochemical model based on the LUE approach, the Carnegie-Ames-Stanford -Approach (CASA, Potter et al., 1993; van der Werf et al., 2010). Croplands were separated into 26 crop types as described in 3.2.2. We estimated ε^*_{GPP} using 16 eddy covariance flux tower sites (FLUXNET) following Chen et al. (2011) and conducted a literature survey on previously reported ε* values. A combination of these two ε* resources yielded the look-up table of ε^*_{GPP} for the 26 crop types. These steps are explained in more detail below.

3.2.2 LUE model and cropland data

The CASA biogeochemical model with the version described in van der Werf et al. (2010) was used in this study. GPP was calculated by multiplying absorbed photosynthetically active radiation (PAR) and a light use efficiency coefficient, ε (Monteith, 1972; Monteith and Moss, 1977):

$$GPP = PAR \times fPAR \times \varepsilon^*_{GPP} \times T(\varepsilon) \times W(\varepsilon) \quad (3.1)$$

Where fPAR (also known as fAPAR) is the fraction of PAR absorbed by vegetation. Environmental stresses related to temperature and water are indicated by T (ε) and W (ε) respectively. More details about the model structure can be found in Potter et al. (1993).

The monthly distribution of cropland growing data of MIRCA2000 (monthly irrigated and rainfed crop areas, Portmann et al., 2010) was used as the map of global croplands at a 5 arc min spatial resolution. 26 crop types were separated in MIRCA2000. Correspondingly,

5 arc min monthly fPAR data from the Joint Research Centre (JRC) were prepared based on original finer grid records (Gobron et al., 2010) which is further described in Sect. 3.2.3. ε^*_{GPP} was set crop specific, using the values estimated as described in Sect. 3.2.3. International Satellite Cloud Climatology Project (ISCCP) solar radiation data from the Goddard Institute for Space Studies (GISS) (Zhang et al., 2004) were used to generate PAR. Precipitation of the Global Precipitation Climatology Project (GPCP) version 1.1 (Huffman et al., 2001) and temperature of the GISS surface temperature analysis (Hansen et al., 1999) were employed to force environmental stress functions as described in Potter et al. (1993).

3.2.3 The maximum light use efficiency, ε^*_{GPP}

To fulfill the model requirements for the crop types, we needed to estimate and assign ε^*_{GPP} to the 26 crop types of the MIRCA2000 map. ε^*_{GPP} based on direct field measurements are ideal to ensure the parameters in our model are consistent with regard to the vegetation index and environmental factors. Therefore, we applied a similar procedure as in our previous work (Chen et al., 2011) by constraining CASA modelled GPP with field GPP measurements from FLUXNET.

Eddy covariance instrumentation directly measures ecosystem net exchange (NEE), which can then be partitioned into GPP and respiration using various approaches (Reichstein et al., 2005; Lasslop et al., 2010). Combining satellite and eddy covariance tower measurements, ε^*_{GPP} can be directly estimated. FLUXNET offers a high level of global consistency between individual flux tower measurements (see www.fluxdata.org). The FLUXNET dataset contains about 30 cropland sites. To accomplish our purpose of LUE evaluation, we included only those sites where PAR, temperature and precipitation records were available. Besides that, we also collected the rotation histories with details of growing periods and plant types from individual FLUXNET PI's. The information of the sites used in this study is listed in Table 3.2.

Satellite-based fPAR was used to indicate vegetation activity in our study, using JRC collected fPAR products over the FLUXNET sites, available on http://fapar.jrc.ec.europa.eu/Home.php. JRC-fPAR data are generated based on the data collections of SeaWiFS (Sea-viewing Wide Field-of-view Sensor) sensor on the SeaStar satellite and the MERIS (Medium Resolution Imaging Spectrometer) sensor on the Envisat (Environmental Satellite) platform of the European Space Agency. These collections have a 10 day temporal scale and cover 3 by 3 pixels, about 6 × 6 km, around the central pixel where the FLUXNET sites are located. These data are specifically designed for validation of remote sensing products and models or for characterization of field sites. Because usually there are not sufficient fPAR observations on the ground, fPAR from the center pixel is assumed to represent the fPAR influencing the footprint of the tower.

To optimize ε^*_{GPP}, we iteratively changed its value with steps of 0.05 g C MJ^{-1} and choose the ε^*_{GPP} with the lowers RMSE (root mean square error) between CASA and FLUXNET GPP:

$$RMSE = [\frac{1}{N}\sum_{n=1}^{N}(GPP_{CASA} - GPP_{FLUXNET})^2]^{1/2} \quad (3.2)$$

This approach yielded direct estimates of ε^*_{GPP} for 8 crop types out of 26 crops due to the distribution of the FLUXNET sites. To fill in the gaps we conducted a survey of previous studies that reported ε across a wide variety of crop types. However, these previous studies were quite different in their methodology. For example, solar radiation, intercepted PAR and absorbed PAR were interchangeably used to indicate radiation. Direct measurements of dry matter were often used to calculate production while we focused on GPP here. For consistency, we therefore used a conversion equation:

$$\varepsilon^*_{GPP} = \varepsilon_{biomass} \times R_{CB} \times {R_{NG}}^{-1} \times R_{ES} \quad (3.3)$$

where R_{CB} is the carbon content per unit of dry biomass, R_{NG} is the ratio between NPP and GPP and R_{ES} indicates environmental stresses. R_{CB} was found to be quite stable within a 45-50% range (Schlesinger, 1991), and Magnussen and Reed (2004) suggested a conversion rate of 0.475 which was used here (R_{CB} = 0.475). NPP is usually treated as half the value of GPP in most analyses (Beer et al., 2010). Therefore, we used R_{NG} = 0.5 in this paper.

Most of biomass measurements usually only consider above ground dry matter (ADM). To calculate total dry matter (TDM) we used an ADM/TDM ratio of 0.8 (Gallagher and Biscoe, 1978; Steingrobe et al., 2001) when ε values reported were based on ADM measurements only. The maximum light use efficiency concept assumes no environmental stresses, therefore, only the well-watered sites and those without diseases or drought were included in this study ($R_{ES} \approx 1$). As a results, 89 ε^*_{GPP} values using eq. 3.3 were converted based on literature, covering 21 crop types (Table 3.1).

Table 3.1. Experimental light use efficiency values for various crops.

ε^*_{GPP} (g C MJ^{-1})	crop ID	crop type	References	comments
2.46	1	wheat (spring wheat)	Caviglia and Sadras (2001)	
2.53	1	wheat	Muurinen and Peltonen-Sainio (2006)	
2.55	1	wheat	Koizumi et al. (1990)	
2.61	1	wheat	Jamieson et al. (1991)	
2.85	1	wheat barley	Gallagher and Biscoe (1978)	extract from Cannell et al.

				(1987)
2.93	1	wheat	Foulkes et al. (2007)	
3.21	1	wheat (spring wheat)	Abbate et al. (1997)	
3.33	1	wheat	Kiniry et al. (1989)	
3.80	1	wheat	Kemanian et al. (2004)	
3.23	2	maize	Sinclair and Horie (1989)	
4.16	2	maize	Kiniry et al. (1989)	
4.37	2	maize (dentcorn)	Koizumi et al. (1990)	
4.51	2	maize	Lindquist et al. (2005)	
2.57	3	rice	Koizumi et al. (1990)	
2.61	3	rice	Kiniry et al. (1989)	
2.66	3	rice	Sinclair and Horie (1989)	
2.88	3	rice	Katsura et al. (2007)	
3.25	3	rice	Zhang et al. (2009)	
2.43	4	barley	Whitman et al. (1985)	
2.60	4	barley	Muurinen and Peltonen-Sainio (2006)	
2.61	4	barley (spring barley)	Legg et al. (1979)	Extract from Cannell et al. (1987)
2.77	4	barley	Jamieson et al. (1995)	
2.85	4	barley	Koizumi et al. (1990)	
3.12	4	barley	Bingham et al. (2007)	
3.80	4	barley (spring barley)	Kemanian et al. (2004)	
3.09	6	millet	Azam-Ali et al. (1984)	
3.44	6	millet	Begue et al. (1991)	
4.04	6	millet	Mcintyre et al. (1993)	
3.33	7	sorghum	Kiniry et al. (1989)	
3.98	7	sorghum (sweet sorghum)	Varlet-Grancher et al. (1992)	extracted from Dercas and Liakatas (2007)
4.03	7	sorghum (grain sorghum)	Mastrorilli et al. (1995)	
4.11	7	sorghum (grain sorghum)	Rosenthal et al. (1993)	
4.22	7	sorghum (sweet sorghum)	Dercas and Liakatas (2007)	
4.39	7	sorghum (sweet sorghum)	Mastrorilli et al. (1995)	
2.04	8	soybean	Mastrorilli et al. (1995)	
2.09	8	soybean	Muchow et al. (1993)	
2.28	8	soybean	Sinclair and Horie (1989)	

3.04	8	soybean	Unsworth et al. (1984)	
1.98	9	sunflower	Trapani et al. (1992)	
2.61	9	sunflower	Kiniry et al. (1989)	
2.97	9	sunflower	Mastrorilli et al. (1995)	
2.26	10	potato	Shah et al. (2004)	
2.46	10	potato	Haverkort and Harris (1987)	
2.47	10	potato	Kooman et al. (1996)	
2.57	10	potato	Opoku-Ameyaw and Harris (2001)	
3.42	10	potato	Allen and Scott (1980)	extract from Cannell et al. (1987)
4.20	11	cassava	Leepipatpaiboon et al. (2009)	
2.99	12	sugarcane	Muchow et al. (1997)	Kunia, H73-6110
3.18	12	sugarcane	Muchow et al. (1997)	Kunia, H78-7234
3.61	12	sugarcane	Muchow et al. (1997)	Macknade, Q117
3.71	12	sugarcane	Muchow et al. (1997)	Macknade, Q138
4.09	12	sugarcane	Muchow et al. (1997)	Ayr, Q96
4.28	12	sugarcane	Muchow et al. (1997)	Ayr, Q117
2.19	13	sugar beet	Martin (1986a)	
2.47	13	sugar beet	Martin (1986b)	
2.70	13	sugar beet	Clover et al. (2001)	
3.23	13	sugar beet	Scott and Jaggard (1993)	extract from Clover et al. (2001)
3.42	13	sugar beet	Biscoe and Gallagher (1977)	extract from Cannell et al. (1987)
1.90	14	oil palm	Hand et al. (1985)	extract from Cannell et al. (1987)
2.14	14	oil palm	Squire (1990)	chapter 11
3.35	15	Summer Rape	Morrison and Stewart (1995)	
2.28	15	oilseed rape	Mendham et al. (1981)	Justes et al. (2000)
2.22	15	oilseed rape	Justes et al. (2000)	
2.07	16	peanuts	Koizumi et al. (1990)	
2.61	16	peanuts	Bell et al. (1987)	
1.82	17	pigeon pea	Nam et al. (1998)	
2.23	17	mungbean	Muchow et al. (1993)	
2.49	17	cow pea	Muchow et al. (1993)	
2.92	17	pigeon pea	Hughes and Keatinge (1983)	
4.87	17	field beans	Fasheun and Dennett (1982)	
1.48	21	cotton	Pinter et al. (1994)	

1.56	21	cotton 'TamcotCD3H'	Rosenthal and Gerik (1991)	
1.73	21	cotton 'Deltapine 50'	Rosenthal and Gerik (1991)	
1.87	21	cotton	Pinter et al. (1994)	
1.90	21	cotton 'Acala SJ-2'	Rosenthal and Gerik (1991)	
2.14	22	cocoa	Squire (1990)	
1.60	24	olive	Mariscal et al. (2000)	
2.61	25	forage and grain legumes	Charles-Edwards (1982)	extract from Cannell et al. (1987)
3.04	25	lucerne	Brown et al. (2006)	
3.90	25	Italian ryegrass	Koizumi et al. (1990)	
1.52	26	bell pepper	Vieira et al. (2009)	
1.73	26	sweet pepper	del Amor and Gomez-Lopez (2009)	
2.26	26	fibre hemp	Meijer et al. (1995)	
2.38	26	Garlic	Rizzalli et al. (2002)	
2.54	26	Oat	Muurinen and Peltonen-Sainio (2006)	
3.18	26	Quinoas	Ruiz and Bertero (2008)	
3.44	26	Garlic	Rizzalli et al. (2002)	
4.16	26	Lettuce	Hand et al. (1985)	extract from Cannell et al. (1987)
2.09	26	Chrysanthemum	Charles-Edwards (1982)	extract from Cannell et al. (1987)

Table 3.2. Rotation history of the eddy covariance flux sites used in our study.

site ID	Country	latitude	longitude	crop type	period (yy-mm)	PI / references
BE_Lon	Belgium	50.5522	4.74494	sugar beet winter wheat potato	2004-04, 2004-09 2004-10, 2005-09 2006-10, 2006-12 2005-10, 2006-04	Aubinet et al. (2009); Moors et al. (2010)
CN_Du1	China	42.0456	116.671	wheat	2005-05, 2005-09	Chen et al. (2009)
DE_Geb	Germany	51.1001	10.9143	rapeseed winter barley sugar beet	2003-08, 2004-08 2004-09, 2005-07 2005-11, 2006-09	Kutsch et al. (2010); Moors et al. (2010)
DE_Kli	Germany	50.8929	13.5225	rapeseed winter wheat	2004-09, 2005-08 2005-10, 2006-09	Christian Bernhofer

DK_Ris	Denmark	55.5303	12.0972	winter wheat	2004-01, 2005-12	Henrik Soegaard; Ceschia et al. (2010); Moors et al. (2010)
ES_ES2	Spain	39.2755	-0.31522	rice	2004-05, 2004-09 2005-05, 2005-09 2006-05, 2006-09	Maria Jose Sanz; Moors et al. (2010); Kutsch et al. (2010); Ceschia et al. (2010)
FR_Gri	France	48.844	1.95243	wheat	2005-11, 2006-07	Pierre Cellier
IE_Ca1	Ireland	52.8588	-6.91814	spring barley	2004-03, 2004-07 2005-03, 2005-07 2006-03, 2006-07	Mike Jones; Ceschia et al. (2010); Moors et al. (2010)
JP_Mas	Japan	36.05397	140.0269	rice	2002-05, 2002-09 2003-05, 2003-09	Akira Miyata
NL_Lan	Netherlands	51.9536	4.9029	maize	2005-06, 2005-10	Eddy Moors; Moors et al. (2010);
US_ARM	USA	36.6058	-97.4888	wheat	2003-01, 2003-07 2003-09, 2004-06	Marc Fischer Fischer et al. (2007)
US_Bo1	USA	40.0062	-88.2904	maize soybean	2001-05, 2001-10 2003-05, 2003-10 2005-05, 2005-10 2000-05, 2000-10 2002-05, 2002-10 2004-05, 2004-10 2006-05, 2006-10	Meyers and Hollinger, (2004); Meyers et al. (2006)
US_Bo2	USA	40.009	-88.29	maize soybean	2004-05, 2004-10 2006-05, 2006-10 2005-05, 2005-10	Carl Bernacchi
US_Ne1	USA	41.1651	-96.4766	maize	2001-06, 2001-10 2002-06, 2002-09 2003-06, 2003-10 2004-06, 2004-10	Shashi Verma; Verma et al. (2005)
US_Ne2	USA	41.1649	-96.4701	maize soybean	2001-05, 2001-10 2003-05, 2003-10 2002-06, 2002-10 2004-06, 2004-10	Shashi Verma; Verma et al. (2005)
US_Ne3	USA	41.1797	-96.4397	maize soybean	2001-05, 2001-10 2003-05, 2003-10 2002-06, 2002-10 2004-06, 2004-10	Shashi Verma; Verma et al. (2005)

3.3 Results

3.3.1 Light use efficiency ε^*_{GPP}

The direct estimates of ε^*_{GPP} using FLUXNET crop sites are listed in Table 3.3. At these sites, the ratios between modelled and observed GPP varied between 0.86 and 1.23 and were on average 1.04±0.08 (standard deviation). The corresponding correlation coefficients of monthly modelled and observed GPP over each site were on average 0.85±0.14 (standard deviation). We summarized these measured ε^*_{GPP} and the ones derived from the literature for the 26 crop types in MIRCA2000 in Table 3.4. 8 of 26 crop types were directly calculated in this paper, covering 55% of the global cropland areas (Portmann et al., 2010). FLUXNET-based ε^*_{GPP} varied between crop types with potato having the lowest value (1.5 g C MJ^{-1}) and maize having the highest (2.84 g C MJ^{-1}). Our estimates and those of previous studies (Lobell et al., 2002; Chen et al., 2011; Table 3.1) thus confirm a higher LUE value for maize than most other crops. On average our ε^*_{GPP} values are higher than those used in Zhao and Running (2010) (i.e. 1.044 g C MJ^{-1}) and the default values in CASA model (i.e. 1 g C MJ^{-1}), but are still within the range of values reported based on site measurements previously (e.g. Lobell et al., 2002; Table 3.1).

As shown in Fig. 3.1a, our direct estimates are generally lower than the literature based values. We prefer to use our directly estimates based on FLUXNET measurements because this enables us to upscale our site level results to large domains using identical JRC fPAR data. To harmonize our ε^*_{GPP} values, a linear regression was calculated when both FLUXNET and literature based ε^*_{GPP} were available (Fig. 3.1b). The linear relation was applied to generate the ε^*_{GPP} for the crop types that were not included in FLUXNET based ε^*_{GPP} as:

$$\varepsilon^*_{GPP\_FLUXNET} = 0.6757 \times \varepsilon^*_{GPP\_literature} + 0.1252 \quad (3.4)$$

Because ε^*_{GPP} should be always larger than zero, we kept the physically unrealistic offset (i.e. 0.1252) to best preserve the relation within the range of estimates. For 5 crop types we had neither FLUXNET nor literature values available. For rye the same ε^*_{GPP} of wheat was assigned because rye is a member of wheat tribe. The other 4 types (citrus, date palm, grapes and coffee) were all assigned 1.2 g C MJ^{-1}. This value is close to the lowest value of our estimates for other perennial crops (1.21 g C MJ^{-1}) and to the values used by Zhao and Running (2010).

Table 3.3. Statistics of GPP_{CASA} to $GPP_{FLUXNET}$ relation and ε^*_{GPP} estimates at FLUXNET sites.

site code	crop types	correlation coefficient	standard deviation[1]	centered RMSE[1]	GPP_{CASA}/ $GPP_{FLUXNET}$	ε^*_{GPP} (g C MJ^{-1})
BE_Lon	Sugarbeet	0.47	0.46	0.88	1.00	2.90
	Winterwheat	0.72	0.75	0.69	0.95	2.40
	Potato	0.98	0.39	0.61	1.12	1.50
CN_Du1	Wheat	0.83	0.56	0.62	1.10	1.65
DE_Geb	Rapeseed	0.94	0.89	0.36	1.04	2.30
	Winter Barley	0.72	0.79	0.70	0.86	1.55
	Sugarbeet	0.90	0.84	0.43	1.23	1.00
DE_Kli	Rapeseed	0.81	0.87	0.59	0.94	1.80
	Winter Wheat	0.95	0.83	0.33	1.20	2.45
DK_Ris	Winter Wheat	0.92	0.98	0.41	0.95	2.25
ES_ES2	Rice	0.94	0.94	0.33	1.01	2.90
FR_Gri	Winter Wheat	0.92	0.93	0.40	0.96	2.80
IE_Ca1	Spring Barley	0.83	0.66	0.58	1.09	1.90
JP_Mas	Rice	0.90	0.53	0.57	1.07	2.60
NL_Lan	Maize	0.47	0.52	0.88	1.00	2.35
US_AR	Wheat	0.96	1.02	0.30	0.94	1.25
US_Bo1	Soybean	0.87	0.75	0.51	1.12	1.55
	Maize	0.96	0.85	0.31	1.06	2.00
US_Bo2	Maize	0.99	0.87	0.16	1.09	2.90
	Soybean	0.96	0.85	0.29	1.07	1.45
US_Ne1	Maize	0.90	0.61	0.53	1.11	2.95
US_Ne2	Maize	0.92	0.71	0.45	1.10	3.45
	Soybean	0.79	0.63	0.63	1.07	1.75
US_Ne3	Maize	0.84	0.65	0.58	1.10	3.40
	Soybean	0.74	0.64	0.68	1.03	1.80

[1] both modelled standard deviation and centered RMSE were nondimensionalized by dividing the standard deviation of the corresponding observation. More details are in section 3.2 of Taylor (2001)

Table 3.4. ε^*_{GPP} used in our study and global cropland GPP estimates for various crop types.

ID	crop types	$\varepsilon^*_{GPP\_FLUXNET}$ ±std	$\varepsilon^*_{GPP\_literature}$ ±std	$\varepsilon^*_{GPP\_regress}$	$\varepsilon^*_{GPP\_model}$	GPP (Pg C yr^{-1})
1	Wheat	2.13±0.57	2.92±0.45	2.10	2.13	1.384
2	Maize	2.84±0.57	4.07±0.58	2.87	2.84	1.545
3	Rice	2.75±0.21	2.79±0.28	2.01	2.75	1.514
4	Barley	1.73±0.25	2.88±0.46	2.07	1.73	0.260
5	Rye				2.13	0.109
6	Millet		3.52±0.48	2.51	2.51	0.134
7	Sorghum		4.01±0.66	2.83	2.83	0.272
8	Soybeans	1.64±0.17	2.36±0.46	1.72	1.64	0.491
9	Sunflower		2.52±0.50	1.83	1.83	0.112
10	Potatoes	1.50	2.63±0.45	1.91	1.50	0.091
11	Cassava		4.20	2.96	2.96	0.612
12	Sugar cane		3.64±0.50	2.59	2.59	0.494
13	Sugar beet	1.95±1.34	2.80±0.52	2.02	1.95	0.040
14	Oil palm		2.02±0.17	1.49	1.49	0.210
15	Rape seed	2.05±0.35	2.62±0.64	1.89	2.05	0.115
16	Groundnuts		2.34±0.38	1.71	1.71	0.105
17	Pulses		2.87±1.19	2.06	2.06	0.353
18	Citrus				1.2	0.064
19	Date palm				1.2	0.001
20	Grapes				1.2	0.041
21	Cotton		1.71±0.19	1.28	1.28	0.123
22	Cocoa		2.14	1.57	1.57	0.132
23	Coffee				1.2	0.158
24	Others perennial		1.60	1.21	1.21	0.795
25	Fodder grasses		3.18±0.65	2.28	2.28	1.389
26	Others annual.		2.59±0.85	1.87	1.87	0.508
	global					11.050

3.3.2 Global cropland monthly GPP in the year 2000

We calculated monthly GPP for these 26 crop types at 5 arc min resolution for the year 2000, the only year for which the cropland distribution was available (Portmann et al., 2010). Global annual GPP amounts for each crop type as well as for all cropland combined are listed in Table 3.4. The annual global cropland GPP was 11.05 Pg C yr^{-1} in the year 2000. This estimate was in between the 8.2 Pg C yr^{-1} and 14.8 Pg C yr^{-1} reported previous by Beer et al. (2010) and Saugier et al. (2001), respectively. Maize, rice and wheat had the 3 highest GPP values for grains, contributing 40% of the global cropland GPP. Fodder grasses are the most important crop type that is not grain and ranked third in all crops. The 8 crop types where GPP was calculated using ε^*_{GPP} based on FLUXNET sites contributed 49% of the global cropland GPP.

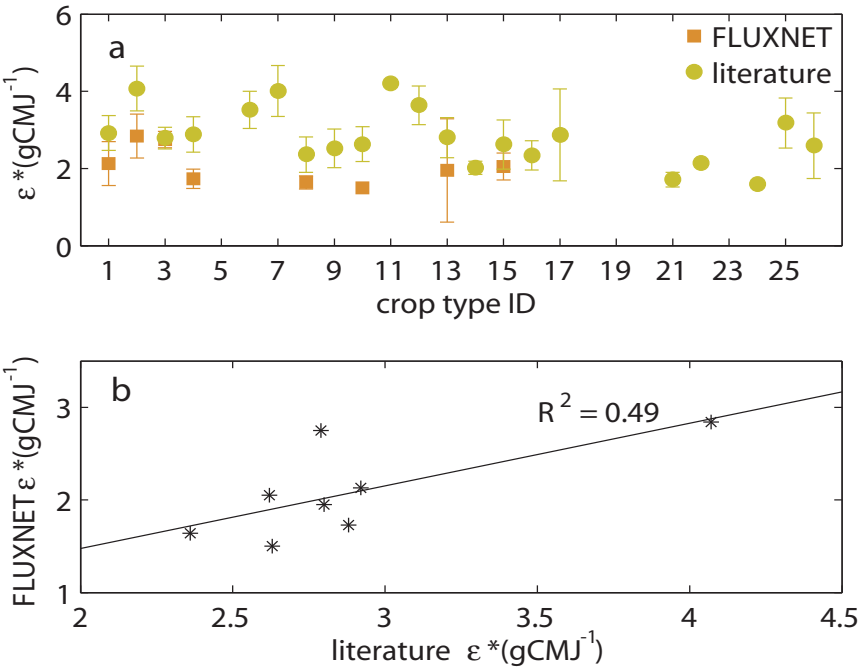

Figure 3.1. Maximum light use efficiency (ε^*_{GPP} in g C MJ^{-1}) for a) different crop types based on FLUXNET and literature with error bars representing two standard deviations of ε^*_{GPP}. Crop type ID value refers Table 3.4. b) Linear relation between FLUXNET based and literature based ε^*_{GPP} estimations for 8 crop types listed in Table 3.4.

Figure 3.2 illustrates the global spatial distribution of annual global cropland GPP. High GPP regions extend mostly in the warm humid or semi-humid plains of the northern hemisphere, such as the central and eastern part of United States, Europe, the eastern plain of China and the Ganges plain of South Asia. Per unit area, tropical regions had the highest GPP, such as in the lower reaches of the Ganges River over the contiguous areas of India and Bangladesh, and the lower reaches of the Niger River in Nigeria.

Asia produced over one third of global cropland GPP, which is more than two times that of any other continents (Table 3.5). Within the 26 types, rice contributed the most (1336.3 Tg C yr^{-1}) to the annual GPP in Asia. GPP of rice in Asia contributed 88.3% of global rice GPP. North America and Europe accounted for respectively 16.6% and 16.2% of the global cropland GPP. The United States is the main producer of maize and soybean in the world, and this is reflected in the proportion of maize and soybean (Table 3.5). Africa was the fourth most important region (13.5%) with the most cassava GPP (57.9%) of the world. Annual cropland GPP in South America (12.8%) was very close to that of Africa. Maize and soybean contributed most to the cropland GPP in South America (Table 3.5). The cropland GPP in Oceania was the lowest of the continents, due to the small areas of croplands.

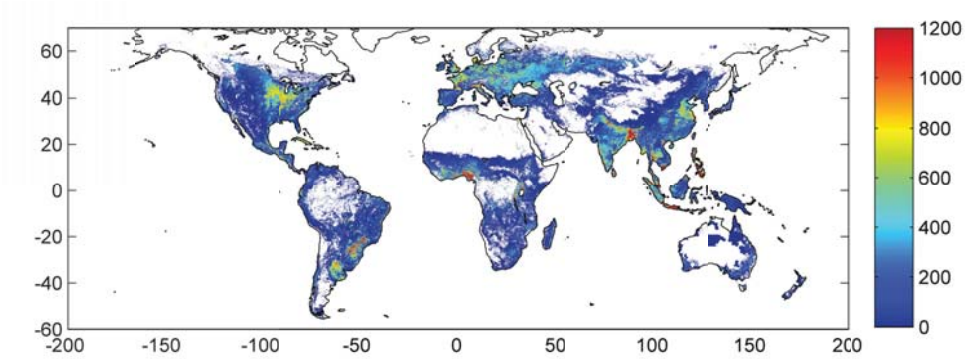

Figure 3.2. Spatial distribution of annual GPP flux (g C m^{-2} yr^{-1}) for each 5 arc min grid cell in the year 2000 with values capped at 1200 g C m^{-2} yr^{-1}. The range of the color bar was chose for visual purpose. Annual GPP flux values of some grid cells in the tropics are larger than 2000 g C m^{-2} yr^{-1}.

3.4 Discussion

3.4.1 Model performance

After the initial development of the LUE approach (Monteith, 1972; Monteith and Moss, 1977) to estimate ecosystem production (GPP or NPP), considerable efforts have been made to evaluate ε to meet the need of the model parameterizations. We chose to estimate ε^*_{GPP} directly by combining FLUXNET measurements and JRC fPAR, the same vegetation index as we used in our model. Our estimates of ε^*_{GPP} are within the range reported previously by field measurements (Table 3.1, 3.3 and 3.4). In our model we treated the directly estimated ε^*_{GPP} as superior to the literature based values. On average, the ε^*_{GPP} values based on biomass (dry matter) measurements are higher than our estimates based on FLUXNET observations. Therefore, we adjusted the literature-based ε^*_{GPP} values using ratios between the FLUXNET and literature based estimates when available. The ε^*_{GPP} values finally used in our model are therefore higher than those used in other models (Zhao and Running, 2010; Lobell et al., 2002; Field et al., 1995; Potter et al., 1993). A look-up table of ε^*_{GPP} for 26 crop types was created, offering

a much more sophisticated parameters of the LUE empirical models than previous studies.

Table 3.5. Annual GPP (Tg C yr^{-1}) for different regions in the year 2000.

Crop types	North America[1]	South America	Europe[2]	Asia	Africa	Oceania
Wheat	196.4	87.5	481.6	525.4	35.4	58.2
Maize	504.2	277.2	204.6	342.6	215.5	1.0
Rice	22.0	78.1	3.6	1336.3	73.2	0.9
Barley	24.5	5.5	149.4	55.0	9.9	16.2
Rye	1.7	0.7	98.4	7.2	0.4	0.2
Millet	0.9	0.3	3.6	62.7	65.9	0.2
Sorghum	54.1	28.3	1.4	70.4	112.0	5.6
Soybeans	215.1	198.2	5.5	65.8	5.9	0.2
Sunflower	9.3	24.4	53.7	19.2	4.5	0.5
Potatoes	3.9	5.1	49.3	28.6	3.8	0.3
Cassava	9.9	103.9	0.0	143.6	354.4	0.8
Sugar cane	85.2	180.8	0.0	186.8	30.4	11.0
Sugar beet	3.0	0.3	32.0	3.8	0.4	0.0
Oil palm	2.6	6.9	0.0	138.0	60.8	2.1
Rape seed	16.2	0.4	36.6	56.4	0.1	5.4
Groundnuts	6.5	3.8	0.1	55.4	39.4	0.2
Pulses	29.8	54.4	25.7	143.8	92.5	6.6
Citrus	12.3	18.8	3.3	18.9	10.2	0.3
Date palm	0.0	0.0	0.0	0.6	0.8	0.0
Grapes	2.5	3.4	27.2	6.0	1.2	1.0
Cotton	31.6	11.9	1.5	54.2	21.3	2.2
Cocoa	6.2	28.7	0.0	14.2	80.3	2.9
Coffee	33.2	56.2	0.0	36.0	30.7	1.6
Others perennial	34.2	64.7	55.9	505.1	121.1	14.3
Fodder grasses	494.5	135.6	504.2	205.3	26.0	24.2
Others annual.	31.9	37.2	117.7	215.6	95.8	9.5
Total	1831.7	1412.1	1855.4	4297.0	1492.0	165.5
Percent (%)	16.6	12.8	16.8	38.9	13.5	1.5

[1]North America includes Central America. [2]Europe does not contain Russia east of the Ural.

Global cropland GPP was estimated to be 11.05 Pg C yr^{-1}, which is within the range of previous studies (Beer et al., 2010; Saugier et al., 2001). Several model studies found that ε^*_{GPP} or ε^*_{NPP} values based on site measurements could not be used in models directly because this would lead to excessively high cropland GPP values (Lobell et al., 2002; Potter et al., 1993). For example, a value of 0.5 g C MJ^{-1} for ε^*_{NPP} was initially used in CASA (Potter et al., 1993). Because if ε^*_{NPP} was set 1.25 g C MJ^{-1} as Heimann and Keeling (1989) did, annual NPP would be an unrealistic 185 Pg C yr^{-1} (Potter et al., 1993).

Even if we double 0.5 g C MJ^{-1} number to account for the GPP/NPP ratio of about 2, the value is much below the ε^*_{NPP} values in our study.

The difference between in-situ measurements of ε^*_{GPP} and the values used in models may reflect model structural biases which have to be compensated for by adjusting parameters. Therefore, we echo the findings of Lobell et al. (2002) who used both CASA and harvest records. Cropland NPP for continental United States (excluding Alaska and Hawaii) was estimated to be 0.62 Pg C yr^{-1}, or 1.24 Pg C yr^{-1} GPP by doubling NPP (Lobell et al., 2002). ε^*_{NPP} in Lobell et al. (2002) was estimated by constraining the model results with harvest data based NPP across each county. In our estimations, GPP in United States was 1.28 Pg C yr^{-1} which is very close to the value obtained in Lobell et al. (2002). However, the ε^*_{GPP} values in Lobell et al. (2002) by doubling ε^*_{NPP} are still much smaller than the values we used here. There is therefore no conflict between field based ε^*_{GPP} and the direct parameterization application in our model. The main distinction between the current and previous studies are the two main innovations of our study: 1) we use cropland areas distribution data to define the cropland types by month in order to distinguish the growing and fallow periods; 2) we assigned the 26 crops each a different ε^*_{GPP} value.

Compared with natural ecosystems, usually croplands have three important distinct features which influence their carbon exchange. First, the plant types are much more homogeneous than natural ecosystems due to management practice of farmers. Second, the plant types change much faster than natural ecosystems due to crop rotation schemes used, which means the land cover type does not uniquely determine plant types as in more natural ecosystems. Third, planting, ploughing and harvesting activities change the ecosystems in croplands abruptly and leave land fallow for long periods, sometimes even in the growing season. Therefore, croplands distributions from survey data are the only option to separate crop rotation and planting times fully at present. However, the spatial resolution of this data is still larger than a single field, implying that one cell still contains several crop yields and types. These crops have different light use efficiencies in reality but are treated in models with the same vegetation index and environmental factors.

3.4.2 Uncertainties

Current global scale estimates of gross primary production (GPP) are still subject to large uncertainties (Beer et al., 2010; Koffi et al., 2012), although GPP is the largest flux of the terrestrial carbon cycle. Usually, model structure and input data are the main sources of these uncertainties (Jung et al., 2007). Previous studies have also demonstrated that it is difficult to quantify these uncertainties accurately, but that they rather quantify the sensitivity of model results to various sources (June et al., 2007; Zhao et al., 2006). In this section, the current state of global GPP estimates and the uncertainties of the datasets created in this thesis will be addressed.

Due to the large variability of plant species and growth, existing direct observational data are still far from sufficient to generate an accurate GPP estimate alone. Therefore, although photosynthesis processes at leaf level have been well known, current global GPP estimates rely very much on model and observation-model fusion methods or other proxy datasets (Field et al., 1995; Knorr and Heimann, 1995; Potter et al., 1993; Ruimy et al., 1994; Zhao et al., 2005; Ryu et al., 2011; Koffi et al., 2012; Beer et al., 2010; Suntharalingam et al., 2008; Welp et al., 2011).

Several independent methods have been developed to estimate global GPP. GPP can be roughly estimated by doubling NPP because autotrophic respiration (R_a) is suggested to usually take up about half of GPP (Waring et al., 1998), but with large changes across plant types and sites (Litton et al., 2007; DeLucia et al., 2007; Luyssaert et al., 2007). NPP can be estimated by measuring above ground dry matter or total dry matter in field. Particularly for croplands, harvested data are also found to be well linked to NPP (Haberl et al., 2007; Monfreda et al., 2008; Lobell et al., 2002). Therefore, doubling NPP acts as an indirect way to infer GPP. The biochemical processes of photosynthesis will change some isotope concentrations in the atmosphere, modifying the atmospheric ^{18}O and ^{16}O ratios ($^{18}O/^{16}O$) in a measureable way. Several studies have demonstrated the usage of $^{18}O/^{16}O$ in these GPP estimations (Ciais et al., 1997; Farquhar et al., 1993 nature; Welp et al., 2011). GPP calculated from on $^{18}O/^{16}O$ ranges from 150-175 Pg C yr^{-1} based on the latest results (Welp et al., 2011). Carbonyl sulphide (OCS) is also absorbed by plants during the photosynthesis processes when CO_2 is being taken up by ecosystems, which could be further used to constraint terrestrial GPP (Suntharalingam et al., 2008; Asaf et al., 2013).

Flux towers based eddy covariance methods offer directly field measurements of the CO_2 flux between atmosphere and terrestrial ecosystems, which can then be further converted to GPP and ecosystem respiration (Lasslop et al., 2010; Reichstein et al., 2005). After decades of developments, more than one thousand flux towers have been established worldwide. From these and using additional, primarily satellite data sources, Beer et al., 2010 estimated global GPP 123±8 Pg C yr^{-1} by combining FLUXNET measurements and several models. Although this number was questioned by Welp et al. (2011) as mentioned above, 123 Pg C yr^{-1} is still treated as a benchmark in several studies (Bonan et al., 2011; Chen et al., 2012).

Importantly, most of the studies listed above only can be used to estimate annual mean of global GPP, which is still subject to large uncertainties. Temporal continuously and spatially specified GPP is usually the first step in terrestrial carbon cycle calculated in models. The LUE method used here (Monteith, 1972; Monteith and Moss, 1977) is an empirical approach. Therefore, besides input data and model structure, the look-up table of the key parameter (i.e. ε^*_{GPP}) also contributes considerably to the uncertainties. As shown in equation 3.1, PAR, fPAR, temperature and precipitation are the main forcing datasets. PAR, temperature and precipitation are meteorological variables, describing the environmental stresses in the equation. GPP is very sensitive to PAR in a linear way.

Temperature and precipitation is the main meteorological drivers, which were found impact models results significantly, especially interannual variations of GPP (Jung et al., 2007). For example, using MOD17 algorithm which is also based on LUE method, Zhao et al. (2006) found that different reanalysis data sets could infer over 20 Pg C yr^{-1} bias of global GPP. Only the relative importance could be evaluated and it is hard to reduce biases from meteorological inputs. Therefore, choosing widely used and well evaluated meteorological data sets is ultimately important.

Besides meteorological variables, vegetation monitoring data sets exhibited large biases across different data sets. A large difference was demonstrated after comparing four well-known fPAR data sets (McCallum et al., 2010). Only croplands were analyzed in this thesis, and fortunately, which exhibit the highest agreement across fPAR data sets (McCallum et al., 2010). As discussed above, in this study ε^*_{GPP} values were calculated first using same fPAR data at site level. Therefore, fPAR data set and ε^*_{GPP} values are closely related, which means the bias using different fPAR data sets were partly reduced by ε^*_{GPP} evaluations. In other words, fPAR should be coherent at site level for ε^*_{GPP} parameter calculations and at large scale for GPP modelling. This strategy is similar to previous studies, such as when ε^*_{NPP} was reset from 0.39 g C MJ^{-1} PAR using fPAR to 0.55 g C MJ^{-1} PAR using EVI (enhanced vegetation index) in a variant of CASA (Potter et al., 2007).

LUE is an empirical method, requiring well evaluated look-up table of ε^*_{GPP}. Current look-up table of ε^*_{GPP} for these 26 crop types are still far from accurate. At site level, biases in ε^*_{GPP} calculations were constrained by data quality of tower measurements, the overlap of remote sensed fPAR pixel and tower footprint. At current, ε^*_{GPP} only represents the annual mean of the linear relationship between the terms in equation 3.1. This implies that monthly biases integrated are much larger than those at annual timescales. ε^*_{GPP} values based on flux tower measurements were treated as the reference here to convert literature based ε^*_{GPP} to generate the final look-up table. Unfortunately, previous studies lacked uniformity in field measurements. A conversion equation was thus created (equation 3.4), which of course implicitly relies on a set of assumptions.

The use of 26 different ε^*_{GPP} for these crop types is the innovative aspect of this study compared with previous studies. Measurements constrained ε^*_{GPP} of each crop type have a range as shown in Table 3.4. Thus only the mean values were chosen to drive the model, generating uncertainties in two ways. Biases of regional GPP estimates would be relative larger than that of global. The mean value of ε^*_{GPP} used in the model may also different with the theoretical accurate value. Usually enlarging the number of evaluation sites leads to more accurate estimates. Compared to previous studies, it is assured that the use of 26 ε^*_{GPP} will reduce the biases in spatial distribution of croplands GPP because more plant specified information is considered. For example, as a C_4 plant, ε^*_{GPP} of maize is much larger than most other crops. If only one value of ε^*_{GPP} was assigned for all crops, the crop GPP in the region where maize is the dominating plant will be under-estimated.

Therefore, although large uncertainties are still involved in global crop land GPP data set from vary sources, improvements were obtained in spatial details and plant specified contributions.

3.5 Conclusions

In this paper, we estimated global cropland GPP using a LUE model with improved input data and parameterization of ε^*_{GPP}. 26 crop types were separated in our model with different ε^*_{GPP} values compared to the previously default parameterization with a constant ε^*_{GPP} for all crop types. To meet the parameterization requirements, we evaluated ε^*_{GPP} based on FLUXNET data for 8 crop types. We also performed a literature survey and gathered 89 ε^*_{GPP} values that met our requirements necessary to harmonize these values. Our FLUXNET based ε^*_{GPP} values are within the range of previous studies but are higher than those usually used in LUE models. Finally, a look-up table of ε^*_{GPP} for the 26 crop types was created based on measurements.

ε^*_{GPP} (assumed equal to 2 times ε^*_{NPP}) based on field measurements and the values used in vegetation models differ widely, as discussed by Potter et al. (1993), Ruimy et al. (1994) and Lobell et al. (2002). Our previous work (Chen et al., 2011) also highlighted the need to improve the LUE parameterization in vegetation models. In this study, we estimated global cropland annual GPP at 11.05 Pg C yr^{-1} using field based ε^*_{GPP}. This in the middle of previous studies indicated 14.2 Pg C yr^{-1} by Beer et al. (2010) and 8.2 Pg C yr^{-1} by Saugier et al (2001). GPP in United State was estimated to be 1.28 Pg C yr^{-1}, close to the 1.24 Pg C yr^{-1} reported by Lobell et al. (2002). Our results demonstrate a successful usage of directly estimated ε^*_{GPP} in a LUE approach based vegetation model. Our improvements, separating croplands which are generally treated as one biome in global models into different plant types with corresponding spatial distribution and using more specific ε^*_{GPP} values for each types, may lead to more realistic cropland GPP estimates.

Chapter 4 A global analysis of the impact of drought on net primary productivity[3]

Abstract

We investigated the impact of drought on interannual variability of net primary productivity (NPP) from 1997 to 2009 using the standardized precipitation evapotranspiration index (SPEI) drought index and satellite-derived vegetation greenness converted to NPP. SPEI is positive for wet conditions and negative for dry conditions. We found that SPEI and NPP were coupled and showed in-phase behaviour on a global scale. We then used the Köppen climate classification to study the SPEI-NPP relations regionally and found that while NPP and SPEI were positively related (high SPEI, high NPP) in arid and in seasonal dry regions, the opposite occurs in most boreal regions (high SPEI, low NPP). High intensity drought events, such as the 2003 drought in Europe were picked up by our analysis. Our findings suggest that the strong positive relation between global average moisture availability and NPP consists of a composite of the positive relation across dry regions and the coherent NPP decline during and after intensive drought events in humid regions. Importantly, we also found that there are many areas on the globe that show no strong correlation between drought and NPP.

4.1 Introduction

Terrestrial ecosystems constitute a substantial CO_2 sink, currently in the order of a quarter of emissions from fossil fuels and deforestation (Le Quéré et al., 2009). They exhibit considerable interannual variability, which is to a large extent reflected in the variability of the mean global atmospheric CO_2 growth rate (Knorr et al., 2007; Le Quéré et al., 2009; Zhao and Running, 2010). Zhao and Running (2010) suggested a strong correlation between the occurrence of global drought and NPP (Net Primary Production) using the Moderate Resolution Imaging Spectroradiometer (MODIS) NPP algorithm and the Palmer Drought Severity Index (PDSI) as a proxy for soil moisture.

Extreme droughts can impact the terrestrial productivity in a significant way and reduce the sink strength at (sub) continental scale (Ciais et al., 2005; Reichstein et al., 2007a; van der Molen et al., 2011). Several recent droughts, such as those in Australia (2002-2009), Europe (2003), and Amazonia (2005, 2010) have had a clear detectable impact on plant productivity (Gobron et al., 2010; Zhao and Running, 2010). Since the occurrence and severity of droughts is likely to increase in the near future as a result of global warming (Dai, 2013, but see also Sheffield et al., 2012), there is a clear need to

[3] This chapter is based on Chen, T., van der Werf, G. R., de Jeu, R. A. M., Wang, G., and Dolman, A. J.: A global analysis of the impact of drought on net primary productivity, Hydrol. Earth Syst. Sci., 17, 3885-3894, DOI: 10.5194/hess-17-3885-2013, 2013.

understand whether the global average results found by Zhao and Running (2010) also apply at smaller spatial scales, and perhaps arguably more important, whether at the level and scale of biomes and climate zones different relationships occur.

Droughts have traditionally been described based on their intensity, duration and spatial extent, or a mixture of this. Precipitation anomalies are often used as a proxy because precipitation is the main water source to the soils. However, the local water balance also depends on evaporation, soil moisture storage, and runoff. Compared with precipitation, drought indices have the advantage that they quantitatively describe both the character of drought events and long term variations in the mean dry and wet conditions. Furthermore, drought indices have significant advantages over precipitation in analytical applications, as they address the potential impacts much more explicitly, for instance by taking into account the duration and cumulative severity. However Sheffield et al. (2012) also point out that care has to be exercised when extrapolating drought indices that are not based on a full physical description of the relevant processes. While recently remotely sensed soil moisture data have become available for 30 years (Dorigo et al., 2012; Liu et al., 2012), these data unfortunately suffer sometimes from gaps in the time series and refer in principle only to the first few, variable centimetres of the soil, making their global application in drought studies not yet straight forward.

The previously mentioned drought-vegetation studies generally suggest that at the global scale relationships exist that hide the underlying composite of several regional responses at smaller spatial scales. Importantly then, not only meteorological variability plays a role, but also the general sensitivity or adaptation of the vegetation to drought stresses. Savannah vegetation for instance is likely to be more adapted to periodic drought than a temperate forest that experiences a drought only once in a few years. This calls for the inclusion of biome or vegetation information in the drought-carbon impact analysis. We use here a combination of the Köppen climate classification together with a CASA (Carnegie-Ames-Stanford-Approach; Potter et al., 1993; van der Werf et al., 2010) derived NPP and the SPEI (standardized precipitation evapotranspiration index; Vicente-Serrano et al., 2010) drought index to investigate this variability. By doing so, we aim to improve the understanding of the relation of drought with vegetation and also detect whether our hypothesis of regionally varying responses is correct.

By using the SPEI index, we believe to have made the appropriate choice to study drought in a more meaningful way than with for instance the PDSI, or other static drought indices. As demonstrated by Heim (2002), over 10 different drought indices have been developed during the twentieth century, of which SPI (standardized precipitation index; McKee et al., 1993) and PDSI are the most widely used (Ji and Peters, 2003; Lotsch et al., 2003; Rhee et al., 2010). PDSI is more physical based but SPI is easy to calculate and has different time scales. This time scale characteristic of SPI is very important to represent different kinds of droughts (McKee et al., 1993). The World Meteorological Organization (WMO) has recommended SPI as the standard drought

index. Recently, the SPEI was generated, which relies on a similar algorithm as SPI but including temperature to calculate potential evapotranspiration. Therefore, SPEI combines the advantages of SPI (different time scales) and PDSI (both precipitation and temperature play a role), and is considered to provide a more meaningful parameter to detect the impact of drought on vegetation (Vicente-Serrano et al., 2013) in consequence. However, following Sheffield et al. (2012) who showed the importance of using a physically based estimate of evaporation in calculating droughts, we use here the SPEI calculated from Penman-Monteith derived estimates of evaporation.

The objective of this study is thus to investigate how anomalous moisture conditions, as estimated by the SPEI, are related to annual changes in NPP on multiple time and space scales across the globe. We choose NPP as an indicator of carbon sensitivity, so as not having to separate several ecosystem level responses of heterotrophic respiration, R versus Gross Primary Production (GPP). We appreciate that respiration is also sensitive to drought and soil moisture, but this field is only just evolving and we did not wish to further complicate matters. We also note that these components are usually calculated in models from NPP. Therefore NPP tends to be more useful for our study than either R or NEE and more directly related to ecosystem carbon use than GPP. We use the CASA biogeochemical model (Potter et al., 1993; van der Werf et al., 2010) to estimate NPP. We specifically aimed to provide more spatial detail than Zhao and Running (2010), as it is to be expected that soil moisture-NPP relations are strongest in arid areas and those with a pronounced dry season. In contrast, in cold and humid regions we do not expect a clear relation. We suspect that the global relations as found by Zhao and Running (2010) may hide this regional detail that could be important for the future behaviour of the carbon cycle. Note, that it is also important to identify those regions where no clear drought NPP relation exist, as this indicates robustness of the carbon cycle to changes in precipitation and soil moisture in these regions.

4.2 Methods

We used the Carnegie-Ames-Stanford-Approach (CASA) biogeochemical model (Potter et al., 1993; van der Werf et al., 2010) on a 0.5° grid with a monthly time step. NPP was calculated by the light use efficiency approach multiplying absorbed photosynthetically active radiation (PAR) and a light use efficiency coefficient, ε (Monteith, 1972; Monteith and Moss, 1977):

$$NPP = PAR \times fPAR \times \varepsilon^* \times f(\varepsilon) \quad (4.1)$$

Where fPAR is the fraction of PAR absorbed by vegetation, f (ε) accounts for environmental stress governed by temperature and moisture. CASA employs a sub-model to calculate the soil moisture balance. The model keeps a running water balance where the main impact of soil moisture on GPP is given by water stress factor (W_ε) which is calculated as W_ε = 0.5 + 0.5*P/PET, where PET is the potential evapotranspiration and P is the precipitation. This equation, though arguably simple,

contains the primary responses of NPP to soil moisture. The factor 0.5 is chosen to incorporate the effect that in the fPAR data used in CASA, a soil moisture effect would also be visible, because fPAR will decrease when the wilting occurs due to the shortage of soil moisture. More details of f (ε) can be found in Potter et al. (1993). ε* was set to 0.5 g C MJ^{-1} PAR globally to match global NPP values of 60 Pg C $year^{-1}$ (Beer et al., 2010). International Satellite Cloud Climatology Project (ISCCP) solar radiation data (Zhang et al., 2004) were used here to generate PAR. fPAR data were calculated based on Normalized Difference Vegetation Index (NDVI) from the Advanced Very High Resolution Radiometer (AVHRR, Tucker et al., 2005) and Moderate Resolution Imaging Spectroradiometer (MODIS) products (Myneni et al., 2002). Precipitation from the Global Precipitation Climatology Project (GPCP) version 1.1 (Huffman et al., 2001) and temperature of the Goddard Institute for Space Sciences (GISS) surface temperature analysis (Hansen et al., 1999) were employed to quantify environmental drivers. Further details are provided by van der Werf et al., (2010).

We use the latest SPEI v2.2 data (available from https://digital.csic.es/handle/10261/72264) in this study. SPEI v2.2 involves CRU TS3.2 monthly gridded temperature and PET. The FAO (Food and Agricultural Organization) grass reference method, a variant of the Penman-Monteith method, is using in the PET calculation. More details of PET calculation and application limitations across vegetation types can be found in Ekström et al. (2007) and Allen et al. (1994). The difference between precipitation (PPT) and PET, as a simplified water balance, was calculated as

$$D = PPT - PET \tag{4.2}$$

D was calculated for each grid cell and month following

$$D_j^k = \sum_{i=0}^{k-1}\left(PPT_{j-i} - PET_{j-i}\right), j \geq k \tag{4.3}$$

Where *k* is time scale, in months. A three-parameter log-logistic distribution was used to model these D series, with the function given by

$$F(x) = [1 + (\frac{\alpha}{x-\gamma})^{\beta}]^{-1} \tag{4.4}$$

where α, β, and γ indicate scale, shape and origin parameters, respectively. This function was chosen as the best distribution function by L-moment ratio diagrams to fit D series (Vicente-Serrano et al., 2010). Finally, SPEI data were calculated by standardizing F(x). More details are provided in Vicente-Serrano et al. (2010).

Table 4.1. List of regions referred to this paper. Abbreviations consist of the first two letters of Köppen climate classification (indicating climate) and two letters to identify the continent or region. For example, AFAF is first group (A, equatorial) humid (F) in Africa (AF).

Abbreviation	Köppen climate classification	continent or region
AFAF	equatorial climates, humid and monsoon (Af, Am)	Africa
AFEA	equatorial climates, humid and monsoon (Af, Am)	Eurasia and north Oceania
AFSA	equatorial climates, humid and monsoon (Af, Am)	Central and South America
AWAF	equatorial climates with winter dry (Aw)	Africa
AWEA	equatorial climates with winter dry (Aw)	Eurasia and north Oceania
AWSA	equatorial climates with winter dry (Aw)	Central and South America
BBAF	arid climates (BWk, BWh, BSk, BSh)	Africa
BBEA	arid climates (BWk, BWh, BSk, BSh)	Eurasia
BBNA	arid climates (BWk, BWh, BSk, BSh)	North America
BBOC	arid climates (BWk, BWh, BSk, BSh)	Oceania
BBSA	arid climates (BWk, BWh, BSk, BSh)	Central and South America
CFAS	temperate climates, humid (Cfa, Cfb, Cfc)	Asian
CFEU	temperate climates, humid (Cfa, Cfb, Cfc)	Europe
CFNA	temperate climates, humid (Cfa, Cfb, Cfc)	North America
CFOC	temperate climates, humid (Cfa, Cfb, Cfc)	Oceania
CFSA	temperate climates, humid (Cfa, Cfb, Cfc)	Central and South America
CSEA	temperate climates with summer dry (Csa, Csb, Csc)	Mediterranean Sea
CWAF	temperate climates with winter dry (Cwa, Cwb, Cwc)	Africa
CWEA	temperate climates with winter dry (Cwa, Cwb, Cwc)	Eurasia
DFEA	cold climates, humid (Dfa, Dfb, Dfc, Dfd)	Eurasia
DFNA	cold climates, humid (Dfa, Dfb, Dfc, Dfd)	North America
DWEA	cold climates with winter dry (Dwa, Dwb, Dwc, Dwd)	Eurasia
ETAT	polar tundra (ET)	Arctic
ETQT	polar tundra (ET)	Eurasia

The response of hydrological systems to moisture deficits varies over time scales. On short time scales surface runoff and soil moisture are of concern while at longer timescales stream flow and ground water levels are important (Changnon and Easterling, 1989). Mathematically, SPEI can be calculated on any time scale, but typical scales used

are 1-, 3-, 6-, 12-, and 24-months. 3-, 5- and 6-month SPI have been used to indicate soil moisture conditions (Hirschi et al., 2011; Ji and Peters, 2003; Lotsch et al., 2003) and 2-3 months SPI may indicate agricultural drought best (Mishra and Desai, 2005). We focused our analysis on 1-, 3-, and 6-month SPEI values to capture variability in soil moisture conditions from surface to deeper rooting depths.

Annual SPEI data were calculated from original monthly SPEI using all months in the year. Pearson correlation coefficients were calculated for the annual NPP vs. 1-, 3-, and 6-month SPEI values. We removed the linear trends from annual NPP and SPEI time series during correlation calculation. To aid the interpretation of our analyses, we divided the global land surface into 24 climate regions across continents based on both geographical location and the Köppen climate classification (Kottek et al., 2006, Fig. 4.1, Table 4.1). We did not combine all regions with an identical climate type across continents to maintain variability due to region-specific meteorological conditions. In the Köppen climate classification, first letters are used to indicate the main climate groups, i.e. group A concerns equatorial climate; group B arid climates; group C temperate climates; group D continental cold climates and group E consists of polar climates. Within the Köppen climate classification, we separated arid, humid and seasonal (summer or winter) dry types besides the five main groups. Only those classes that occupy at least 1% of the global land surface were included in our study with the exception of temperate humid Oceania (CFOC), which is the second largest climate type there.

4.3 Results

Global CASA calculated NPP showed a decreasing trend for the period of 1997-2009, similar to that found by Zhao and Running (2010), but also displayed substantial interannual variation (Fig. 4.2). The global SPEI series exhibited almost the same trend, and showed a similar pattern that appeared well in phase with NPP. On a global scale, for example, dry conditions happened in 2002-2003, 2005 and 2009 with lower NPP and SPEI values. 2004 was a wet year and NPP and SPEI were above average compared to other years. SPEI values changed somewhat when calculated over different time scales, with the maximum range between 1 and 6 month SPEI occurring in 2006. The annual variance of SPEI was increasing from 1 month to 6 months time scales as shown in Fig. 4.2. However, the interannual pattern was robust and the calculated correlation coefficients between NPP and SPEI were 0.55 ($p < 0.1$), 0.51 ($p< 0.1$) and 0.43 for 1-, 3- and 6-month SPEI respectively (Table 4.2). There was a slight declining trend in both SPEI and CASA derived NPP, similar to Zhao and Running (2010), despite adding the years 1997-1999 to the analysis.

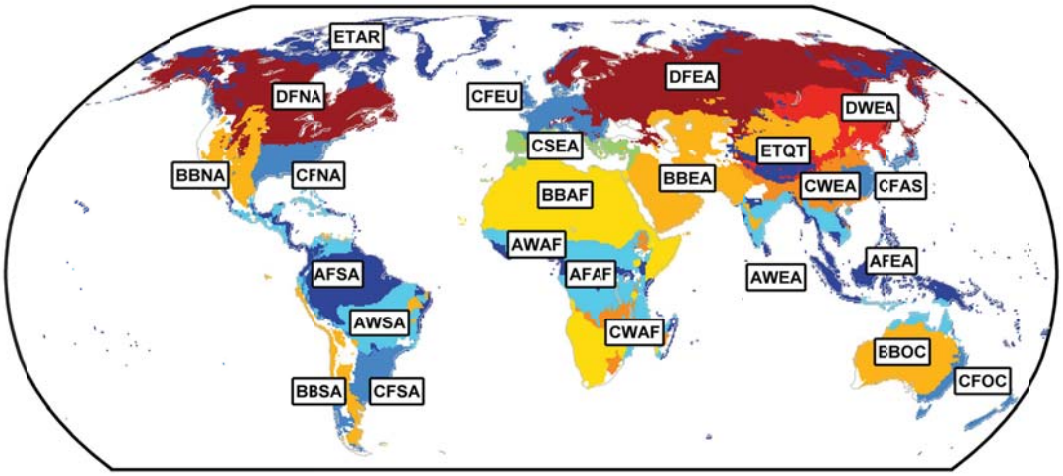

Figure 4.1. Map of 24 regions used in our study. Abbreviations are explained in Table 4.1.

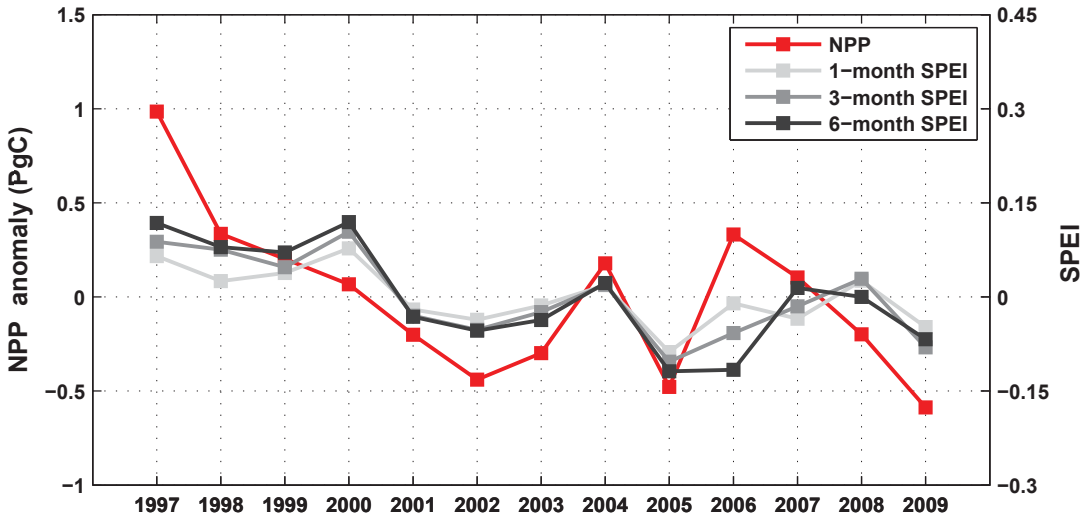

Figure 4.2. Interannual variation in global NPP and SPEI anomalies during 1997-2009. Both NPP and SPEI are area-weighted.

We now proceed to investigate at finer spatial resolution the observed relationships by analysing the correlation between NPP and SPEI at grid cell level. Since the spatial patterns corresponding to 1-, 3-, 6-month SPEI are very similar, we only show the 3-month SPEI-CASA NPP relation (Fig. 4.3). Figure 4.3 illustrates that at 0.5-degree spatial resolution significant positive relations between SPEI and NPP are present. These occur largely at the mid-latitudes of both hemispheres. Significant negative relations were mainly observed in the boreal region. NPP in the Southern hemisphere appeared to be more sensitive to SPEI indicated by high correlation values.

To bring in the vegetation component more explicitly, we now analyze the relationship between SPEI and NPP in more detail using the Köppen climate classification across continents. Compared with the global results of NPP and SPEI, the correlation

coefficients in several regions exhibit much more change with different SPEI time scales, such as the range of 0.57 in cold humid Eurasia (DFEA) (Table 4.2). This implies that the impact of drought on the ecosystems in this area varies with different SPEI time scales, and that NPP is sensitive only to droughts specified by a narrow range of time scales. Significant values occurred at 1 to 3-month scales and the absolute values are much higher than using the 6-month scale, which we suspect is caused by the very short growing period during summer in this region. In contrast, in several other regions, arid South America (BBSA) for example, we observed little change in response when using different time scales (Table 4.2) suggesting that in these cases the vegetation is less sensitive to the precise time scale of the drought.

Complementing Table 4.2, Figure 4.4 shows time series of annual 3-month SPEI and NPP anomalies between 1997 and 2009 for these 24 regions. As expected, NPP and SPEI have similar temporal patterns in arid regions (climate group B, Fig. 4.4g-k), showing significant positive correlation coefficients for the arid regions of North America (BBNA), Eurasian (BBEA), Africa (BBAF) Australia (BBOC) and Central and South America (BBSA). In contrast, NPP and SPEI exhibited out of phase correlations during the whole period in boreal Northern Hemisphere with cold climate (climate group D), i.e. cold-humid North America and North Eurasian (DFNA, DFEA) and cold climates with winter dry North Eurasian (DWEA) as shown in Fig. 4.4t-v.

Table 4.2. Correlation coefficients (R) between annual anomalies of NPP and SPEI for the global and for the 24 regions explained in Table 4.1. Significant values ($p<0.1$) are indicated by *.

SPEI	global	AFAF	AFEA	AFSA	AWAF	AWEA	AWSA	BBAF	BBEA
1	0.55*	0.20	-0.31	0.36	0.91*	0.30	0.79*	0.55*	0.29
2	0.51*	0.34	-0.22	0.30	0.87*	0.56*	0.85*	0.40	0.60*
3	0.43	0.44	0.12	0.34	0.66*	0.67*	0.87*	0.37	0.72*
	BBNA	BBOC	BBSA	CFAS	CFEU	CFNA	CFOC	CFSA	CSEA
1	0.81*	0.74*	0.45	-0.11	0.44	-0.26	0.65*	-0.39	0.30
2	0.86*	0.84*	0.50*	-0.31	0.25	-0.16	0.62*	-0.26	0.41
3	0.93*	0.87*	0.48*	-0.34	0.39	-0.01	0.52*	-0.12	0.58*
	CWAF	CWEA	DFEA	DFNA	DWEA	ETAR	ETQT		
1	0.55*	0.29	-0.68*	-0.46	-0.63*	-0.20	-0.22		
2	0.57*	0.14	-0.53*	-0.48*	-0.63*	-0.26	-0.21		
3	0.45	0.21	-0.11	-0.54*	-0.56*	-0.17	-0.17		

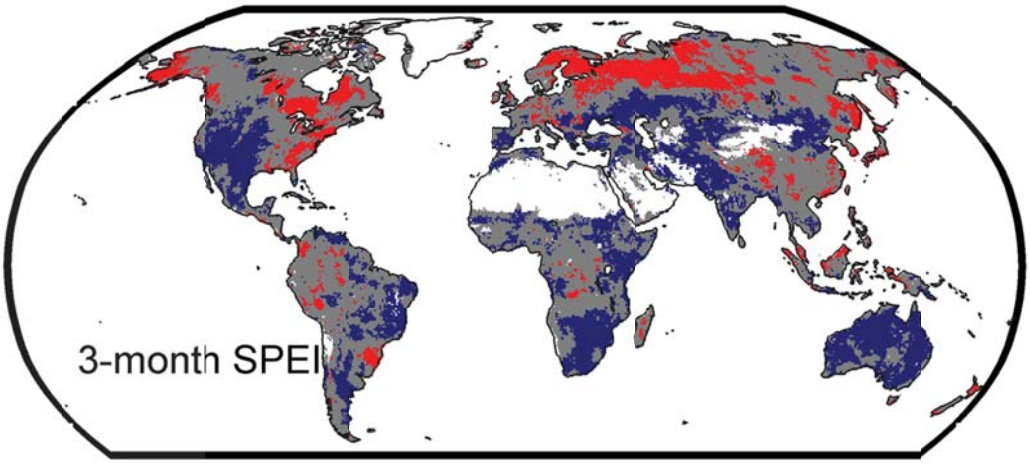

Figure 4.3. Spatial distribution of Pearson's correlation coefficients between annual anomalies of NPP and SPEI (3-months). Correlations that are significant ($p<0.1$) are displayed in blue (positive) and red (negative). Grey areas indicate correlations that are not significant and white areas are not available due to data structure.

Unlike arid and cold regions, other climate zones do not show globally uniform positive or negative patterns. Weak relations are mostly found in temperate humid regions. North America (CFNA), South and Central America (CFSA), Asia (CFAS) and Europe (CFEU) show a mix of both positive and negative correlation coefficients. An exception was Oceania of East Australia and New Zealand (CFOC) where NPP and SPEI had a significant positive relation (Table 4.2).

During 1997-2002 in temperate humid Europe SPEI was in anti-phase (negatively correlated) to NPP (Fig. 4.4m). This suggests that during that period no very strong water limitations were experienced and maybe higher temperatures did lead to more carbon uptake (e.g. Goulden et al., 1996). However, NPP exhibited a sharp decline with SPEI in 2003. In 2003 a severe drought hit Europe during summer and autumn, leading to considerable carbon loss across mid and southern Europe at many ecosystems (Ciais et al., 2005; Reichstein et al., 2007a). Equatorial humid regions show similar behaviour as the temperate humid regions in that they generally have no obvious relation with SPEI (Fig. 4.4a-c, Table 4.2). It is worth noting the absence of these relations, as this suggests that at least for the currently available variability in precipitation, these regions are relatively robust in their NPP. We will discuss this issue further in the discussion.

The regions that have seasonally occurring dry periods including summer or winter dry periods are those in middle latitude and equatorial zones. However, as expected, all the winter dry equatorial regions (AWAF, AWEA and AWSA) have significant correlations between NPP and SPEI (Table 4.2). Further, temperate regions with summer dry regions around the Mediterranean (CSEA) also showed a significant correlation between 6-month SPEI and NPP (Table 4.2). This suggests that once dry seasons are occurring well within the growing season, annual NPP is also positively correlated to SPEI.

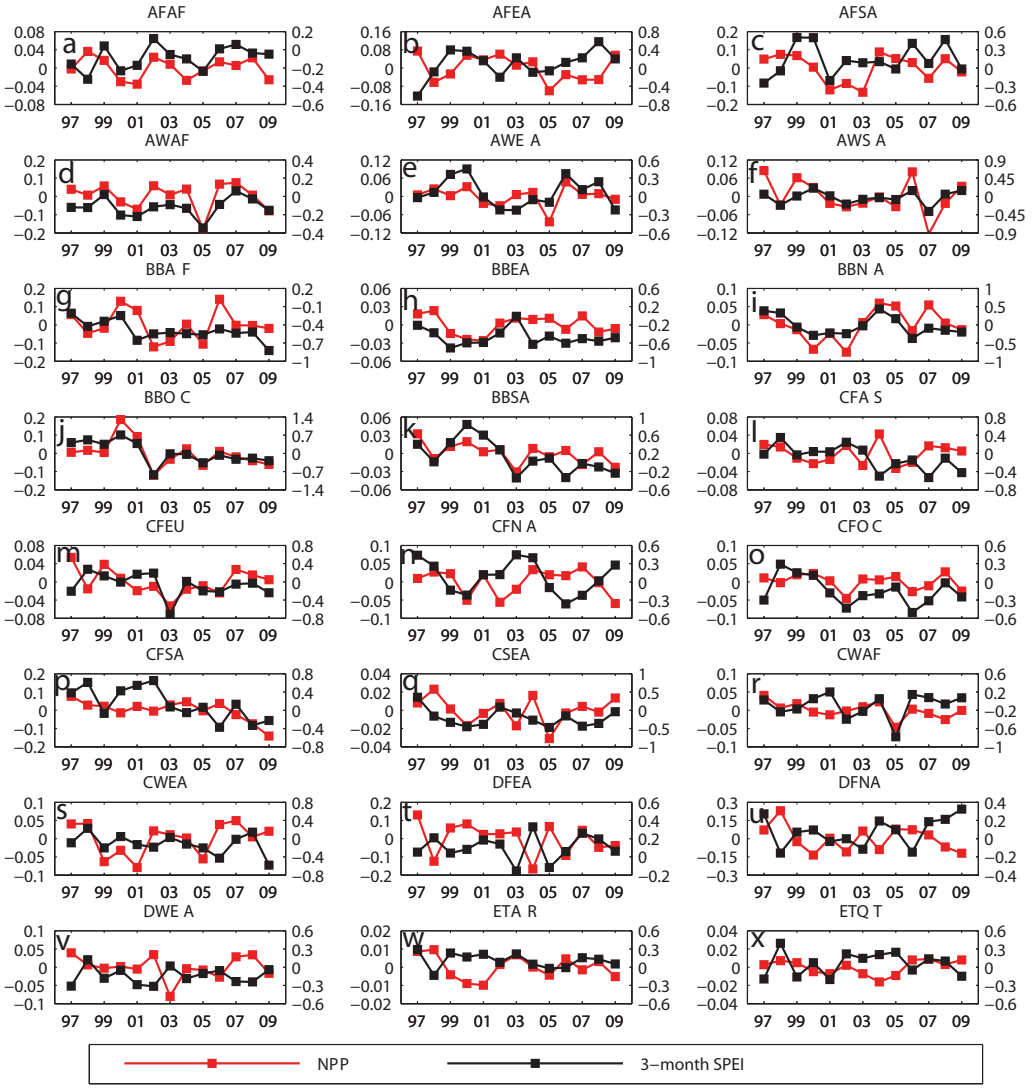

Figure 4.4. Regional average of SPEI and NPP anomalies for the 24 regions listed in Table 4.1.

As shown above, the relationships between NPP and SPEI vary with the regions of the Köppen climate classification. Generally however, different climate zones exist because of the variability of energy and water input with latitude. Therefore, we also show the correlations against latitude and calculated the contribution to global NPP to identify in which areas the sensitivity to global NPP is most pronounced (Fig. 4.5). Figure 4.5 clearly shows the tropics as dominant contributor to global NPP, but with generally low sensitivity to drought. Between 20 and 40 S, and between roughly 20 and 50 N we observe strong positive correlations, as indeed in Zhao and Running (2010) but these areas contribute less to global NPP.

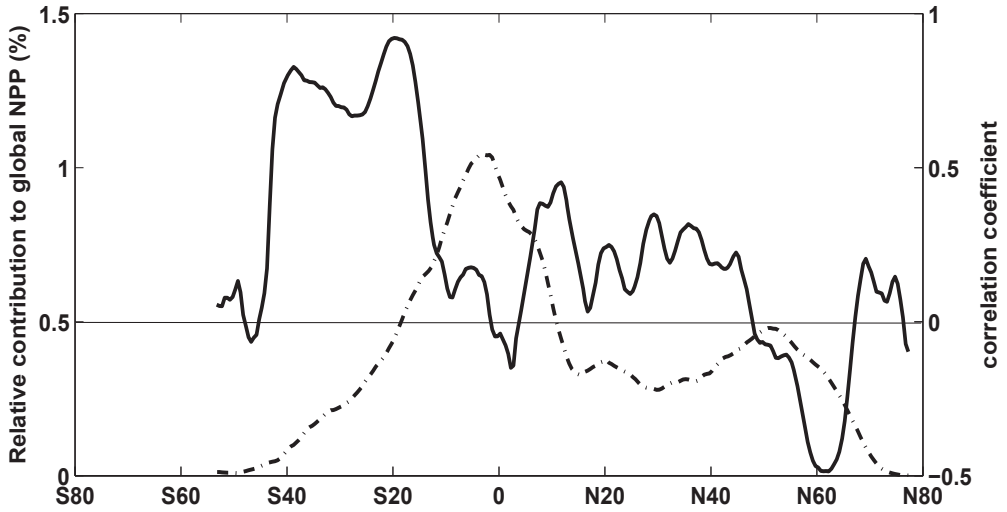

Figure 4.5. Correlation coefficients of latitudinal zone averaged NPP and SPEI (back line) and NPP contributions as a percentage of global NPP (black dash-dot line). 5-degree moving averages were applied to all 0.5-degree steps along latitude.

4.4 Discussion and conclusions

The response of NPP to drought is one of the key dynamic processes of the global carbon cycle. We found a statistically significant relation between global NPP and the drought index SPEI, similar to Zhao and Running (2010) who studied this for a shorter time frame. Although a substantial part of the land surface exhibited opposing patterns, this global relation was for a large part driven by the larger areas of the globe where more soil moisture leads to increased NPP. This was especially obvious in the response that was dominated by the land masses in the Southern hemisphere similar to the soil moisture driven decline in evaporation (Jung et al., 2010) and most probably related to the variability in rainfall caused by the El Niño-La Niña cycle. Although NPP decreased slightly during this period, we prefer to emphasize here its variation rather than the trend because the variations are generally more reliable. Furthermore, our results differ also slightly from the values reported previously due to the use of different models and different time frame. For example, in 2005 the NPP anomaly in the current paper is -0.5 Pg C but Zhao and Running (2010) reported an anomaly of -1.5 Pg C NPP.

Global NPP is one of the prime factors determining the rate of atmospheric CO_2 growth rate (Zhao and Running 2010) and the El Niño/La Niña-Southern Oscillation (ENSO) is known to be correlated strongly to the interannual variability of the growth rate. The mechanism for this is generally attributed to the variation of tropical terrestrial ecosystem NPP driven by variability in precipitation (Zeng et al., 2005) and/or increased fire and deforestation activity during drought years (van der Werf et al., 2004). We have shown how for the tropical landmass with a dry period SPEI shows a clear relation with NPP (Fig. 4.4d-f), which suggests drought impacts are indeed part of this mechanism. However, negative NPP anomalies at northern mid-latitudes caused by drought events,

may also contribute significantly to a lower NPP and the atmospheric CO_2 growth during a moderate El Niño, for example during 2002-2003 (Knorr et al., 2007).

Both regional averages and our grid scale correlation analysis showed spatial variations in the relation between NPP and SPEI. The contrast in response occurred largely between arid regions in the mid-latitudes and the cold humid regions boreal in northern latitudes where NPP and SPEI were correlated positively or negatively respectively.

Global terrestrial ecosystem growth is mainly controlled by radiation, temperature and water availability (Nemani et al., 2003). The arid regions suffer more strongly from water deficits while in those areas radiation and temperature are generally not important limiting factors. For instance, in the western United States, where long-term aridity changes significantly with a warmer climate (Cook et al., 2004), SPEI and NPP exhibited significant correlations (Fig. 4.4i). In contrast, in boreal regions, temperature plays a more important role in explaining NPP variability (Reichstein et al., 2007b). It is important to note that apart from the arid regions, most of seasonally dry regions also show positive relations between NPP and SPEI, particularly if the dry season occurs within the growing season, i.e. the winter dry equatorial regions (AWAF, AWEA and AWSA) and temperate summer dry regions around the Mediterranean (CSEA).

Two regional droughts are important to test the robustness of our results and serve as case studies: the 2003 European heat wave and the 2005 Amazon drought. Vegetation growth over most areas of Europe is generally presumed to be limited primarily by temperature and radiation (Nemani et al., 2003). However, we did find strong NPP and SPEI negative anomalies during 2003 (Fig. 4.4m) that present a substantial change from previous years. This implies that the net effect of temperature, radiation, and water limitation on NPP depends primarily on the intensity of drought. This highlights the sensitivity of the ecosystem carbon cycle in these areas to climate variability, in particular extreme drought and rainfall events. It is however difficult from our analysis to detect a clear threshold that separates the positive from the negative effects of drought on NPP. It is clear that severe droughts, such as those in 2003 in Europe reduce NPP significantly.

In contrast, we are not able to detect an intense NPP decline in Amazon rainforest during 2005 although Phillips et al. (2009) reported substantial tree mortality. Zhao and Running (2010) also found a clear relation between a negative anomaly in soil moisture and a decline in NPP in tropical forests. In our case (not shown here), negative NPP anomalies occur at some regions where a strong decline in biomass is reported by Phillips et al. (2009), but do not overlap fully. We note that whether there was a significant decline in NPP in 2005 in the Amazon is still subject to controversy (Samanta et al., 2011). However, if the CASA model underestimated the Amazon NPP decline in 2005, global SPEI and NPP would show an even stronger in-phase coupled behaviour. Besides these two cases, for the Australian continental drought (2002-2009) we find a very strong relationship between SPEI and NPP.

In this study we aimed to provide more regional and biome detail to the global relations found in Zhao and Running (2010) by analyzing the relation between moisture conditions and NPP at regional to global scales. At a global scale, 1-, 3-, 6-month SPEI and NPP are positively and significantly related, confirming the results of Zhao and Running (2010). We divided the global land surface into different regions based on the Köppen climate classification. SPEI and NPP show significant and positive relations in the arid and seasonally dry in temperate and equatorial zones regions. In contrast, SPEI and NPP in cold regions in the boreal northern hemisphere exhibit a negative relation. At grid level, grids with a significant positive relation occurred more often than those with a negative relation. At a global level, consequently, NPP and SPEI are mostly coupled and in phase.

Our study demonstrates that at annual time scale NPP variance is strongly correlated to the variability in dry and wet condition as expressed by the drought index SPEI. Using a drought index appeared an effective way to estimate the impact of drought on NPP. The spatial non-uniform pattern of drought impact on NPP should be taken into account in further analysis and may serve as benchmark for global vegetation models (Sitch et al., 2008). Our results demonstrate that the strong correlation between global NPP and drought found by Zhao and Running (2010) is a composite of the inherent positive relations in global extend dry regions (arid and seasonal dry) and some extreme drought events in humid areas. Further work in comparing the correlation between several drought indices and NPP may be able to elucidate more clearly some of the contrasting results between previous studies (e.g. Zhao and Running, 2010).

From our analysis we cannot unequivocally set a threshold to define the drought impact on ecosystems. However, with global climate change expected to lead to more frequent droughts (Dai, 2013; Sheffield et al., 2012), we can expect further large regional declines in NPP to occur. How these are counterbalanced by areas with increases in NPP, or whether they lead to an overall negative trend in NPP, can only be studied by increased monitoring of droughts and NPP, preferably through satellite remote sensing (Dolman and de Jeu, 2010).

Chapter 5 Using satellite based soil moisture to quantify the water driven variability in NDVI: a case study over mainland Australia[4]

Abstract

Soil moisture is crucial in regulating vegetation productivity and controlling terrestrial carbon uptake. This study aims to quantify the impact of soil moisture on vegetation at large spatial and long-term temporal scales using independent satellite observations. We used a newly developed satellite-derived soil moisture product and the Normalized Difference Vegetation Index (NDVI) to investigate the impact of soil moisture on vegetation across mainland Australia between 1991 and 2009. Our approach relied on multiple statistical methods including: (i) windowed cross correlation; (ii) quantile regression; (iii) piecewise linear regression. We found a strong positive relationship between soil moisture and NDVI, with NDVI typically lagging behind soil moisture by one month. The temporal characteristics of this relation show substantial regional variability. Dry regions with low vegetation density are more sensitive to soil moisture for the high end of the distribution of NDVI than moist regions, suggesting that soil moisture enhances vegetation growth in dry regions and in the early stage in wet regions. Using piecewise linear regression, we detected three periods with different soil moisture trends over the 19 years. The changes in NDVI trends are significant ($p<0.01$) with turning points of soil moisture in the beginning of 2000 and the end of 2002. Our findings illustrate the usefulness of the new soil moisture product by demonstrating the impacts of soil moisture on vegetation at various temporal scales. This analysis could be used as a benchmark for coupled vegetation climate models.

5.1 Introduction

Knowledge of the response of vegetation to climate change is crucial in understanding ecosystem dynamics. The growth of atmospheric CO_2 concentration has caused green foliage increased at least during last three decades (Donohue et al., 2013). Water availability, solar radiation and temperature are the main climatic constraints that determine the spatial distribution of ecosystems and plant growth (Churkina and Running, 1998; Nemani et al., 2003; Stephenson, 1990). The impacts of these factors on vegetation are relatively well investigated (Lotsch et al., 2003; Mercado et al., 2009; Myneni et al., 1997; Piao et al., 2008). For example, an increase in plant growth has been

[4] This chapter is based on Chen, T., de Jeu, R. A. M., Liu, Y. Y., van der Werf, G. R., and Dolman, A. J.: Using satellite based soilmoisture to quantify thewater driven variability in NDVI: A case study over mainland Australia, Remote Sensing of Environment, 140, 330-338, DOI: 10.1016/j.rse.2013.08.022, 2014.

observed in high latitudes, and was ascribed to the lengthening of the growing season (Myneni et al., 1997). However, climate-ecosystem interactions are complex and autumn warming could also lead to net CO_2 losses in northern ecosystems (Piao et al., 2008).

The availability of water influences more than half of the primary productivity of the world's terrestrial ecosystems (Heimann and Reichstein, 2008), highlighting the constraints of hydrological processes to vegetation. Unfortunately, this effect is probably the lesser understood of the three above-mentioned constraints on plant growth. Water limitation reduces the ability of leaves to take up CO_2, even under conditions of sufficient light, due to a restriction in stomatal conductance and limited root water (van der Molen et al., 2011). Thus, over regions where temperature and radiation are expected to be non-limiting, water availability is an important factor determining vegetation dynamics. Almost classic examples are the 2005 and 2010 droughts in the Amazon basin that caused large-scale mortality and associated reductions in living biomass (Lewis et al., 2011; Phillips et al., 2009). An obvious reduction in GPP was found during 2003 across Europe. At the site level, FLUXNET analysis suggests that this reduction was caused by water limitation rather than by high temperatures (Ciais et al., 2005). Further support for a large impact of water availability on the carbon uptake of terrestrial ecosystem can be found in Angert et al. (2005), Phillips et al. (2009) and Reichstein et al. (2007a).

Importantly, these results were often obtained without adequate observations of soil moisture. Model based soil moisture and several drought indices that are related to actual soil moisture in different ways were often used as a proxy (Hirschi et al., 2011; Lotsch et al., 2003; Nicholson et al., 1990) to study the relationship between vegetation dynamics and water availability. In addition, other researchers used other components of the water balance like precipitation to capture the hydrological impact on vegetation (e.g. Donohue et al., 2009; Wang et al., 2003) or used a combination of water and temperature in non-linear models to study the leaf phenology (e.g. Williams et at., 1997; Choler et al., 2011). These studies provide insights of ecohydrological processes, they also had their limitations as they were based on models and/or indirect observations of water availability.

Observed soil moisture is arguably the best representation of the actual amount of water contained in the soil, and is key to understanding the climate-soil-vegetation system both in space and time (Porporato and Rodriguez-Iturbe, 2002; Rodriguez-Iturbe, 2000). Soil moisture is more directly associated with dynamics in plant photosynthesis and respiration processes than precipitation, of which a variable amount will be lost through interception and runoff (e.g., Miralles et al., 2010). Until recently, no long-term global scale observed soil moisture product was available. This situation has changed dramatically in the last few years. Near-surface soil moisture (several centimetres) from space borne passive and active microwave instruments have been shown to provide effective observations at regional and global scales (Gao et al., 2006; McCabe et al., 2005; Njoku et al., 2002; Owe et al., 2008; Wagner et al., 2003; Wen et al., 2003). The passive and active microwave soil moisture products, respectively, give robust estimates over

sparsely and moderately vegetated regions (de Jeu et al., 2008; Dorigo et al., 2010). Based on previous studies, further blending passive and active microwave soil moisture retrievals from various satellites have led to a long-term improved product with better spatial and temporal coverage (Liu et al., 2011, 2012). These satellite soil moisture products have shown their value in climate studies (e.g. Jung et al., 2010; Taylor et al., 2012) and hydrological studies (Brocca et al., 2011) but are currently still not often used in biogeochemical studies.

Here, we used a newly derived merged product of soil moisture (Liu et al., 2012; Dorigo et al., 2012) to quantify the impact of soil moisture on vegetation dynamics with a range of temporal and spatial scales. The Normalized Difference Vegetation Index (NDVI) product derived from the Advanced Very High Resolution Radiometer (AVHRR) instruments was used to represent vegetation conditions (Tucker et al., 2005). Our objectives are twofold. Firstly to determine the usefulness of the satellite derived products in estimating short and long term variability in the relation between soil moisture and vegetation and secondly to shed light on these relations and trends for mainland Australia. We analyzed these relationships with a multi-statistical approach including variation coherence, time scale, trends and extremes. We selected Australia as a case study because the satellite derived soil moisture has been extensively evaluated by ground based soil moisture and rainfall over Australia (Draper et al., 2009) and the product has an established high data quality over this area (Parinussa et al., 2011). Australia is a water-limited continent (McVicar et al., 2012) where vegetation growth is mainly controlled by water conditions (Donohue et al., 2009; Williams et al., 1997). Australia also contains a large variety in vegetation types, from desert to tropical rainforest. All these components provide an appropriate test bed for this study. Section 2 describes the soil moisture and NDVI products and the statistical methods applied here. Section 3 presents the results, while the last section discusses the results and the performance of the soil moisture product in establishing these relationships.

5.2 Data and Methods

5.2.1 Data

5.2.1.1 Soil moisture

The monthly 0.25 degree spatial resolution soil moisture dataset used (1991 – 2009) was extracted from the European Space Agency Climate Change Initiative data portal (ESA, see http://www.esa-soilmoisture-cci.org). This product was recently developed by merging the active microwave soil moisture products developed by Bartalis et al. (2007) and Wagner et al. (1999) with the passive microwave soil moisture products developed by the VU University Amsterdam in collaboration with NASA (de Jeu et al., 2008; Owe et al., 2008), representing surface soil moisture (not deeper than 10 cm, Liu et al., 2011). A short description of this approach is given below and a more thorough description can be found in Liu et al. (2011, 2012). The harmonization approach is based on two steps. At

first all individual datasets are converted into one soil moisture range (Vol. %) using cumulative distribution functions. Then all the datasets are statistically ranked based on their quality (as derived from triple collocation analysis) and harmonized into one consistent dataset.

This approach primarily addresses three major challenges: i.e., (1) differences in instrument specifications resulting in different absolute soil moisture values; (2) the global passive and active microwave retrieval methods producing conceptually different quantities (expressed in the volumetric soil moisture (m^3 m^{-3}) and degree of saturation (%), respectively); (3) products varying in their relative performances depending on vegetation cover (Dorigo et al., 2010; Scipal et al., 2008). While this approach changes the absolute values of soil moisture, it preserves the relative dynamics (e.g., seasonality and inter-annual variations) of the original satellite derived retrievals and this makes it particularly well suited for our purpose. The long-term changes, as evident in the original soil moisture products, are also preserved (Liu et al., 2012). Although the original data are daily, there are too many gaps because each scan of the satellites can't cover the whole region. Therefore, we averaged the original daily product into monthly data to produce spatially covered maps of mainland Australia. Fig.5.1 gives an overview of the general spatial soil moisture conditions over time for this study area with relative wet conditions in the south in the winter (JJA) and wet conditions in the summer (DJF) in the north.

5.2.1.2 NDVI

The Normalized Difference Vegetation Index (NDVI) is a normalized ratio calculated from reflected radiation in the red and near-infrared spectral regions. In general, productive plants use the energy available in the red part of the spectrum for photosynthesis and reflect the near infrared. NDVI is calculated as (NIR-VIS) / (NIR+VIS), where NIR and VIS indicate the spectral reflectance at the near-infrared and visible (red) spectral band range, respectively. NDVI has been widely used to indicate vegetation dynamics or growth (Donohue et al., 2009, 2013; Myneni et al., 1997; Nemani et al., 2003; Piao et al., 2011; Tucker et al., 1986). Here we used the long term time series of NDVI observation from the Global Inventory Modelling and Mapping (GIMMS) group derived from NOAA AVHRR imagery (Tucker et al., 2005, Beck et al., 2011). NDVI used here is averaged at monthly and 0.25 degree resolution for direct comparison with the monthly soil moisture maps. In Fig. 5.1, spatial patterns of annual averaged NDVI were shown to present the general vegetation conditions. In addition the main ecoregions (Department of the Environment, Water, Heritage and the Arts, 2012a) are mapped in Fig. 5.2.

Both soil moisture and NDVI have a strong seasonal cycle, and here we only used the monthly anomalies (i.e. the monthly anomaly was calculated by subtracting the monthly time series from the monthly climatology based on the 19 year data record).

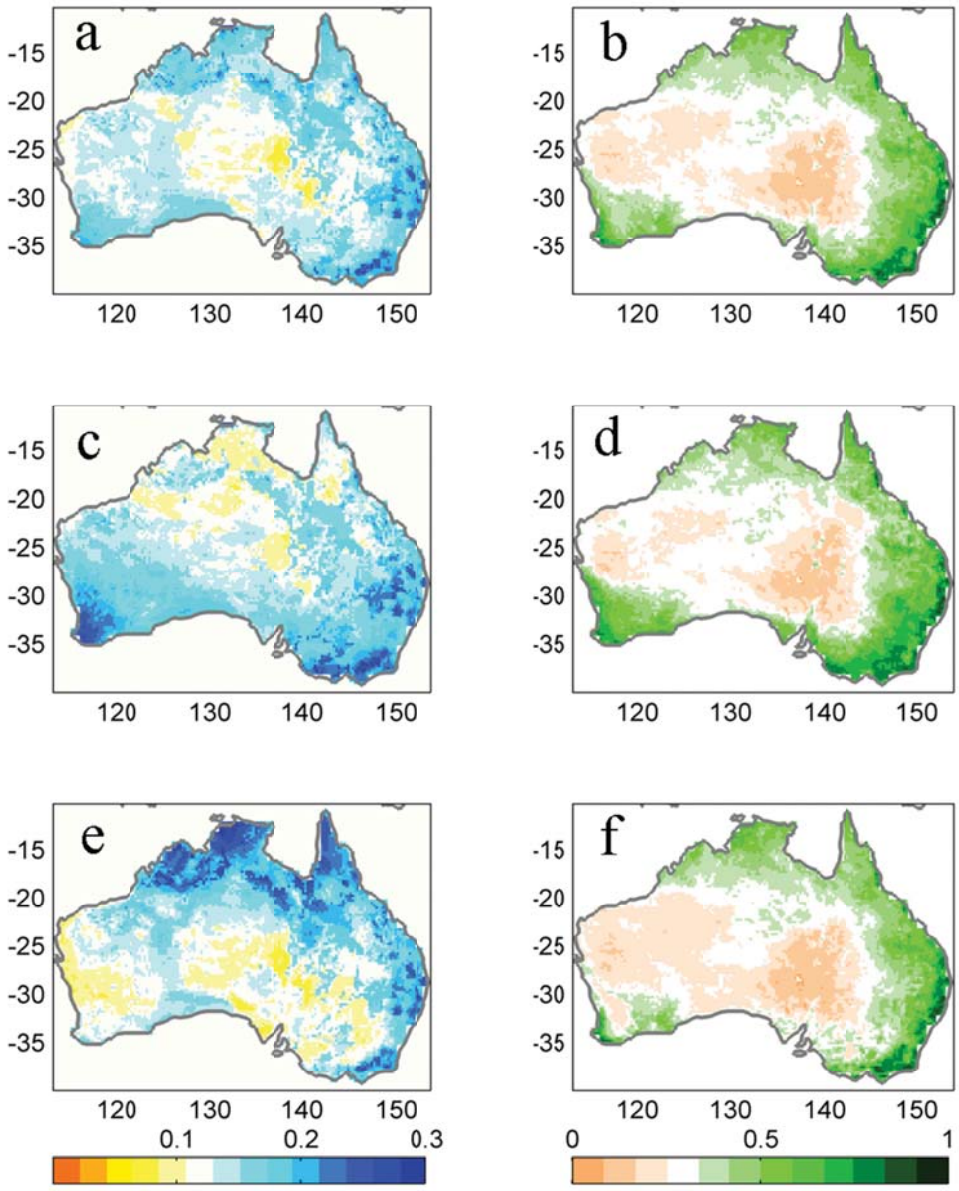

Figure 5.1. Average soil moisture (left panels, m^3 m^{-3}) and NDVI (right panels) during 1991-2009. Panels a-b, c-d, e-f are annual, Southern Hemisphere winter (JJA) and summer (DJF) separately.

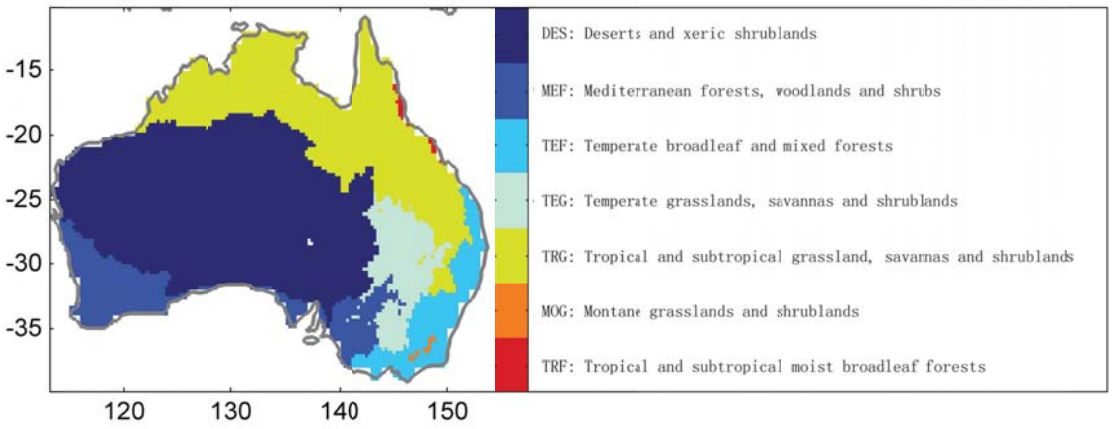

Figure 5.2. Terrestrial ecoregions of Australia (derived from Department of the Environment, Water, Heritage and the Arts, 2012a) at 0.25 degree resolution in this study.

5.2.2 Statistical methods

The impact of soil moisture on vegetation is so complex that a simple correlation analysis is not fully capable to determine their co-relationship. Instead, we used three methods to more comprehensively characterize their co-relationship. Firstly, the Windowed Cross Correlation (WCC) was applied to analyze the lagged relation between soil moisture and vegetation. Secondly, Quantile Regression (QR) was used to further enhance our knowledge on the relation between vegetation and the wet and dry end of soil moisture distribution within a pixel. Thirdly and, the piecewise linear regression (PLR) was applied to analyze the coherence in trends between the two satellite data products. Together, these techniques comprehensively illustrate the spatiotemporal relationship between soil moisture and vegetation for this study area.

5.2.2.1 Windowed Cross Correlation (WCC)

The impact of soil moisture on NDVI is expected to show finite time lags due to variability in temporal response of vegetation to soil moisture. To quantify these time scales, we applied Windowed Cross Correlation (WCC) to determine the time lag in the response.
The common cross correlation of two time series (X, Y) at lag ς is given by,

$$\gamma(X,Y,\varsigma) = \frac{1}{N-\varsigma}\sum_{t=1}^{N-\varsigma}\frac{(X_t-\mu_x)(Y_t-\mu_y)}{\sigma_x\sigma_y} \qquad (5.1)$$

where ς indicates time in months, ranging from 1 to N. μ_x and μ_y are the averages of X and Y. σ_x and σ_y are the standard deviations of X and Y respectively. As an improvement, the windowed cross correlation (WCC) was developed by Boker et al. (2002). In this technique, a temporal window is selected and moved forward from the beginning to the end. A series of cross correlations can then be applied on the windowed X and Y to

examine the correlation changes over time. This advantage is particular important in this study because climatic variables usually have periodic characteristics and the lagged relation can be analyzed (i.e. with this method you can analyze the time it takes time before vegetation will respond on a change in hydrological conditions). More details on this analysis can be found in Boker et al. (2002).

In the WCC method, the window, or length of the time series in each calculation, for the analysis is chosen manually, but has two requirements. Firstly, the window has to be sufficiently long to contain enough samples to calculate statistically meaningful correlation coefficients within the window. Secondly, the length of the data series to evaluate the temporal variation of the strength of the relationship has to be long enough to encompass the variability. Here we used a 10-year long window with 120 monthly points, i.e., N=120.

5.2.2.2 Quantile Regression (QR)

We explored the behaviour of the relations for the extremes by using a quantile regression technique, as it is likely that the effect of soil moisture (shortage) will not often be expressed through a decline in the mean, but rather through the extremes. Quantile regression (Koenker and Bassett 1978) was developed to investigate the conditional quantiles of a response variable distribution. Compared to ordinary least square regression, which responds largely to the mean of a distribution, quantile regression advantageously responds to both the lower and upper end of the distribution. This is particularly relevant in our case, both to assess the probability of NDVI response to extreme drought or wetness. This response could vary across wet or dry regions due to the change of water-limited strength and other landscape features impacts (e.g. soil and vegetation types). Additionally, quantile regression could assess whether the satellite soil moisture data-based analysis is sensitive enough to determine these. The method has been widely used in biology (Cade and Noon, 2003) and geosciences (Hirschi et al., 2011).

The τ-th sample (τ Є (0, 1)) quantile can be formulated as a simple optimization problem of random variable y:

$$min_{\xi \in R} \sum \rho_\tau (y_i - \xi) \tag{5.2}$$

and

$$\rho_\tau(\mu) = \begin{cases} \tau\mu & if \ \ \mu \geq 0 \\ (\tau - 1)\mu & if \ \ \mu < 0 \end{cases} \tag{5.3}$$

where i is used to indicate each value, ξ is a real number. In the case of quantile regression (Koenker and Bassett, 1978; Koenker and Hallock, 2001) the linear quantile function can be obtained by solving for

$$\beta_\tau = \arg min_{\beta \epsilon R^P} \sum_{i=1}^{n} \rho_\tau (y_i - x_i' \beta) \quad (5.4)$$

where ' denotes the transpose; $x_i'\beta$ is the inner product of vectors x_i and β. For a one argument condition, p = 1.

5.2.2.3 Piecewise Linear Regression (PLR)

To investigate the coherence in trends of soil moisture and NDVI we applied piecewise linear regression (PLR) approach (Toms and Lesperance 2003), which is also called segmented linear regression. To our knowledge, there is unfortunately no optimal way to determine the segments number when segments are more than two, other than by visual inspection or trial and error. A significance test can then be applied to determine the segmentation reasonableness. In our case, three intervals were selected based on the time series general shapes, and hence each time series has two turning points. Minimizing the residuals of segmented linear fits then determines these turning points. A linear regression approach (Toms and Lesperance 2003) was applied to each successive two interval segments to test the turning-point significance by a t-test against the null hypothesis. The model is given by:

$$Y = \begin{cases} \beta_0 + \beta_1 X + \varepsilon & X \leq \alpha \\ \beta_0 + \beta_1 X + \beta_2 (X - \alpha) + \varepsilon & X > \alpha \end{cases} \quad (5.5)$$

where X is time and Y is soil moisture or NDVI. As time series are stochastic process, we adjusted this model β_0 to β' for trend analysis when X>α. A t- test was applied to test if β_2 is not equal to zero. Both the soil moisture and NDVI continental average series were standardized to achieve parity in the regressions.

5.3 Results

5.3.1 Time lag and spatial response

Figure 5.3 illustrates the windowed cross correlation analysis of continental average soil moisture and NDVI. Strong positive relations were found, particularly when soil moisture precedes NDVI by one month. Fig. 5.3a shows that the correlation coefficients vary considerably with different time lags. In general, positive correlation coefficients are found more often, in particular where the soil moisture preceded, or is concurrent with the NDVI (Fig. 5.3a). This means that soil moisture leads the behaviour of vegetation. The highest correlation coefficients are observed when soil moisture precedes NDVI by one

month. Fig. 5.3b shows the temporal pattern of correlation coefficients between soil moisture for this case. The correlation coefficients are statistically significant ($p < 0.01$) and appear to become stronger with time, rapidly rising from around 0.4 in 1996 to 0.6 in 2001 and levelling off afterwards, which is in line with the 'Big Dry' drought during the first decade of this century (Leblanc et al., 2012; Verdon-Kidd and Kiem, 2009; Wei et al., 2011). This finding suggests that water availability became a stronger factor in the ecosystem dynamics as the drought progressed. We were not able to detect any impact of the different satellite systems used in the analysis of the merged soil moisture product or NDVI.

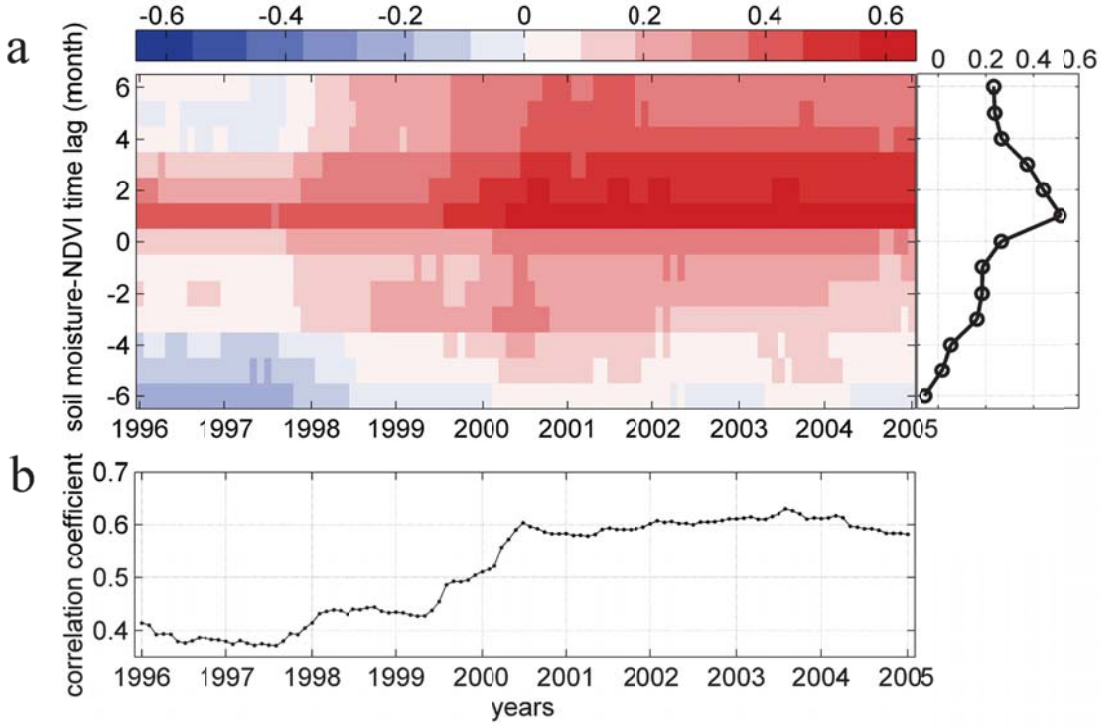

Figure 5.3. a) Windowed cross correlations between soil moisture and NDVI over Australia. Both soil moisture and NDVI are area weighted (using grid areas as weighting coefficients). A decadal (N = 120) window is chosen, therefore, the midpoints for display range from 1996 to 2005 comparing data length of 1991-2009. Positive numbers in lag indicate soil moisture proceeds NDVI. The inset on the right shows the average correlation coefficients of each lag. b) String diagram of a) only when soil moisture precedes NDVI by one month.

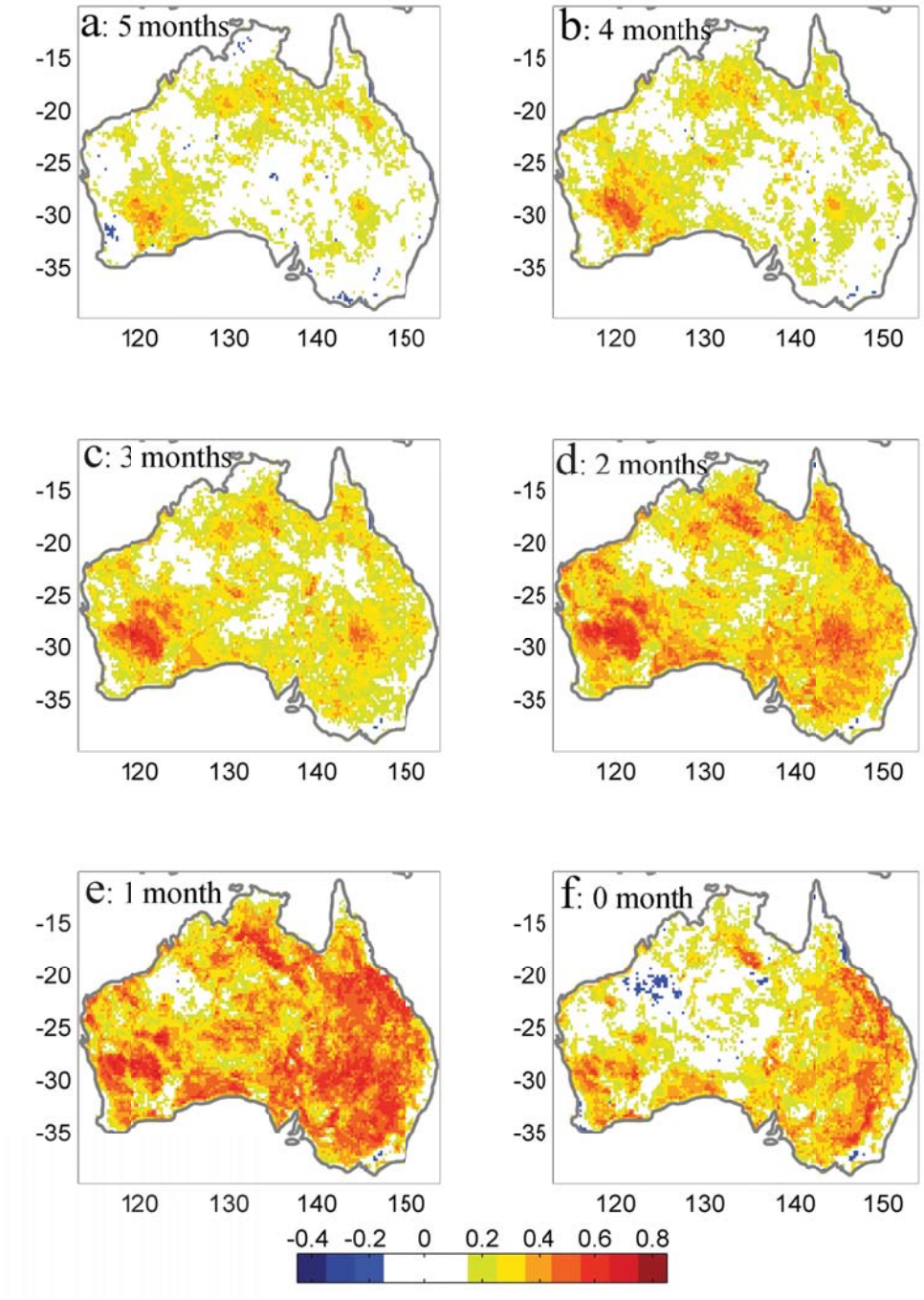

Figure 5.4. Cross correlation coefficients between soil moisture and NDVI across Australia between 1991 and 2009. The labels of panels a-f indicate the time scales of 5-0 months respectively. Positive scales indicate soil moisture preceding NDVI.

We further investigated the spatial patterns of soil moisture – NDVI relationship. The rate of significant grids reaches the peak (93%) when the time lag is 1 month. And the rates when time lag ranges from 1 to 6 months are much higher than that when time lag ranges from -6 to -1 months, i.e. 40%-93% versus 27%-52%. In Fig. 5.4 we only show the zero up to five months cases. Soil moisture and NDVI show strong correlations in most grid cells across the mainland Australia with a time lag of zero up to four months. For

most grid cells (73%), the highest positive correlations are found when again soil moisture is one month ahead of the NDVI (Fig. 5.4e), which agrees with the continental average results as shown in Fig. 5.3. Over the inland southwest where mixed woodlands and many lakes exist soil moisture and NDVI are positively related for a range of temporal scale (lag time from 0 to 5 months). More quickly responding (lag < 1 month) areas are found in the east and southwest corner which are dominated by subtropical and temperate grasslands and rainfed agriculture (both pasture and crops) (Fig. 5.4f). The results from the WCC were further confirmed in Fig. 5.5. High correlations are generally distributed over the continent with the exception of low correlations in northwest Australia. The optimized month map showed the highest correlation during the months with the strongest precipitation signal (i.e. generally in February in the northwest and September/October in the southeast). The lag plot (Fig. 5.5c) gave a general lag value of 1 month throughout country.

Table 5.1. Statistical summary for the 5 dominant ecoregions in continental Australia as given in Fig. 5.2. The other two ecoregions (i.e. MOG, TRF in Fig. 5.2) were ignored because their areas are too small to be accurately described at 0.25 degree resolution in this study.

region	soil moisture	NDVI	WCC analysis		QR slopes				
	(ave ± std)	(ave ± std)	Opt.lag	R	τ=0.1	τ=0.3	τ=0.5	τ=0.7	τ=0.9
DES	0.13±0.04	0.24±0.07	1	0.48	0.05	0.09	0.20	0.21	0.29
MEF	0.15±0.04	0.43±0.15	1	0.47	0.53	0.60	0.70	0.74	0.52
TEF	0.19±0.04	0.67±0.15	1	0.47	1.73	0.77	0.76	0.78	0.87
TEG	0.14±0.04	0.40±0.13	1	0.64	0.78	0.83	0.61	0.73	0.75
TRG	0.16±0.06	0.42±0.13	1	0.62	0.13	0.32	0.32	0.43	0.61

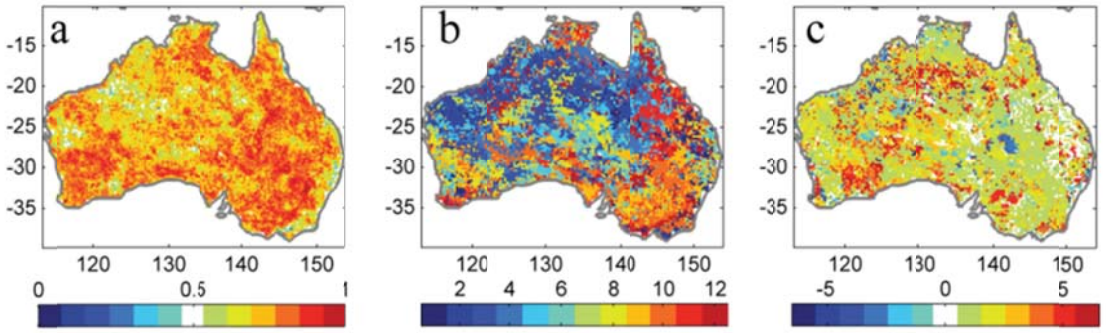

Figure 5.5. Results from cross correlation analysis of monthly NDVI and soil moisture for 1991-2009 and a time increment of one year. Part a) represents the maximum obtained correlation coefficients; part b) the optimized month that produces the highest correlation and part c) the optimized lag in months.

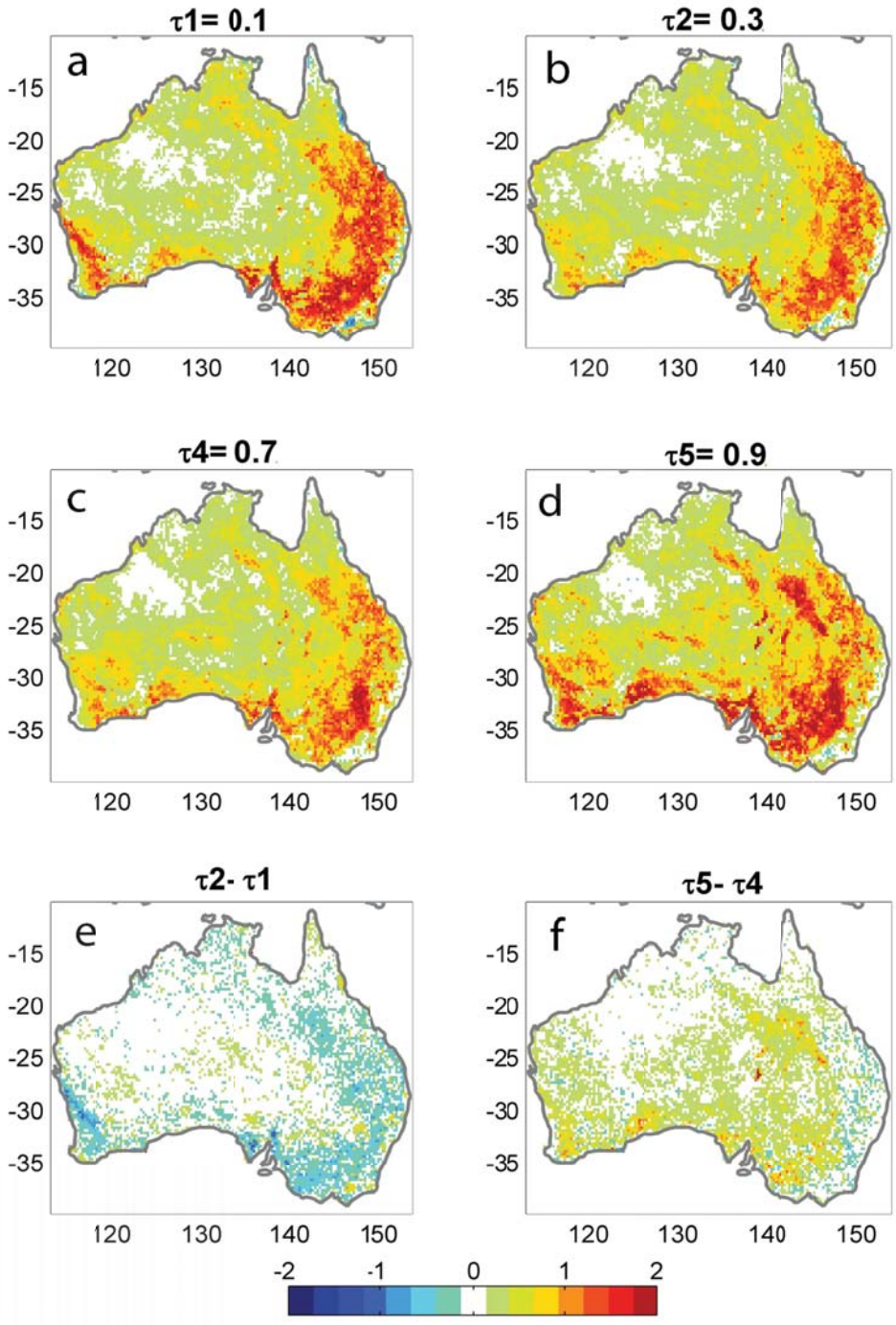

Figure 5.6. Spatial patterns of quantile regression slopes (NDVI/soil moisture) across Australia. τ values are 0.1, 0, 3, 0.7 and 0.9 (top 4 panels indicated by a-d, τ value shown in top of each panel). Bottom two panels show τ2-τ1 (e) and τ5-τ4 (f).

We further analyzed the spatial relation of soil moisture and NDVI by looking at the extremes of the probability distributions. The spatial patterns of the quantile regression slopes are shown in Fig. 5.6. This illustrates the slope of NDVI versus soil moisture when NDVI is lagged one month with respect to soil moisture. We selected distinct quantiles of 0.1, 0.3, 0.5 (median), 0.7 and 0.9, covering a broad range within the distribution. For the first order quantile regression, the rate of change (slope) of NDVI to soil moisture is the

element we are interested in. The spatial patterns of slopes of the quantile regression vary with quantiles. In the more densely vegetated areas including temperate forests and Mediterranean forests in the east, north and southwest corners where persistent vegetation cover locates (Lu et al., 2003; Donohue et al., 2009), high slope values seem linked to low quantiles of NDVI as shown by Fig. 5.6e and ecoregion TEF in Table 5.1. By contrast, in other parts of the continent, such as in semiarid areas with grasslands, the highest slope values of NDVI to soil moisture occur within the upper quantiles of NDVI (Fig. 5.6f, ecoregion DES and TRG in Table 5.1). However, the smallest slope of ecoregion TEF (i.e. 0.87) is still higher than the slopes of other regions, which means persistent vegetation also change with water condition or droughts (Pook et al., 1997). The slope trends with quantiles of densely (decrease) and low vegetated areas (increase) are contrary (Table 5.1). In more densely vegetated areas, this indicates that soil moisture is more inclined to constrain early stage of growth. Whereas in low vegetated areas, higher precipitation/soil moisture events results in additional growth (boost) once these events are sufficient to overcome the lost from canopy interception (Dunkerley 2000, 2008; Dunkerley and Booth 1999) or quick evaporation of the soil surface (Dunkerley 2002). In addition, in the persistent hummock grasslands or Acacia open woodlands, ephemerals or biennial grasses wound response to higher precipitation events obviously (Masters 1993; Southgate and Masters 1996). However, there is a particular region in the southwest corner of Western Australia that shows a different behaviour. This triangular region is a winter cereal-cropping zone (Donohue et al., 2009), and clearly shows a distinct pattern in both Fig. 5.6e and Fig. 5.6f. Donohue et al. (2009) demonstrated that this region shows anomalous vegetation response which is probably due to agricultural practices.

5.3.2 Trends in soils moisture and NDVI

As shown in Fig. 5.3, the strength of the correlation between NDVI and soil moisture increased since approximately 2000. Furthermore, our data show that Australia has experienced an overall decline in surface soil moisture during 1991-2009 at the rate of $-1.0*10^{-3}$ m^3 m^{-3} yr^{-1}; as demonstrated by Dorigo et al. (2012), decreases in West and Central Australia dominant.

During the same period, NDVI decreased at a rate of $-1.1*10^{-4}$ yr^{-1}. However, both the NDVI and soil moisture trends are very small and do not change monotonically during the whole period. We applied a piecewise linear regression to investigate these trends in more detail and determine the turning points in these trends.

For the full study period, the trends in both soil moisture and NDVI are best described by a three segmented model (Fig. 5.7). The different trends of the adjacent segments are separated by turning points (TP) and these all are significant (T-test, $p < 0.01$). Both soil moisture and NDVI show an increase in the early 1990s, a decrease until early 2000s and after that increase again (Fig. 5.7a, b). The TP positions for soil moisture and NDVI series are however different. Following a previous application of this method (Piao et al., 2011),

we further analyze the NDVI series using by the TPs of soil moisture (Fig. 5.7c). In this case, the TPs of soil moisture series are also significant ($p<0.01$) to the NDVI series. Besides, Fig. 5.8 demonstrates the spatial patterns of soil moisture and NDVI trends using TPs of soil moisture. And these patterns of soil moisture and NDVI are generally coherent. This strongly suggests that our results are robust and that the observed trend in NDVI can be attributed, to a large extent, at least statistically, to a trend in soil moisture. This soil moisture trend is obviously related to rainfall variability, but soil moisture here provides the direct relation to vegetation activity as expressed through the NDVI series.

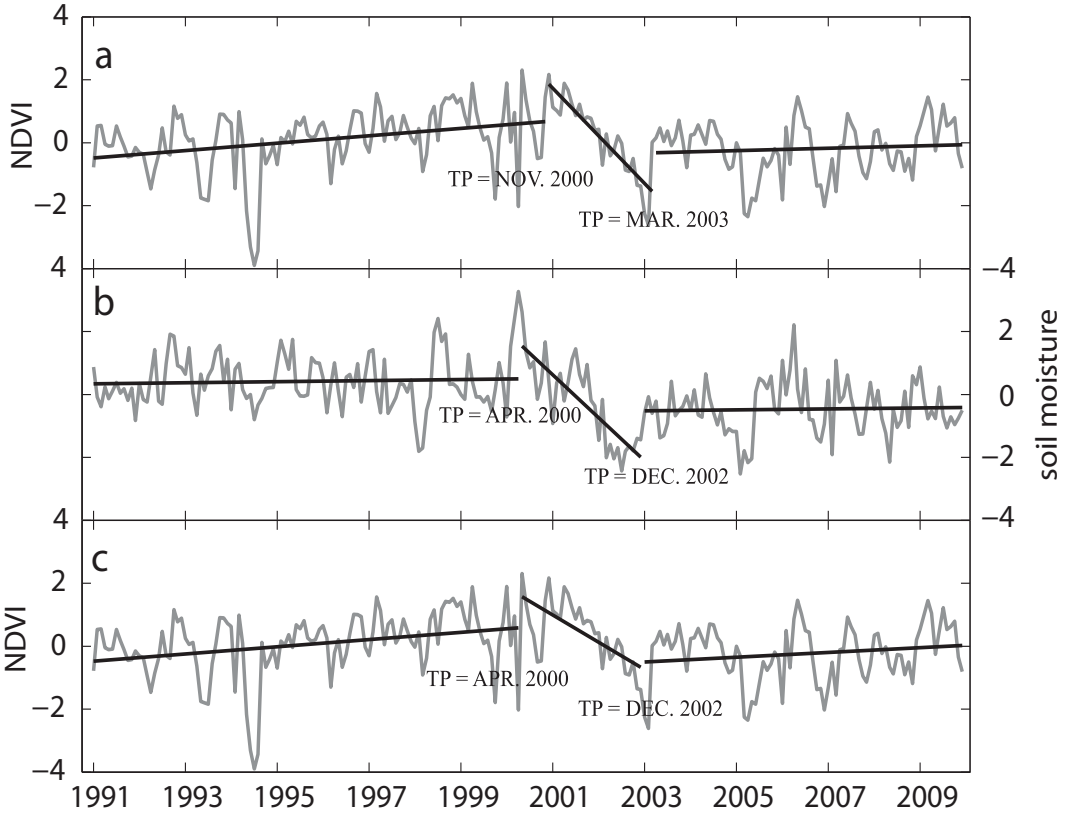

Figure 5.7. Piecewise analysis on the continental averages of soil moisture and NDVI anomalies series. Both are normalized. Part a) three-segment trends of NDVI series separated by NDVI turning-points; part b) three -segment trend of soil moisture series separated by soil moisture turning-points; part c) three-segment trends of NDVI series separated by soil moisture turning-points.

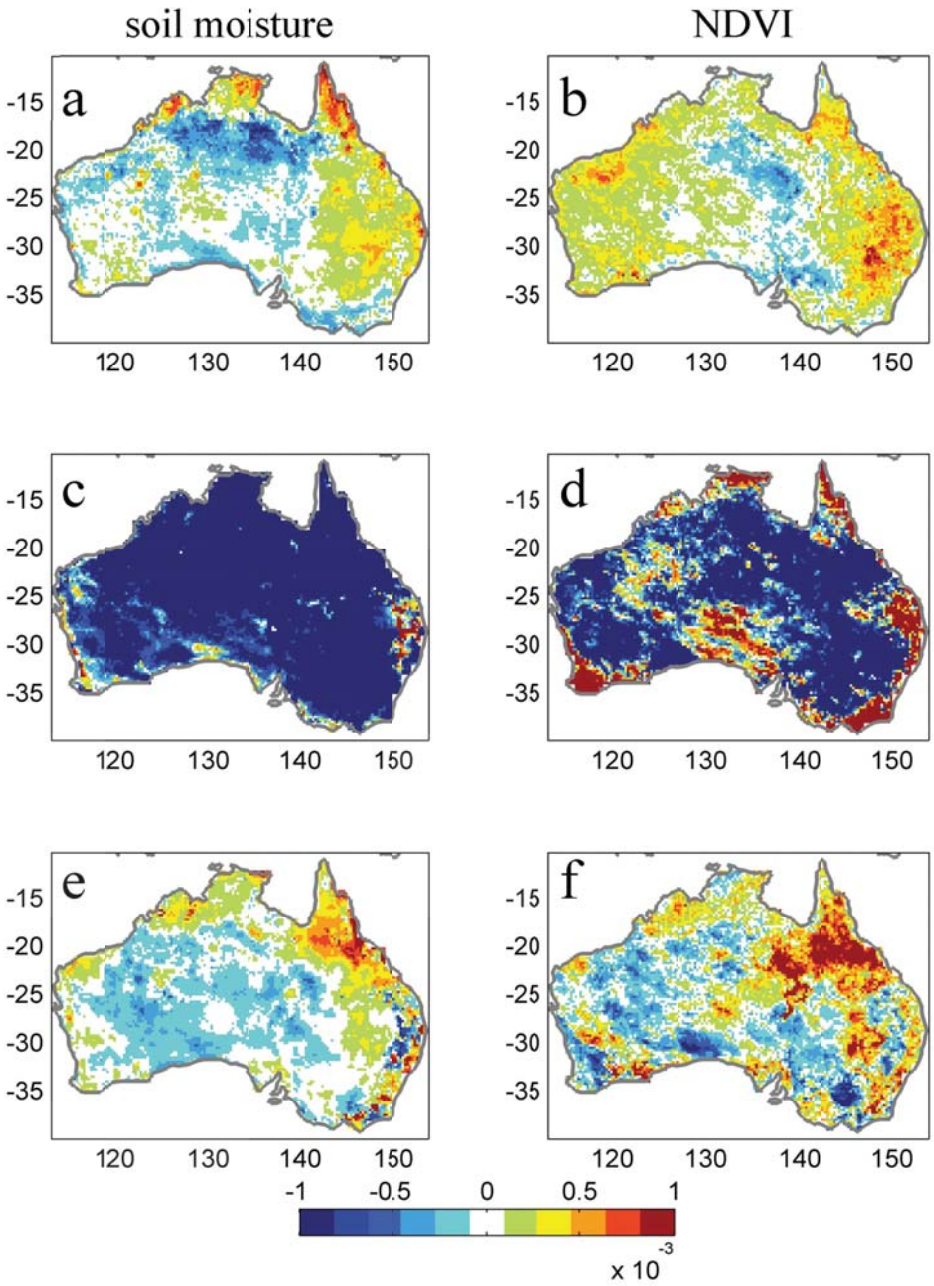

Figure 5.8. Grid trends (per month) of soil moisture (left panels, $m^3\ m^{-3}$) and NDVI (right panels) during the three periods divided by the soil moisture TPs corresponding to Fig. 5.7, i.e. Jan. 1991 – Apr. 2000 for a) and b); Apr. 2000 – Dec. 2002 for c) and d); Dec. 2002 – Dec. 2009 for e) and f). Units for soil moisture are $m^3 m^{-3} month^{-1}$; and for the NDVI are $month^{-1}$.

5.3.3 Vegetation Prediction

The results from the CWW demonstrate the possibility to use satellite soil moisture data to predict vegetation dynamics. This finding is further analyzed and Fig. 5.9 illustrates the anomalies of soil moisture (January to February 2009) and NDVI (February to March 2009). Both soil moisture and NDVI exhibit positive anomalies in the north Australia. We

also checked previous and following months (December 2008 to May 2009) to determine the whole cycle of this case. In these five months of the growing season, we notice that, in particular January and February 2009, soil moisture predicts well the spatial extent of NDVI in February and March respectively (Fig. 5.9). Again, soil moisture clearly precedes NDVI by one month. Importantly, and supporting our earlier findings, the spatial details of the preceding soil moisture matches that of NDVI very well and demonstrates a vegetation forecast application for soil moisture for water-limited regions of Australia.

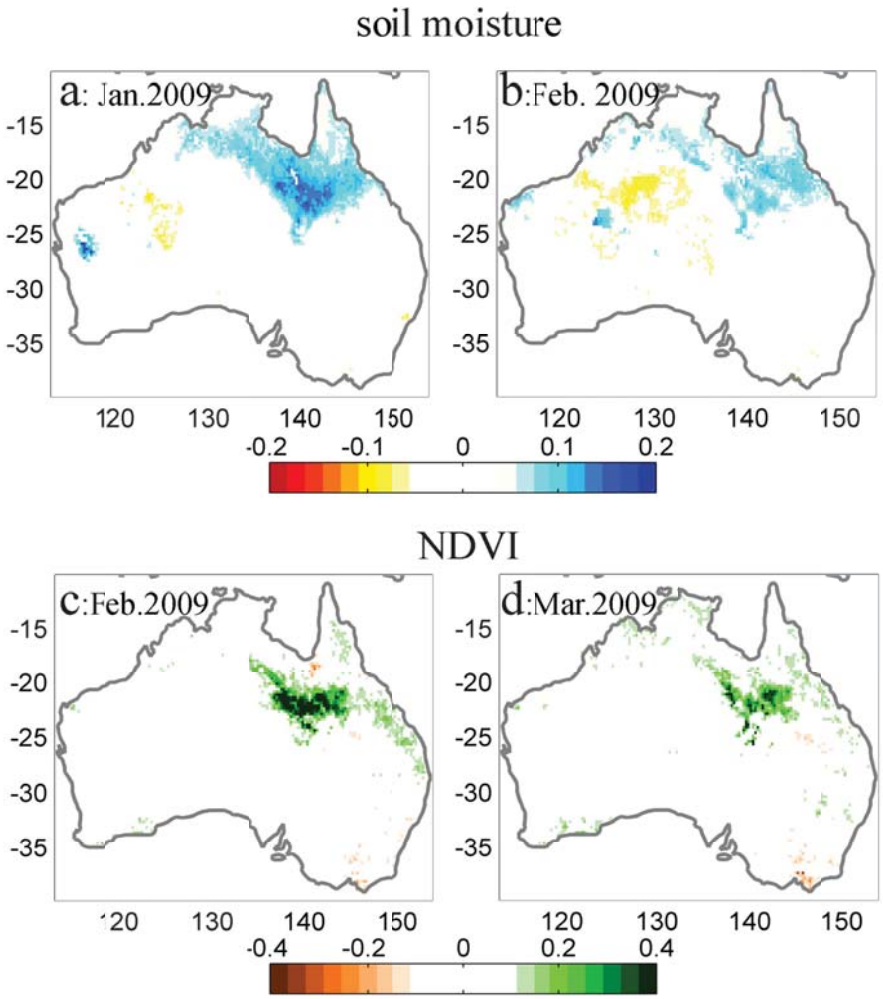

Figure 5.9. A case study of coherent positive anomalies between soil moisture and NDVI. The upper panels are soil moisture anomalies from a) January 2009 to b) February 2009. Correspondingly, lower panels indicate NDVI anomalies from c) February 2009 to d) March 2009.

5.4 Discussion

Hydrological processes generally regulate vegetation at multi spatial and temporal scales. Our aim was to show the usefulness of satellite derived soil moisture products in

determining these relationships in Australia, a continent with a strong gradient in rainfall rates leading to vegetation types ranging from desert shrubs to tropical rainforest.

We showed that soil moisture and NDVI co-vary both temporally and spatially. In the temporal domain, this relation became stronger during the last decade and soil moisture generally precedes the NDVI variances with a typical scale of one month during the whole period. Both soil moisture and NDVI exhibit coherent trend changes during the whole study period. The response of vegetation to changes in soil moisture varied over a gradient from arid to moist conditions. The quality of soil moisture data changes with time, as more and better satellites became available during the latter period of the analysis. However, the typical lag character between soil moisture and NDVI occurs during the whole period. Precipitation-induced changes are apparently greater than the changes between satellites sensors. Our first objective to detect relations between observed soil moisture and the vegetation characteristic NDVI, is thus successful. We note that the microwave-derived product is representative of variable, but shallow depth of soil moisture. However, the shallow depth observations can be representative value for soil moisture dynamics at the root zone layer. This was clearly demonstrated by Rebel et al. (2012) where they found high correlations between the satellite product and modelled root zone soil moisture using the measurements of 15 eddy flux sites.

The spatial pattern of the slopes that are obtained for the quantile regression changed across the continent. For the low-density vegetation areas (Fig. 5.1; Glenn et al., 2011; Liu et al., 2007), high values of the slope for the upper distributions of NDVI quantiles, 0.7 and 0.9, reveal that positive anomalies of soil moisture are more likely to cause distinct vegetation growth (see also Table 5.1). Thus, higher soil moisture (low probability) causes a rapid vegetation growth, indicated by faster increasing rate of NDVI. In contrast, we obtain high values of the slope (the sensitivity) for the low values of NDVI in the more densely vegetated areas (Fig. 5.1; Table 5.1; Glenn et al., 2011; Liu et al., 2007). Slopes of East Australia decline with higher quantiles (Fig. 5.6e-f), because during a quite wet condition plants will not be responsive to soil moisture intensely and exclusively.

In general, the dynamics and location of available water has a large effect on the vegetation distribution. For example, humid areas exhibit much higher vegetation densities than semi-arid or desert regions (Glenn et al., 2011). In water-limited areas a sudden change in the water regime (e.g. strong precipitation event) results in a rapid vegetation change, as the case study shown by Fig. 5.9.

Although Australia is mostly water-limited (McVicar et al., 2012), a wide range of vegetation types and ecohydrological conditions exist indicated by National Dynamic Land Cover Dataset (Lymburner, et al., 2010) and IBRA7 (Department of the Environment, Water, Heritage and the Arts, 2012b, Donohue et al., 2012). In this study, we used the terrestrial ecoregions based on IBRA7 in analysis (Fig. 5.2; Table 5.1). As shown in the results above, pasture and crops have a shorter response time scale to soil moisture

anomalies than shrubs. Plants in humid and dry regions have different sensitive stages to soil moisture indicated by the results of quantile regression analysis. This is in agreement with the different response mechanisms of vegetation response to drought (van der Molen et al., 2011) and shows the usefulness of using spatial information such as soil moisture from satellites to detect these relationships. Besides, groundwater dependent ecosystems (spring, wetland and some forests) may not respond strongly on land surface moisture conditions. The landscapes where the soil moisture conditions are driven by lateral flow or ground-water are hard to be remotely sensed. Meanwhile, the adaption of plants to arid conditions, including roots exploration and even species alternation, may impact the relationships found above.

Soil moisture and NDVI show three periods where the trends change, based on the linear piecewise regression analysis. Using the turning points of soil moisture for NDVI generated three significant segments. This suggests that during the entire period of 1991-2009, soil moisture and NDVI trends together demonstrate a strong relationship. We emphasize that the statistical methods used here do not determine the “direction” or “causality” of the impact. To achieve this, physical and physiological mechanisms which can only be studies by models (Lucht et al., 2002; Nemani et al., 2003) need to be invoked. However, the fact that switching the TPs yields similar trends suggests that the behaviour is independent on the exact location of those, and that the long-term changes in NDVI for much of the Australia are indeed strongly linked to changes in soil moisture.

5.5 Conclusions

We investigated the impact of soil moisture on vegetation across the Australian continent. Soil moisture and NDVI are significantly ($p< 0.1$) positive related in both regional average and most areas at grid level, with a typical time scale of soil moisture preceding NDVI by one month. We also showed that the sensitivity of NDVI to soil moisture depended on vegetation cover density. Both soil moisture and NDVI exhibit coherent trends during our study period. We conclude that soil moisture influences NDVI in both the monthly variance and in the longer term trend changes. Because soil moisture and NDVI are independently derived remote sensing products, our results show that monitoring soil moisture could help to predict vegetation changes.

Previous studies suggested that precipitation is a predictor of NDVI, with a lag of one to several months (Richard and Poccard 1998; Wang et al., 2003). Our study illustrates that remotely sensed soil moisture data can as well be a good predictor for vegetation growth. The relations found here could be used to improve the link between hydrological processes and biogeochemical processes in land surface models, as suggested by Rebel et al. (2012) who used a similar soil moisture product to evaluate the performance of a Dynamic Global Vegetation Model. The relationships found here provide useful benchmarks for modelling studies using coupled vegetation climate models. Whether the relationship we found also holds for other water-limited or ‘equitant’ regions (McVicar et al 2012) of the globe requires further study.

Chapter 6 Synthesis

6.1 Introduction

The work presented in this thesis covers two closely related topics in Earth system sciences. One is the estimation of global cropland GPP (gross primary production) and NPP (net primary production). The other investigates soil moisture constraints on terrestrial ecosystems and the carbon cycle. In this synthesis, integration of the findings of the work in this thesis and other related studies are presented in section 6.2. After that, a discussion of existing limitations and future perspectives is given in section 6.3.

6.2 Research purposes and main findings

6.2.1 Cropland GPP and NPP estimations

In chapter 2 and 3 of this thesis, we focused on cropland GPP and NPP estimates, essential components in the terrestrial carbon cycle. The light use efficiency (LUE) approach, a well evaluated empirical method developed by Monteith (1972), was used here. Usually, empirical methods require look-up tables of key parameters to quantify the diversity of ecosystems. Therefore the maximum light use efficiency approach (ε*) was evaluated and a look-up table was generated for 26 crop types. A new monthly global cropland GPP dataset was created based on this look-up table and a more sophisticated LUE model.

The objective of this study was to improve GPP estimates. GPP is the largest carbon flux in the terrestrial carbon cycle and provides the main carbon input into terrestrial ecosystems, ranging from about 120 to 150 Pg C yr^{-1} (Beer et al., 2010; Welp et al., 2011). About half the GPP is used by plants for maintenance (autotrophic respiration, R_a), the remainder being available for plant growth as net primary production (NPP). Because direct field measurements are far from sufficient to generate global GPP and NPP due to large variability in plant species and growth, a sophisticated modelling approach is required. Current global GPP and NPP estimates mainly rely on model results, observations, model fusion methods and atmospheric isotopes changes (Field et al., 1995; Knorr and Heimann, 1995; Potter et al., 1993; Ruimy et al., 1994; Zhao et al., 2005; Ryu et al., 2011; Koffi et al., 2012; Beer et al., 2010; Welp et al., 2011). However, considerable differences exist among various studies. For example, global annual GPP is estimated at 123±8 Pg C yr^{-1} versus 150-175 Pg C yr^{-1} suggested by Beer et al. (2010) and Welp et al. (2011) respectively.

The light use efficiency (LUE) approach (Monteith, 1972; Monteith and Moss, 1977) and carboxylation rate calculation (Collatz et al., 1991; Collatz et al., 1992) are the two main methods used to estimate GPP and NPP in biogeochemical or land surface models. The LUE approach was developed realizing that growth of plant biomass is directly

proportional to absorbed solar radiation. These observations suggest that environmental variables, such as radiation can be used to estimate plant productivity circumventing the complicated calculation of detailed biochemical processes (Field et al., 1995; Knorr and Heimann, 1995; Potter et al., 1993; Ruimy et al., 1994, 1996, 1999; Prince and Goward, 1995). LUE-based models are relatively easy to apply and are still under development with more and more proxy data becoming available to drive models (Goerner et al., 2011; Jin et al 2013).

The LUE method is an effective empirical approach, therefore, parameter evaluations have been widely applied across global different plant types, and this kind of work will continue in the future. Currently, using flux tower measurements to evaluate LUE models is becoming the standard way of model evaluation. There are several widely used LUE models or algorithms, such as Moderate Resolution Imaging Spectroradiometer Primary Productivity (MODIS MOD17 product, Zhao and Running, 2010), Carnegie-Ames-Stanford Approach (CASA, Potter et al., 1993), Vegetation Photosynthesis Model (VPM, Xiao et al., 2005). Evaluation using eddy flux towers at site level (about $1km^2$) has been applied across various plant types worldwide although large biases were found. Turner et al. (2006) showed that MODIS GPP products had no overall bias over 9 sites covering several plant and land use types. However, more evaluation work suggests the ε* of MODIS GPP should be adjusted to better estimate GPP for local ecosystems. For instance, after testing MOD17 products with eddy flux tower measurements over 12 African sites, Sjöström et al. (2013) suggested ε* were underestimated in 10 savanna or grass land sites. Wang et al. (2012b) validated MOD17 products at 10 flux sites in northern China, and also found that site based ε* values were larger than that used in MOD17. The work in Chapter 2 and the first part of Chapter 3 used similar methods to evaluate ε* of cropland globally based on flux tower records and remotely sensed vegetation index.

Although the empirical characteristics of the LUE method requires plant type specific parameter values, only less than 20 vegetation type globally were separated (i.e. MODIS MOD17 product; Zhao and Running 2010) and many studies even set ε* constant globally (Potter et al., 2007). In addition, cropland usually is treated as one vegetation type, using a constant ε* in consequence in these models. However, among these main vegetation types globally, the bias is particular large over croplands (Sjöström et al., 2013; Wang et al., 2012b). The results in this thesis demonstrated a clear underestimate of model default ε* values over 8 crop types, which is in consistent with previous results. An important improvement presented in this thesis is the large number of crop types that were studied independently. ε^*_{GPP} ranged from 1.21 g C MJ^{-1} (Other perennial) to 2.96 g C MJ^{-1} (Cassava). Parallel studies found similar results which led for example to modifying the cropland ε^*_{GPP} value of the MOD17 product to 1.044 g C MJ^{-1} (Zhao and Running, 2010) compared with the previously used value of 0.68 g C MJ^{-1} (Heinsch et al., 2003).

Based on previous studies and the results in this thesis, ε^*_{GPP} in croplands exhibits a very large range. The ε^*_{GPP} value used in models usually try to represent the global average conditions, making the results at that scale match or look reasonable. An inevitable problem is then the bias at local scales or site level. Some efforts have been made to separate C_3 and C_4 plants in the models, for instance in the global production efficiency model (GLO-PEM; Prince and Goward, 1995). This is however, still far from an evaluation based on site measurements. A key question is to determine how many crop types are needed for an overall credible global result. Distinguishing hundreds of crop types in global models is unrealistic. Separating some main crops, like maize, wheat, rice and so on to cover the most important crop types is suggested in this thesis. Using both previous site results and the ε^*_{GPP} values calculated in chapter 3, maize has a larger ε^*_{GPP} value than most other crops. It is also suggested that the range of maize ε^*_{GPP} is much smaller than that of all crop types. Therefore, it is possible, and effective, to separate some widely cultivated plants rather than treat global croplands as a whole.

The creation of a new dataset of global cropland GPP is the direct consequence of the parameter valuation executed in this study. There are several widely used LUE models, however, only a few of them have publicly released their outputs. MOD17 GPP and NPP datasets are evaluated worldwide as illustrated previously in this synthesis. NPP based on CASA model is still being updated (Potter et al., 2012), and CASA is also used to further calculate fire emissions (van der Werf et al., 2010). As discussed above, to improve the dataset using LUE method, separating more plant types is an efficient way.

In addition to separating more crop types, information on the extent of different crop types is crucial to create a new cropland GPP map. Portmann et al. (2010) created such a crop type map, separating 26 crop types. This dataset was used in Chapter 3 along with a newly developed look-up table of ε^*_{GPP} combining several input data sources. The spatial resolution is 1/12 degree, which is higher than most of other current models.

A look-up table of ε^*_{GPP} for these 26 crop types is the first main task. Only 8 types could be evaluated directly using flux tower measurements as shown in Chapter 2 and 3. Fortunately, croplands are the most studied plant category previously and hundreds of ε values are available by measuring dry matter, either only above ground or total dry matter. Because these ε values cannot be used to build the look-up table directly, a conversion method was created in chapter 3 to convert ε to ε^*_{GPP} based on the assumption that environmental stresses could be ignored for well watered croplands. As a result, a global look-up table of 26 crop types was created based observational records.

A dataset of global cropland GPP in the year 2000 was created in Chapter 3 at monthly temporal and 1/12 of a degree spatial scales. There are still evaluations needed in the future to further validate this dataset. Currently, its performance over North America was confirmed by comparing with harvest based estimate (Lobell et al., 2002). Importantly, this work may also contribute to resolving an outstanding issue. Usually, ε^* values in LUE-based models are much smaller than field-based values (Lobell et al., 2002;

Potter et al., 1993; Zhang et al., 2008). This dataset only uses observational ε^*_{GPP} values. Global cropland GPP was estimated to be 11.05 Pg C yr^{-1}, falling in the middle of previous studies indicating 14.2 Pg C yr^{-1} by Beer et al. (2010) and 8.2 Pg C yr^{-1} by Saugier et al (2001). This suggests how to merge the difference between field-based ε^*_{GPP} and that in models.

The main conclusions of chapter 2 and 3 can be summarized as follows:

- The light use efficiency (LUE) approach is very suitable to estimate cropland GPP and NPP.
- FLUXNET-based ε* values are comparable to previous values reported by field measurements based on dry matter measurements.
- Cropland ε* at field level, including FLUXNET-based and literature-based in this thesis, are substantially higher than used in most vegetation models.
- A more accurate description of cropland distribution (crop types and growing periods) and sophisticated parameterization for individual crop types, will help to better use field based ε^*_{GPP} in vegetation models.
- A dataset of global monthly GPP in the year 2000 was developed at a spatial resolution of 1/12 degree yielding a global cropland GPP of 11.05 Pg C yr^{-1}.

6.2.2 Soil moisture constraints on vegetation

In chapter 4 and 5 of this thesis, we focussed on the soil moisture related impacts on vegetation, using both a drought index and remotely sensed soil moisture. A global analysis of SPEI (standardized precipitation evapotranspiration index) and NPP was presented to complement previous studies of spatial patterns of the relationship between anomalous dry or wet conditions and NPP. The Köppen climate classification was used to classify the spatial pattern into some main categories. Besides, a very prior attempt was made in chapter 5 to quantify the relationship between observational soil moisture and vegetation.

The objective of this study is to contribute to the knowledge of vegetation response to climate change, which is crucial in understanding and predicting future terrestrial carbon cycle behaviour. The spatial distribution of ecosystems as well as their growth is mainly determined by climatic factors, including water availability, solar radiation and temperature (Churkina and Running, 1998; Nemani et al., 2003; Stephenson, 1990). Water availability is a primary constraint compared to radiation and temperature (Heimann and Reichstein, 2008). Drought events impact terrestrial production and reduce the sink strength at (sub) continental scale (Ciais et al., 2005; Reichstein et al., 2007a, 2013; van der Molen et al., 2011). More importantly, since the occurrence and severity of drought are likely to increase or at least continue in the future (Dai, 2013, but see also Sheffield et al., 2012), there is a clear need to further evaluate the relationships between soil moisture and vegetation.

Reichstein et al. (2013) reviewed the impacts of climate extremes on the terrestrial carbon cycle and pointed out that drought and storms have the potential to cancel the expected increase of terrestrial carbon stocks. As mentioned above, usually this kind of studies focused on some typical extreme cases, such as the 2003 heat wave in Europe (Ciais et al., 2005; Reichstein et al., 2007a) and 2005 drought in Amazon (Phillips et al., 2009). These kinds of case studies have made robust conclusions by comprehensive analysis. In addition, some others tried to investigate the globally integrated effects of dry/wet conditions on vegetation (Gobron et al., 2010; Zhao and Running, 2010). Previous studies found that on a global scale, drought and NPP are strongly related in a positive way. It is easy to expect some spatial differences to occur, however, details of the spatial patterns of this relation are not clear. Therefore, in chapter 4 of this thesis, the spatial patterns of the relationship between SPEI and NPP are presented. Also, the rules governing those spatial patterns are key to understand. As a further step, the Köppen climate classification was used here to categorize the spatial pattern successfully. As a result, this study provides a stronger regional focus than previous work.

Drought indices have their advantages in application because usually precipitation and temperature data used to calculate drought indices are relatively well known. Drought indices are powerful tools to describe intensity, duration and spatial extent of droughts and have been widely used in analytical applications. Additionally, soil moisture data are still being developed and remarkable achievements have been reached using satellite derived indices (de Jeu et al., 2008; Dolman and de Jeu, 2010; Liu et al., 2011, 2012). Therefore, firstly, a drought index was used in chapter 4 to make a global analysis. The work in chapter 5 uses remotely sensed soil moisture directly, but on a more regional scale.

Soil moisture is an essential component in understanding the climate-soil-vegetation system both in space and time, and is directly associated with the dynamics of plant photosynthesis and respiration. Remote sensing based data are able to measure large-scale surface soil moisture continuously (de Jeu et al., 2008; Owe et al., 2008). In the last few years, near-surface soil moisture from space borne passive and active microwave instruments provided robust estimates of surface soil moisture at regional and global scales. Blending passive and active microwave soil moisture retrievals from various satellites has led to a long-term improved product with better spatial and temporal coverage than previous data sets (Liu et at., 2011, 2012). These remotely sensed soil moisture estimates offer the opportunity to evaluate the relationships between water availability and vegetation.

Global scale application is still limited due to data gaps in the time series. Therefore, a first attempt was made focusing on mainland Australia because the soil moisture data there have been well evaluated with ground-based measurements (Draper et al., 2009). Several statistical methods were used to perform a comprehensive analysis between remotely sensed soil moisture and vegetation index (i.e. NDVI).

The main conclusions of chapter 4 and 5 are summarized here:

- Drought indices, such as SPEI, are an effective and useful way to estimate the impact of drought on vegetation.
- The strong positive relation between SPEI and NPP that exists on a global scale is the result of a generally positive relation in dry regions and a coherent NPP decline with intensive drought event in humid regions, whereas NPP and SPEI were negatively related in most boreal regions.
- The spatial patterns of drought impact on NPP could be analysed using the Köppen climate classification, which suggests that the adequate prediction of vegetation in the different climate zones maybe crucial to the quantification of the behaviour of the future terrestrial carbon cycle.
- Remotely sensed soil moisture is positive related with NDVI in mainland Australia.
- NDVI typically lags behind soil moisture by one month and this indicates a typical scale of vegetation response to soil moisture shortages.
- Dry regions with low vegetation density are more sensitive to soil moisture for the high end of the distribution of NDVI than moist regions, suggesting that soil moisture enhances vegetation growth in dry regions and in the early stage in wet regions.

6.3 Limitations and future perspective

6.3.1 LUE application in GPP estimation

As discussed previously, improvements of GPP estimates using the LUE methods depend on the parameterization of ε* and model structure to present vegetation conditions and environmental stresses more accurately. Several aspects are included, such as evaluation of ε*, environmental stress description, vegetation index and the model's spatial and temporal resolution. Several vegetation indices and descriptions of environmental stresses are used in different models (Goerner et al., 2011, Jin et al 2013; Potter et al., 1993; Zhao and Running, 2010). Usually water and temperature condition are the two main factors. These models generally perform well in evaluation studies while large uncertainties still exist. Currently, all these aspects are requiring further work.

In this thesis, the global cropland GPP dataset created in chapter 3 highlights the importance of crop type separation and parameterization in dataset environments. Here, the limitations of the current work are obvious. For example, the survey data that could separate crop types over croplands was only available for the year of 2000 (Portmann et al., 2010). Croplands were separated into 26 crop types. However, not all the ε* values were estimated directly using flux tower measurements. Even a combination of FLUXNET-based and literature-based ε* values could not cover all the 26 crops. More direct field estimations of ε* with crop type information are thus needed. Besides, irrigated and rainfed croplands should be separated in the future as natural water stresses can be larger for the rainfed croplands.

6.3.2 Soil moisture constraints on vegetation

Both model and field measurement confirmed that drought could reduce vegetation production significantly. However, on large scales (regional to global), the relationships between drought and NPP are also determined by the accuracy of the modelled NPP and the data used to calculate drought index. For example, NPP values in rain forests still have great uncertainties, partly related to the low sensitivity of satellite productivity data in highly productive areas (Samanta et al., 2011; Zhao and Running 2010).

Besides the calculated drought index, soil moisture observations are in principle a better and more robust way to quantify water availability. However, the remote sensing approach also has its inherent shortcomings. Passive remote sensed soil moisture data have large errors over regions with high vegetation density (Parinussa et al., 2011). Therefore, semi-arid or arid regions were chosen where soil moisture data are more reliable to evaluate the relationships between soil moisture and NDVI. A further complication is that only the surface layer soil moisture content can be obtained by satellite observations, not that of the full root zone. Thus, currently, the analysis in this thesis could only quantify the surface hydrological cycles and its impact on vegetation. However, the shallow depth observations can be representative for soil moisture dynamics at the root zone layer. This was clearly demonstrated by Rebel et al. (2012) where they found high correlations between the satellite product and modelled root zone soil moisture.

In the future, more work on several aspects of this study is needed. The work in this thesis only quantifies the relationship between remotely sensed soil moisture and NDVI over mainland Australia. It is a typical region and a clear global conclusion in general cannot be reached yet. Extending similar work over other regions is needed, but this also depends on the data quality. Filling gaps is a precondition over many regions, and is still under development (Wang et al., 2012a). In addition, remotely sensed soil moisture offers observational records of soil water condition. Both soil moisture-NPP and precipitation-NDVI relationships have been established. Further comparison work is required to demonstrate whether there are some advantages using soil moisture than precipitation under specified conditions.

6.3.3 Integration

The amount of global GPP is not a constant but changes with time, although there are still large uncertainties in the estimate of annual average GPP. In a foreseeable future, the concentrations of atmospheric CO_2 will continue to increase due to anthropogenic carbon emission. It is clear that greenhouse gases have caused global warming, based on the latest IPCC report AR5 (Stocker et al., 2013). Due to the fertilization effects of atmospheric CO_2, modelled GPP and NPP would exhibit significant increase in the future as shown by Free-Air CO_2 Enrichment (FACE) experiments (Piao et al., 2013). Climate change will lead to different environmental stresses on plant photosynthesis processes.

The proportions of vegetation types will also change due to vegetation adaptability. Land surface cover change could be caused by both natural and anthropogenic changes. For instance, herbaceous vegetation would replace woody vegetation in some tropical areas in the future (Sitch et al., 2008). But importantly, this might also occur due to human activities, known as land use or land cover changes, such as deforestations and croplands extensions (Houghton et al., 2012). Therefore, due to human activities, croplands will contribute more to global terrestrial GPP. To improve the estimate of global croplands GPP could become more and more important.

Meanwhile, agricultural activities primarily rely on water availability, particular the case for rainfed agriculture. Even irrigated croplands are constrained by vulnerable ground water conditions. Therefore, integrating the analysis of global cropland GPP and soil moisture constraints on vegetation is a necessary next step. Current estimate of croplands GPP only focuses on the one year due to the data limitations. It is possible to extend its temporal scales, for example, using history crop areas records during 1700 to 2007 (Ramankutty and Foley 1999). If these trends continue, the prediction of cropland GPP could be also based on some designed scenarios. How well to quantify the environmental stresses on GPP needs be based on the knowledge of soil moisture constraints on vegetation. Therefore, the two topics in this thesis are closely related and will contribute to the future understanding of terrestrial carbon cycle in a combined way.

Chapter 7 Samenvatting

Dit proefschrift gaat over twee gerelateerde onderwerpen die van belang zijn bij het bestuderen van de planten en gewasgroei op land: 1) het afschatten van de productie en dus de CO_2 opname van landbouwgewassen, en 2) patronen tussen de hoeveelheid bodemvocht enerzijds en de productiviteit van vegetatie op land anderzijds. Een van de unieke aspecten van dit werk is dat beide onderwerpen op grote schalen zijn bekeken waarbij veelvuldig gebruik is gemaakt van satellietdata.

Landbouwgewassen nemen ongeveer 12% van het ijsvrije landoppervlak in beslag en vormen dus een belangrijk en dynamisch deel van de mondiale koolstofcyclus. Helaas is niet goed bekend hoeveel koolstof deze gewassen op mondiale schaal vastleggen. Door meetgegevens te vergelijken met modelgegevens heb ik allereerst laten zien dat de rol van deze gewassen in veel modellen wordt onderschat.

De belangrijkste reden van deze onderschatting is dat veel van de zogenaamde lichtgebruiksmodellen geen rekening houden met het feit dat landbouwgewassen efficiënter zijn dan de natuurlijke gewassen waar ze van afstammen. Dit heeft vele oorzaken en ik heb laten zien dat er grote verschillen in de efficiëntie van verschillende gewassen zijn. Door deze afzonderlijk te bepalen voor verschillende gewastypes op basis van metingen en literatuur, en daarna deze gegevens te combineren met een nieuwe mondiale kaart van gewastypes heb ik nauwkeurigere schattingen kunnen maken van de rol van landbouwgewassen in de mondiale koolstofcyclus. Mijn nieuwe schatting was 11×10^{15} gram koolstof per jaar, dit getal ligt ongeveer halverwege de eerdere schattingen.

Planten hebben water nodig om te groeien en droogtes beperken dus meestal plantengroei maar de exacte relaties tussen gebrek aan water en de invloed daarvan op planten is niet goed bekend. Door een nieuwe index die droogtes beter beschrijft te combineren met satellietdata van vegetatie productiviteit heb ik laten zien hoe verschillende gebieden reageren op droogte. Eerdere studies hebben laten zien dat op mondiale schaal droge jaren overeenkomen met jaren waarin de plantenwereld minder productief is, maar ik laat zien dat er belangrijke regionale verschillen zijn: in relatief droge gebieden neemt productiviteit weliswaar af met droogte maar in koudere streken neemt het vaak toe. Dit kan bijvoorbeeld doordat droogtes vaak voorkomen in periodes waarin het warm is en er veel zonlicht tot de aarde doordringt.

Ik heb deze relaties verder onderzocht door gedetailleerd Australië te bestuderen, een continent waar droogtes een negatieve invloed hebben op planten. Hier bleek dat er gemiddeld een maand vertraging zat tussen de periodes van droogte en de reactie van de plantenwereld daarop. In extreem droge gebieden reageerde de vegetatie nog sneller. Door met een aantal statistische methodes de trends te bekijken kon ik daarnaast aantonen hoe Australië in de afgelopen jaren door drie fases van droge en natte

periodes is gegaan. Dit onderzoek kan gebruikt worden om de vegetatieproductiviteit te voorspellen op basis van neerslagdata.

References

Abbate, P. E., Andrade, F. H., Culot, J. P., and Bindraban, P. S.: Grain yield in wheat: Effects of radiation during spike growth period, Field Crop. Res., 54, 245-257, DOI: 10.1016/S0378-4290(97)00059-2, 1997.

Allen, R. G., Smith, M., Pereira, L. S. and Perrier, A.: An update for the calculation of reference evapotranspiration, ICID bulletin, 43 (2), 35-92, 1994.

Allen, E. J., and Scott, R. K.: An Analysis of Growth of the Potato Crop, J Agr Sci, 94, 583-606, 1980.

Angert, A., Biraud, S., Bonfils, C., Henning, C. C., Buermann, W., Pinzon, J., Tucker, C. J., and Fung, I.: Drier summers cancel out the CO_2 uptake enhancement induced by warmer springs, P Natl Acad Sci USA, 102, 10823-10827, DOI: 10.1073/pnas.0501647102, 2005.

Asaf, D., Rotenberg, E., Tatarinov, F., Dicken, U., Montzka, S. A., and Yakir, D.: Ecosystem photosynthesis inferred from measurements of carbonyl sulphide flux, Nature Geosci, 6, 186-190, DOI: 10.1038/ngeo1730, 2013.

Asrar, G., Fuchs, M., Kanemasu, E. T., and Hatfield, J. L.: Estimating absorbed photosynthetic radiation and leaf-area index from spectral reflectance in wheat, Agron J, 76, 300-306, ,DOI: 10.2134/agronj1984.00021962007600020029x, 1984.

Aubinet, M., Moureaux, C., Bodson, B., Dufranne, D., Heinesch, B., Suleau, M., Vancutsem, F., and Vilret, A.: Carbon sequestration by a crop over a 4-year sugar beet/winter wheat/seed potato/winter wheat rotation cycle, Agr. Forest. Meteorol., 149, 407-418, DOI: 10.1016/j.agrformet.2008.09.003, 2009.

Azam-Ali, S. N., Gregory, P. J., and Monteith, J. L.: Effects of Planting Density on Water Use and Productivity of Pearl Millet (Pennisetum Typhoides) Grown on Stored Water. II. Water Use, Light Interception and Dry Matter Production, Exp Agr, 20, 215-224, DOI: 10.1017/S0014479700017786, 1984.

Baldocchi, D., Falge, E., Gu, L. H., Olson, R., Hollinger, D., Running, S., Anthoni, P., Bernhofer, C., Davis, K., Evans, R., Fuentes, J., Goldstein, A., Katul, G., Law, B., Lee, X. H., Malhi, Y., Meyers, T., Munger, W., Oechel, W., U, K. T. P., Pilegaard, K., Schmid, H. P., Valentini, R., Verma, S., Vesala, T., Wilson, K., and Wofsy, S.: FLUXNET: A new tool to study the temporal and spatial variability of ecosystem-scale carbon dioxide, water vapor, and energy flux densities, B Am Meteorol Soc, 82, 2415-2434, DOI: 10.1175/1520-0477(2001)082<2415:FANTTS>2.3.CO;2 , 2001.

Ballantyne, A. P., Alden, C. B., Miller, J. B., Tans, P. P., and White, J. W. C.: Increase in observed net carbon dioxide uptake by land and oceans during the past 50 years, Nature, 488, 70–72, DOI: 10.1038/nature11299, 2012.

Bartalis, Z., Wagner, W., Naeimi, V., Hasenauer, S., Scipal, K., Bonekamp, H., Figa, J., and Anderson, C.: Initial soil moisture retrievals from the METOP-A Advanced Scatterometer (ASCAT), Geophys Res Lett, 34, L20401, DOI: 10.1029/2007gl091088, 2007.

Beck, H. E., McVicar, T. R., van Dijk, A. I. J. M., Schellekens, J., de Jeu, R. A. M., and Bruijnzeel, L. A.: Global evaluation of four AVHRR-NDVI data sets: Intercomparison and assessment against Landsat imagery, Remote Sensing of Environment, 115, 2547-2563, DOI: 10.1016/j.rse.2011.05.012, 2011.

Beer, C., Reichstein, M., Tomelleri, E., Ciais, P., Jung, M., Carvalhais, N., Rodenbeck, C., Arain, M. A., Baldocchi, D., Bonan, G. B., Bondeau, A., Cescatti, A., Lasslop, G., Lindroth, A., Lomas, M., Luyssaert, S., Margolis, H., Oleson, K. W., Roupsard, O., Veenendaal, E., Viovy, N., Williams, C., Woodward, F. I., and Papale, D.: Terrestrial gross carbon dioxide uptake: global distribution and covariation with climate, Science, 329, 834-838, DOI: 10.1126/science.1184984, 2010.

Begue, A., Desprat, J. F., Imbernon, J., and Baret, F.: Radiation use efficiency of Pearl-Millet in the Sahelian zone, Agr. Forest. Meteorol., 56, 93-110, DOI: 10.1016/0168-1923(91)90106-Z, 1991.

Bell, M. J., Muchow, R. C., and Wilson, G. L.: The Effect of plant-population on peanuts (arachis-hypogaea) in a monsoonal tropical environment, Field Crop. Res., 17, 91-107, DOI: 10.1016/0378-4290(87)90085-2, 1987.

Bingham, I. J., Blake, J., Foulkes, M. J., and Spink, J.: Is barley yield in the UK sink limited? I. Post-anthesis radiation interception, radiation-use efficiency and source-sink balance, Field Crop. Res., 101, 198-211, DOI: 10.1016/j.fcr.2006.11.005, 2007.

Biscoe, P. V., and Gallagher, J. N.: Weather, dry matter production and yield. Environmental Effects on Crop Physiology (Ed. by J.J. Landsberg & C. V. Cutting), pp. 75-100. Academic Press, London, 1977.

Brown, H. E., Moot, D. J., and Teixeira, E. I.: Radiation use efficiency and biomass partitioning of lucerne (Medicago sativa) in a temperate climate, Eur. J. Agron., 25, 319-327, 2006.

Boden, T.A., Marland, G. and Andres R.J.: Global, Regional, and National Fossil-Fuel CO_2 Emissions. Carbon Dioxide Information Analysis Center, Oak Ridge National Laboratory, U.S. Department of Energy, Oak Ridge, Tenn., U.S.A. DOI: 10.3334/CDIAC/00001_V2012, 2012.

Boker, S. M., Xu, M. Q., Rotondo, J. L., and King, K.: Windowed cross-correlation and peak picking for the analysis of variability in the association between behavioral time series, Psychol Methods, 7, 338-355, DOI: 10.1037//1082-989x.7.3.338, 2002.

Bonan, G. B., Lawrence, P. J., Oleson, K. W., Levis, S., Jung, M., Reichstein, M., Lawrence, D. M., and Swenson, S. C.: Improving canopy processes in the Community Land Model version 4 (CLM4) using global flux fields empirically inferred from FLUXNET data, J Geophys Res-Biogeo, 116, G02014, DOI: 10.1029/2010jg001593, 2011.

Brocca, L., Hasenauer, S., Lacava, T., Melone, F., Moramarco, T., Wagner, W., Dorigo, W., Matgen, P., Martinez-Fernandez, J., Llorens, P., Latron, J., Martin, C., and Bittelli, M.: Soil moisture estimation through ASCAT and AMSR-E sensors: An intercomparison and validation study across Europe, Remote Sensing of Environment, 115, 3390-3408, DOI: 10.1016/j.rse.2011.08.003, 2011.

Cade, B. S., and Noon, B. R.: A gentle introduction to quantile regression for ecologists, Front Ecol Environ, 1, 412-420, DOI: 10.1890/1540-9295(2003)001[0412:AGITQR]2.0.CO;2, 2003.

Caldeira, K., and Wickett, M. E.: Anthropogenic carbon and ocean pH, Nature, 425, 365-365, DOI: 10.1038/425365a, 2003.

Canadell, J. G., Le Quéré, C., Raupach, M. R., Field, C. B., Buitenhuis, E. T., Ciais, P., Conway, T. J., Gillett, N. P., Houghton, R. A., and Marland, G.: Contributions to accelerating atmospheric CO_2 growth from economic activity, carbon intensity, and efficiency of natural sinks, P Natl Acad Sci USA, 104, 18866-18870, DOI: 10.1073/pnas.0702737104, 2007.

Cannell, M. G. R., Milne, R., Sheppard, L. J., and Unsworth, M. H.: Radiation interception and productivity of willow, J Appl Ecol, 24, 261-278, 1987.

Caviglia, O. P., and Sadras, V. O.: Effect of nitrogen supply on crop conductance, water- and radiation-use efficiency of wheat, Field Crop. Res., 69, 259-266, DOI: 10.1016/S0378-4290(00)00149-0, 2001.

Ceschia, E., Beziat, P., Dejoux, J. F., Aubinet, M., Bernhofer, C., Bodson, B., Buchmann, N., Carrara, A., Cellier, P., Di Tommasi, P., Elbers, J. A., Eugster, W., Grunwald, T., Jacobs, C. M. J., Jans, W. W. P., Jones, M., Kutsch, W., Lanigan, G., Magliulo, E., Marloie, O., Moors, E. J., Moureaux, C., Olioso, A., Osborne, B., Sanz, M. J., Saunders, M., Smith, P., Soegaard, H., and Wattenbach, M.: Management effects on net ecosystem carbon and GHG budgets at European crop sites, Agr. Ecosyst. Environ., 139, 363-383, DOI: 10.1016/j.agee.2010.09.020, 2010.

Changnon, S. A., and Easterling, W. E.: Measuring drought impacts - the Illinois case, Water Resour Bull, 25, 27-42, DOI: 10.1111/j.1752-1688.1989.tb05663.x, 1989.

Charles-Edwards, D. A.: Physiological Determinants of Crop Growth. Academic Press, London. 1982.

Chen, J. M., Chen, B. Z., Higuchi, K., Liu, J., Chan, D., Worthy, D., Tans, P., and Black, A.: Boreal ecosystems sequestered more carbon in warmer years, Geophys Res Lett, 33, L10803, DOI: 10.1029/2006gl025919, 2006.

Chen, J. M., Mo, G., Pisek, J., Liu, J., Deng, F., Ishizawa, M., and Chan, D.: Effects of foliage clumping on the estimation of global terrestrial gross primary productivity, Global Biogeochem Cy, 26, GB1019, DOI: 10.1029/2010gb003996, 2012.

Chen, S. P., Chen, J. Q., Lin, G. H., Zhang, W. L., Miao, H. X., Wei, L., Huang, J. H., and Han, X. G.: Energy balance and partition in Inner Mongolia steppe ecosystems with different land use types, Agr. Forest. Meteorol., 149, 1800-1809, DOI: 10.1016/j.agrformet.2009.06.009, 2009.

Chen, T. X., van der Werf, G. R., Dolman, A. J., and Groenendijk, M.: Evaluation of cropland maximum light use efficiency using eddy flux measurements in North America and Europe, Geophys Res Lett, 38, L14707, DOI: 10.1029/2011gl047533, 2011.

Choler, P., Sea, W., and Leuning, R.: A benchmark test for ecohydrological models of interannual variability of NDVI in semi-arid tropical grasslands, Ecosystems, 14, 183-197, DOI: 10.1007/s10021-010-9403-9, 2011.

Churkina, G., and Running, S. W.: Contrasting climatic controls on the estimated productivity of global terrestrial biomes, Ecosystems, 1, 206-215, DOI: 10.1007/s100219900016, 1998.

Ciais, P., Denning, A. S., Tans, P. P., Berry, J. A., Randall, D. A., Collatz, G. J., Sellers, P. J., White, J. W. C., Trolier, M., Meijer, H. A. J., Francey, R. J., Monfray, P., and Heimann, M.: A three-dimensional synthesis study of δ18O in atmospheric CO_2: 1. Surface fluxes, Journal of Geophysical Research: Atmospheres, 102, 5857-5872, DOI: 10.1029/96JD02360, 1997.

Ciais, P., Reichstein, M., Viovy, N., Granier, A., Ogee, J., Allard, V., Aubinet, M., Buchmann, N., Bernhofer, C., Carrara, A., Chevallier, F., De Noblet, N., Friend, A. D., Friedlingstein, P., Grunwald, T., Heinesch, B., Keronen, P., Knohl, A., Krinner, G., Loustau, D., Manca, G., Matteucci, G., Miglietta, F., Ourcival, J. M., Papale, D., Pilegaard, K., Rambal, S., Seufert, G., Soussana, J. F., Sanz, M. J., Schulze, E. D., Vesala, T., and Valentini, R.: Europe-wide reduction in primary productivity caused by the heat and drought in 2003, Nature, 437, 529-533, DOI: 10.1038/Nature03972, 2005.

Clover, G. R. G., Jaggard, K. W., Smith, H. G., and Azam-Ali, S. N.: The use of radiation interception and transpiration to predict the yield of healthy, droughted and virus-infected sugar beet, J Agr Sci, 136, 169-178, 2001.

Collatz, G. J., Ball, J. T., Grivet, C., and Berry, J. A.: Physiological and environmental-regulation of stomatal conductance, photosynthesis and transpiration - a model that includes a laminar boundary-layer, Agr Forest Meteorol, 54, 107-136, DOI: 10.1016/0168-1923(91)90002-8, 1991.

Collatz, G. J., Ribas-Carbo, M., and Berry, J. A.: Coupled photosynthesis-stomatal conductance model for leaves of C_4 plants, Aust J Plant Physiol, 19, 519-538, DOI: 10.1071/PP9920519, 1992.

Connolly, J., Roulet, N. T., Seaquist, J. W., Holden, N. M., Lafleur, P. M., Humphreys, E. R., Heumann, B. W., and Ward, S. M.: Using MODIS derived fPAR with ground based flux tower measurements to derive the light use efficiency for two Canadian peatlands, Biogeosciences, 6, 225-234, DOI: 10.5194/bg-6-225-2009, 2009.

Cook, E. R., Woodhouse, C. A., Eakin, C. M., Meko, D. M., and Stahle, D. W.: Long-term aridity changes in the western United States, Science, 306, 1015-1018, DOI: 10.1126/science.1102586, 2004.

Dai, A. G.: Increasing drought under global warming in observations and models, Nat Clim Change, 3, 52-58, DOI: 10.1038/Nclimate1633, 2013.

de Jeu, R. A. M., Wagner, W., Holmes, T. R. H., Dolman, A. J., van de Giesen, N. C., and Friesen, J.: Global soil moisture patterns observed by space borne microwave radiometers and scatterometers, Surv Geophys, 29, 399-420, DOI: 10.1007/s10712-008-9044-0, 2008.

del Amor, F. M., and Gomez-Lopez, M. D.: Agronomical response and water use efficiency of sweet pepper plants grown in different greenhouse substrates, Hortscience, 44, 810-814, 2009.

DeLucia, E. H., Drake, J. E., Thomas, R. B., and Gonzalez-Meler, M.: Forest carbon use efficiency: is respiration a constant fraction of gross primary production? Global Change Biol, 13, 1157-1167, DOI: 10.1111/j.1365-2486.2007.01365.x, 2007.

Department of the Environment, Water, Heritage and the Arts (2012a).Interim Biogeographic Regionalisation for Australia, (IBRA), Version 7. http: //www.environment.gov.au/parks/nrs/ science/bioregion-framework/ibra/index.html, (last accessed June, 2013).

Department of the Environment, Water, Heritage and the Arts (2012b).TerrestrialEcoregions in Australia. http: //www.environment.gov.au/parks/nrs/science/bioregion-framework/ terrestrial-habitats.html, (last accessed June, 2013).

Dercas, N., and Liakatas, A.: Water and radiation effect on sweet sorghum productivity, Water Resour. Manag., 21, 1585-1600, 10.1007/s11269-006-9115-2, 2007.

Ed Dlugokencky and Pieter Tans, NOAA/ESRL (www.esrl.noaa.gov/gmd/ccgg/trends/).

Dolman, A. J., and de Jeu, R. A. M.: Evaporation in focus, Nat Geosci, 3, 296-296, DOI: 10.1038/Cgeo849, 2010.

Donohue, R. J., McVicar, T. R., and Roderick, M. L.: Climate-related trends in Australian vegetation cover as inferred from satellite observations, 1981-2006, Global Change Biol, 15, 1025-1039, DOI: 10.1111/j.1365-2486.2008.01746.x, 2009.

Donohue, R. J., Roderick, M. L., and McVicar, T. R.: Roots, storms and soil pores: Incorporating key ecohydrological processes into Budyko's hydrological model, J Hydrol, 436, 35-50, DOI: 10.1016/j.jhydrol.2012.02.033, 2012.

Donohue, R. J., Roderick, M. L., McVicar, T. R., and Farquhar, G. D.: Impact of CO_2 fertilization on maximum foliage cover across the globe's warm, arid environments, Geophys Res Lett, 40, 3031-3035, DOI: 10.1002/grl.50563, 2013.

Dorigo, W., de Jeu, R., Chung, D., Parinussa, R., Liu, Y., Wagner, W., and Fernandez-Prieto, D.: Evaluating global trends (1988-2010) in harmonized multi-satellite surface soil moisture, Geophys Res Lett, 39, L18405, DOI: 10.1029/2012gl052988, 2012.

Dorigo, W. A., Scipal, K., Parinussa, R. M., Liu, Y. Y., Wagner, W., de Jeu, R. A. M., and Naeimi, V.: Error characterisation of global active and passive microwave soil moisture datasets, Hydrol Earth Syst Sc, 14, 2605-2616, DOI: 10.5194/hess-14-2605-2010, 2010.

Draper, C. S., Walker, J. P., Steinle, P. J., de Jeu, R. A. M., and Holmes, T. R. H.: An evaluation of AMSR-E derived soil moisture over Australia, Remote Sensing of Environment, 113, 703-710, DOI: 10.1016/j.rse.2008.11.011, 2009.

Dunkerley, D.: Measuring interception loss and canopy storage in dryland vegetation: a brief review and evaluation of available research strategies, Hydrol Process, 14, 669-678, DOI: 10.1002/(SICI)1099-1085(200003)14: 4<669: : AID-HYP965>3.0.CO;2-I, 2000.

Dunkerley, D. L., and Booth, T. L.: Plant canopy interception of rainfall and its significance in a banded landscape, arid western New South Wales, Australia, Water Resour Res, 35, 1581-1586, DOI: 10.1029/1999WR900003, 1999.

Dunkerley, D. L.: Infiltration rates and soil moisture in a groved mulga community near Alice Springs, arid central Australia: evidence for complex internal rainwater redistribution in a runoff-runon landscape, J Arid Environ, 51, 199-219, DOI: 10.1006/jare.2001.0941, 2002.

Dunkerley, D. L.: Intra-storm evaporation as a component of canopy interception loss in dryland shrubs: observations from Fowlers Gap, Australia, Hydrol Process, 22, 1985-1995, DOI: 10.1002/hyp.6783, 2008.

Ekström, M., Jones, P. D., Fowler, H. J., Lenderink, G., Buishand, T. A., and Conway, D.: Regional climate model data used within the SWURVE project 1: projected changes in seasonal patterns and estimation of PET, Hydrol Earth Syst Sc, 11, 1069-1083, DOI: 10.5194/hess-11-1069-2007, 2007.

Farquhar, G. D., Lloyd, J., Taylor, J. A., Flanagan, L. B., Syvertsen, J. P., Hubick, K. T., Wong, S. C., and Ehleringer, J. R.: Vegetation effects on the isotope composition of oxygen in atmospheric CO_2, Nature, 363, 439-443, 1993.

Fasheun, A., and Dennett, M. D.: Interception of radiation and growth efficiency in field beans (Vicia-Faba L), Agr. Meteorol., 26, 221-229, DOI: 10.1016/0002-1571(82)90033-4, 1982.

Field, C. B., Randerson, J. T., and Malmstrom, C. M.: Global net primary production - combining ecology and remote-sensing, Remote Sensing of Environment, 51, 74-88, DOI: 10.1016/0034-4257(94)00066-V, 1995.

Field, C. B., Behrenfeld, M. J., Randerson, J. T., and Falkowski, P.: Primary production of the biosphere: Integrating terrestrial and oceanic components, Science, 281, 237-240, DOI: 10.1126/science.281.5374.237, 1998.

Fischer, M. L., Billesbach, D. P., Berry, J. A., Riley, W. J., and Torn, M. S.: Spatiotemporal variations in growing season exchanges of CO_2, H_2O, and sensible heat in agricultural fields of the Southern Great Plains, Earth Interact., 11, DOI: 10.1175/EI231.1 2007.

Foulkes, M. J., Snape, J. W., Shearman, V. J., Reynolds, M. P., Gaju, O., and Sylvester-Bradley, R.: Genetic progress in yield potential in wheat: recent advances and future prospects, J. Agr. Sci., 145, 17-29, DOI: 10.1017/S0021859607006740, 2007.

Friedlingstein, P., Cox, P., Betts, R., Bopp, L., Von Bloh, W., Brovkin, V., Cadule, P., Doney, S., Eby, M., Fung, I., Bala, G., John, J., Jones, C., Joos, F., Kato, T., Kawamiya, M., Knorr, W., Lindsay, K., Matthews, H. D., Raddatz, T., Rayner, P., Reick, C., Roeckner, E., Schnitzler, K. G., Schnur, R., Strassmann, K., Weaver, A. J., Yoshikawa, C., and Zeng, N.: Climate-carbon cycle feedback analysis: Results from the (CMIP)-M-4 model intercomparison, J Climate, 19, 3337-3353, DOI: 10.1175/JCLI3800.1, 2006.

Friedlingstein, P., Houghton, R. A., Marland, G., Hackler, J., Boden, T. A., Conway, T. J., Canadell, J. G., Raupach, M. R., Ciais, P., and Le Quéré, C.: Update on CO_2 emissions, Nat Geosci, 3, 811-812, DOI: 10.1038/ngeo1022, 2010.

Gallagher, J. N., and Biscoe, P. V.: Radiation absorption, growth and yield of cereals, J. Agr. Sci., 91, 47-60, 1978.

Gao, H., Wood, E. F., Jackson, T. J., Drusch, M., and Bindlish, R.: Using TRMM/TMI to retrieve surface soil moisture over the southern United States from 1998 to 2002, J Hydrometeorol, 7, 23-38, DOI: 10.1175/JHM473.1, 2006.

Glenn, E. P., Doody, T. M., Guerschman, J. P., Huete, A. R., King, E. A., McVicar, T. R., Van Dijk, A. I. J. M., Van Niel, T. G., Yebra, M., and Zhang, Y. Q.: Actual evapotranspiration estimation by ground and remote sensing methods: the Australian experience, Hydrol Process, 25, 4103-4116, DOI: 10.1002/hyp.8391, 2011.

Gobron, N., Belward, A., Pinty, B., and Knorr, W.: Monitoring biosphere vegetation 1998-2009, Geophys Res Lett, 37, L15402, DOI: 10.1029/2010gl043870, 2010.

Goerner, A., Reichstein, M., Tomelleri, E., Hanan, N., Rambal, S., Papale, D., Dragoni, D., and Schmullius, C.: Remote sensing of ecosystem light use efficiency with MODIS-based PRI, Biogeosciences, 8, 189-202, DOI: 10.5194/bg-8-189-2011, 2011.

Goulden, M. L., Munger, J. W., Fan, S. M., Daube, B. C., and Wofsy, S. C.: Exchange of carbon dioxide by a deciduous forest: Response to interannual climate variability, Science, 271, 1576-1578, DOI: 10.1126/science.271.5255.1576, 1996.

Haberl, H., Erb, K. H., Krausmann, F., Gaube, V., Bondeau, A., Plutzar, C., Gingrich, S., Lucht, W., and Fischer-Kowalski, M.: Quantifying and mapping the human appropriation of net primary production in earth's terrestrial ecosystems, Proceedings of the National Academy of Sciences, 104, 12942-12947, DOI: 10.1073/pnas.0704243104, 2007.

Hand, D. W., Sweeney, D. G., Hunt, R., and Wilson, J. W.: Integrated analysis of growth and light interception in winter lettuce .2. differences between cultivars, Ann. Bot-London, 56, 673-682, 1985.

Hansen, J., Ruedy, R., Glascoe, J., and Sato, M.: GISS analysis of surface temperature change, J Geophys Res-Atmos, 104, 30997-31022, DOI: 10.1029/1999jd900835, 1999.

Haverkort, A. J., and Harris, P. M.: A model for potato growth and yield under tropical highland conditions, Agr. Forest. Meteorol., 39, 271-282, DOI: 10.1016/0168-1923(87)90020-7, 1987.

Haxeltine, A., and Prentice, I. C.: A general model for the light-use efficiency of primary production, Funct. Ecol., 10, 551-561, 1996.

Heim, R. R.: A review of twentieth-century drought indices used in the United States, B Am Meteorol Soc, 83, 1149-1165, 2002.

Heimann, M. and Keeling, C. D.: A three-dimensional model of atmospheric CO_2 transport based on observed winds: 2. Model description and simulated tracer experiments. In: Aspects of Climate Variability in the Pacific and the Western Americas (ed. D. H.Peterson). American Geophysical Union, Washington, D.C., 237–275. 1989.

Heimann, M., and Reichstein, M.: Terrestrial ecosystem carbon dynamics and climate feedbacks, Nature, 451, 289-292, DOI: 10.1038/Nature06591, 2008.

Heinsch, F. A., Reeves, M., Votava, P., Kang, S., Milesi, C., Zhao, M., Glassy, J., Jolly, W. M., Loehman, R., Bowker, C. F., Kimball, J. S., Nemani, R. R., and Running, S. W.: User's Guide, GPP and NPP (MOD17A2/A3) Products, NASA MODIS Land Algorithm, 2003.

Hicke, J. A., Lobell, D. B., and Asner, G. P.: Cropland area and Net Primary Production computed from 30 years of USDA agricultural harvest data, Earth Interact., 8, 1-20, DOI: 10.1175/1087-3562 (2004)008<0001:CAANPP>2.0.CO; 2, 2004.

Hirschi, M., Seneviratne, S. I., Alexandrov, V., Boberg, F., Boroneant, C., Christensen, O. B., Formayer, H., Orlowsky, B., and Stepanek, P.: Observational evidence for soil-moisture impact on hot extremes in southeastern Europe, Nat Geosci, 4, 17-21, DOI: 10.1038/ngeo1032, 2011.

Houghton, R. A., House, J. I., Pongratz, J., van der Werf, G. R., DeFries, R. S., Hansen, M. C., Le Quéré, C., and Ramankutty, N.: Carbon emissions from land use and land-cover change, Biogeosciences, 9, 5125-5142, DOI: 10.5194/bg-9-5125-2012, 2012.

Huffman, G. J., Adler, R. F., Morrissey, M. M., Bolvin, D. T., Curtis, S., Joyce, R., McGavock, B., and Susskind, J.: Global precipitation at one-degree daily resolution from multisatellite observations, J Hydrometeorol, 2, 36-50, DOI: 10.1175/1525-7541(2001)002<0036: GPAODD>2.0.CO;2, 2001.

Hughes, G., and Keatinge, J. D. H.: Solar-radiation interception, dry-matter production and yield in pigeonpea (cajanus-cajan (l) millspaugh), Field Crop. Res., 6, 171-178, DOI: 10.1016/0378-4290(83)90058-8, 1983.

Indermuhle, A., Stocker, T. F., Joos, F., Fischer, H., Smith, H. J., Wahlen, M., Deck, B., Mastroianni, D., Tschumi, J., Blunier, T., Meyer, R., and Stauffer, B.: Holocene carbon-cycle dynamics based on CO_2 trapped in ice at Taylor Dome, Antarctica, Nature, 398, 121-126, DOI: 10.1038/18158, 1999.

Jamieson, P. D., Porter, J. R., and Wilson, D. R.: A test of the computer-simulation model archwheat1 on wheat crops grown in New-Zealand, Field Crop. Res., 27, 337-350, 1991.

Jamieson, P. D., Martin, R. J., Francis, G. S., and Wilson, D. R.: Drought effects on biomass production and radiation-use efficiency in barley, Field Crop. Res., 43, 77-86, DOI: 10.1016/0378-4290(95)00042-O, 1995.

Ji, L., and Peters, A. J.: Assessing vegetation response to drought in the northern Great Plains using vegetation and drought indices, Remote Sensing of Environment, 87, 85-98, DOI: 10.1016/S0034-4257(03)00174-3, 2003.

Jin, C., Xiao, X. M., Merbold, L., Arneth, A., Veenendaal, E., and Kutsch, W. L.: Phenology and gross primary production of two dominant savanna woodland ecosystems in Southern Africa, Remote Sensing of Environment, 135, 189-201, DOI: 10.1016/j.rse.2013.03.033, 2013.

Jung, M., Reichstein, M., Ciais, P., Seneviratne, S. I., Sheffield, J., Goulden, M. L., Bonan, G., Cescatti, A., Chen, J. Q., de Jeu, R., Dolman, A. J., Eugster, W., Gerten, D., Gianelle, D., Gobron, N., Heinke, J., Kimball, J., Law, B. E., Montagnani, L., Mu, Q. Z., Mueller, B., Oleson, K., Papale, D., Richardson, A. D., Roupsard, O., Running, S., Tomelleri, E., Viovy, N., Weber, U., Williams, C., Wood, E., Zaehle, S., and Zhang, K.: Recent decline in the global land evapotranspiration trend due to limited moisture supply, Nature, 467, 951-954, DOI: 10.1038/Nature09396, 2010.

Jung, M., Vetter, M., Herold, M., Churkina, G., Reichstein, M., Zaehle, S., Ciais, P., Viovy, N., Bondeau, A., Chen, Y., Trusilova, K., Feser, F., and Heimann, M.: Uncertainties of modeling gross primary productivity over Europe: A systematic study on the effects of using different drivers and terrestrial biosphere models, Global Biogeochem Cy, 21, GB4021, DOI: 10.1029/2006gb002915, 2007.

Justes, E., Denoroy, P., Gabrielle, B., and Gosse, G.: Effect of crop nitrogen status and temperature on the radiation use efficiency of winter oilseed rape, Eur. J. Agron., 13, 165-177, DOI: 10.1016/S1161-0301(00)00072-1, 2000.

Katsura, K., Maeda, S., Horie, T., and Shiraiwa, T.: Analysis of yield attributes and crop physiological traits of Liangyoupeijiu, a hybrid rice recently bred in China, Field Crop. Res., 103, 170-177, DOI: 10.1016/j.fcr.2007.06.001, 2007.

Kemanian, A. R., Stockle, C. O., and Huggins, D. R.: Variability of barley radiation-use efficiency, Crop Sci., 44, 1662-1672, DOI: 10.2135/cropsci2004.1662, 2004.

Kiniry, J. R., Jones, C. A., Otoole, J. C., Blanchet, R., Cabelguenne, M., and Spanel, D. A.: Radiation-use efficiency in biomass accumulation prior to grain-filling for 5 grain-crop species, Field Crop Res, 20, 51-64, DOI: 10.1016/0378-4290(89)90023-3, 1989.

Knorr, W., and Heimann, M.: Impact of Drought Stress and Other Factors on Seasonal Land Biosphere CO_2 Exchange Studied through an Atmospheric Tracer Transport Model, Tellus B, 47, 471-489, DOI: 10.1034/j.1600-0889.47.issue4.7.x, 1995.

Knorr, W., Gobron, N., Scholze, M., Kaminski, T., Schnur, R., and Pinty, B.: Impact of terrestrial biosphere carbon exchanges on the anomalous CO_2 increase in 2002-2003, Geophys Res Lett, 34, L09703, DOI: 10.1029/2006GL029019, 2007.

Knorr, W.: Is the airborne fraction of anthropogenic CO_2 emissions increasing? Geophys Res Lett, 36, L21710, DOI: 10.1029/2009GL040613, 2009.

Koenker, R., and Bassett, G.: Regression Quantiles, Econometrica, 46, 33-50, 1978.

Koenker, R., and Hallock, K. F.: Quantile regression, J Econ Perspect, 15, 143-156, 2001.

Koffi, E. N., Rayner, P. J., Scholze, M., and Beer, C.: Atmospheric constraints on gross primary productivity and net ecosystem productivity: Results from a carbon-cycle data assimilation system, Global Biogeochem Cy, 26, Gb1024, DOI: 10.1029/2010gb003900, 2012.

Koizumi, H., Usami, Y., and Satoh, M.: Annual net primary production and efficiency of solar-energy utilization in 3 double-cropping agroecosystems in Japan, Agr. Ecosyst. Environ., 32, 241-255, 1990.

Kooman, P. L., Fahem, M., Tegera, P., and Haverkort, A. J.: Effects of climate on different potato genotypes .1. Radiation interception, total and tuber dry matter production, Eur. J. Agron., 5, 193-205, DOI: 10.1016/S1161-0301(96)02031-X, 1996.

Kottek, M., Grieser, J., Beck, C., Rudolf, B., and Rubel, F.: World map of the Koppen-Geiger climate classification updated, Meteorol Z, 15, 259-263, DOI: 10.1127/0941-2948/2006/0130, 2006.

Kutsch, W. L., Aubinet, M., Buchmann, N., Smith, P., Osborne, B., Eugster, W., Wattenbach, M., Schrumpf, M., Schulze, E. D., Tomelleri, E., Ceschia, E., Bernhofer, C., Beziat, P., Carrara, A., Di Tommasi, P., Grunwald, T., Jones, M., Magliulo, V., Marloie, O., Moureaux, C., Olioso, A., Sanz, M. J., Saunders, M., Sogaard, H., and Ziegler, W.: The net biome production of full crop rotations in Europe, Agr. Ecosyst. Environ., 139, 336-345, DOI: 10.1016/j.agee.2010.07.016, 2010.

Lasslop, G., Reichstein, M., Papale, D., Richardson, A. D., Arneth, A., Barr, A., Stoy, P., and Wohlfahrt, G.: Separation of net ecosystem exchange into assimilation and respiration using a light response curve approach: critical issues and global evaluation, Global Change Biol, 16, 187-208, DOI: 10.DOI: 1/j.1365-2486.2009.02041.x, 2010.

Landsberg, J. J., Prince, S. D., Jarvis, P. G., McMurtrie, R. E., Luxmoore, R., and Medlyn, B. E.: Energy conversion and use in forests: An analysis of forest production in terms of radiation utilisation efficiency (ε). In The use of remote sensing in the modeling of forest productivity, pp. 273-298, Springer Netherlands, 1997.

Le Quéré, C., Andres, R. J., Boden, T., Conway, T., Houghton, R. A., House, J. I., Marland, G., Peters, G. P., van der Werf, G. R., Ahlström, A., Andrew, R. M., Bopp, L., Canadell, J. G., Ciais, P., Doney, S. C., Enright, C., Friedlingstein, P., Huntingford, C., Jain, A. K., Jourdain, C., Kato, E., Keeling, R. F., Klein Goldewijk, K., Levis, S., Levy, P., Lomas, M., Poulter, B., Raupach, M. R., Schwinger, J., Sitch, S., Stocker, B. D., Viovy, N., Zaehle, S., and Zeng, N.: The global carbon budget 1959–2011, Earth Syst. Sci. Data, 5, 165-185, DOI: 10.5194/essd-5-165-2013, 2013.

Le Quéré, C., Raupach, M. R., Canadell, J. G., Marland, G., Bopp, L., Ciais, P., Conway, T. J., Doney, S. C., Feely, R. A., Foster, P., Friedlingstein, P., Gurney, K., Houghton, R. A., House, J. I., Huntingford, C., Levy, P. E., Lomas, M. R., Majkut, J., Metzl, N., Ometto, J. P., Peters, G. P., Prentice, I. C., Randerson, J. T., Running, S. W., Sarmiento, J. L., Schuster, U., Sitch, S., Takahashi, T., Viovy, N., van der Werf, G. R., and Woodward, F. I.: Trends in the sources and sinks of carbon dioxide, Nat Geosci, 2, 831-836, DOI: 10.1038/ngeo689, 2009.

Leblanc, M., Tweed, S., Van Dijk, A., and Timbal, B.: A review of historic and future hydrological changes in the Murray-Darling Basin, Global Planet Change, 80-81, 226-246, DOI: 10.1016/j.gloplacha.2011.10.012, 2012.

Leepipatpaiboon, S., Boonyawat, S., and Sarobol, E.: Estimation of solar radiation use efficiency in paddy and cassava fields, Kasetsart J, Nat. Sci., 43, 642 - 649 2009.

Legg, B. J., Day, W., Lawlor, D. W., and Parkinson, K. J.: Effects of drought on barley growth - models and measurements showing the relative importance of leaf area and photosynthetic rate, J. Agr. Sci., 92, 703-716, 1979.

Lenton, A., Codron, F., Bopp, L., Metzl, N., Cadule, P., Tagliabue, A., and Le Sommer, J.: Stratospheric ozone depletion reduces ocean carbon uptake and enhances ocean acidification, Geophys Res Lett, 36, L12606, DOI: 10.1029/2009gl038227, 2009.

Lewis, S. L., Brando, P. M., Phillips, O. L., van der Heijden, G. M. F., and Nepstad, D.: The 2010 Amazon Drought, Science, 331, 554-554, DOI: 10.1126/science.1200807, 2011.

Lindquist, J. L., Arkebauer, T. J., Walters, D. T., Cassman, K. G., and Dobermann, A.: Maize radiation use efficiency under optimal growth conditions, Agron. J., 97, 72-78, 2005.

Liu, Y., de Jeu, R. A. M., van Dijk, A. I. J.M., and Owe, M.: TRMM-TMI satellite observed soil moisture and vegetation density (1998–2005) show strong connection with El Nino in eastern Australia. Geophysical Research Letters, 34, L15401, DOI: 10.1029/2007GL030311, 2007.

Liu, Y. Y., Parinussa, R. M., Dorigo, W. A., de Jeu, R. A. M., Wagner, W., van Dijk, A. I. J. M., McCabe, M. F., and Evans, J. P.: Developing an improved soil moisture dataset by blending passive and active microwave satellite-based retrievals, Hydrol Earth Syst Sc, 15, 425-436, DOI: 10.5194/hess-15-425-2011, 2011.

Liu, Y. Y., Dorigo, W. A., Parinussa, R. M., de Jeu, R. A. M., Wagner, W., McCabe, M. F., Evans, J. P., and van Dijk, A. I. J. M.: Trend-preserving blending of passive and active microwave soil moisture retrievals, Remote Sensing of Environment, 123, 280-297, DOI: 10.1016/j.rse.2012.03.014, 2012.

Litton, C. M., Raich, J. W., and Ryan, M. G.: Carbon allocation in forest ecosystems, Global Change Biol, 13, 2089-2109, DOI: 10.1111/j.1365-2486.2007.01420.x, 2007.

Lobell, D. B., Hicke, J. A., Asner, G. P., Field, C. B., Tucker, C. J., and Los, S. O.: Satellite estimates of productivity and light use efficiency in United States agriculture, 1982-98, Global Change Biol, 8, 722-735, DOI: 10.1046/j.1365-2486.2002.00503.x, 2002.

Lotsch, A., Friedl, M. A., Anderson, B. T., and Tucker, C. J.: Coupled vegetation-precipitation variability observed from satellite and climate records, Geophys Res Lett, 30, 1774, DOI: 10.1029/2003gl017506, 2003.

Lu, H., Raupach, M. R., McVicar, T. R., and Barrett, D. J.: Decomposition of vegetation cover into woody and herbaceous components using AVHRR NDVI time series. Remote Sensing of Environment, 86, 1–18, DOI: 10.1016/S0034-4257(03)00054-3, 2003.

Lucht, W., Prentice, I. C., Myneni, R. B., Sitch, S., Friedlingstein, P., Cramer, W., Bousquet, P., Buermann, W., and Smith, B.: Climatic control of the high-latitude vegetation greening trend and Pinatubo effect, Science, 296, 1687-1689, DOI: 10.1126/science.1071828, 2002.

Luthi, D., Le Floch, M., Bereiter, B., Blunier, T., Barnola, J. M., Siegenthaler, U., Raynaud, D., Jouzel, J., Fischer, H., Kawamura, K., and Stocker, T. F.: High-resolution carbon dioxide concentration record 650,000-800,000 years before present, Nature, 453, 379-382,DOI: 10.1038/nature06949, 2008.

Luyssaert, S., Inglima, I., Jung, M., Richardson, A. D., Reichstein, M., Papale, D., Piao, S. L., Schulzes, E. D., Wingate, L., Matteucci, G., Aragao, L., Aubinet, M., Beers, C., Bernhofer, C., Black, K. G., Bonal, D., Bonnefond, J. M., Chambers, J., Ciais, P., Cook, B., Davis, K. J., Dolman, A. J., Gielen, B., Goulden, M., Grace, J., Granier, A., Grelle, A., Griffis, T., Grunwald, T., Guidolotti, G., Hanson, P. J., Harding, R., Hollinger, D. Y., Hutyra, L. R., Kolar, P., Kruijt, B., Kutsch, W., Lagergren, F., Laurila, T., Law, B. E., Le Maire, G., Lindroth, A., Loustau, D., Malhi, Y., Mateus, J., Migliavacca, M., Misson, L., Montagnani, L., Moncrieff, J., Moors, E., Munger, J. W., Nikinmaa, E., Ollinger, S. V., Pita, G., Rebmann, C., Roupsard, O., Saigusa, N., Sanz, M. J., Seufert, G., Sierra, C., Smith, M. L., Tang, J., Valentini, R., Vesala, T., and Janssens, I. A.: CO_2 balance of boreal, temperate, and tropical forests derived from a global database, Global Change Biol, 13, 2509-2537, DOI: 10.1111/j.1365-2486.2007.01439.x, 2007.

Lymburner, L., Tan, P., Mueller, N., Thackway, R., Thankappan, M., Islam, A., Randall, L. and Lewis, A.: Australia's first dynamic land cover map, Proceedings of the 15th Australasian Remote Sensing & Photogrammetry Conference, 13–17 September 2010, Alice Springs, viewed 5 January 2010, www.scribd.com/doc/37457498/15arspc-Submission-96, 2010.

Magnussen, S., and Reed, D.: Modelling for estimation and monitoring, (FAO-IUFRO), 2004.

Mariscal, M. J., Orgaz, F., and Villalobos, F. J.: Radiation-use efficiency and dry matter partitioning of a young olive (Olea europaea) orchard, Tree Physiol., 20, 65-72, DOI: 10.1093/treephys/20.1.65, 2000.

Martin, R. J.: Radiation interception and growth of sugar-beet at different sowing dates in canterbury, New Zeal J. Agr. Res., 29, 381-390, DOI: 10.1080/00288233.1986.10423490, 1986a.

Martin, R. J.: Growth of sugar-beet crops in Canterbury, New Zeal J. Agr. Res., 29, 391-400, DOI: 10.1080/00288233.1986.10423491, 1986b.

Mastrorilli, M., Katerji, N., Rana, G., and Steduto, P.: Sweet sorghum in Mediterranean climate: radiation use and biomass water use efficiencies, Industrial Crops And Products, 253-260, DOI: 10.1016/0926-6690(94)00002-G, 1995.

Masters, P.: The effects of fire-driven succession and rainfall on small Mammals in Spinifex Grassland at Uluru-National-Park, Northern-Territory, Wildlife Res, 20, 803-813, DOI: 10.1071/WR9930803, 1993.

McCabe, M. F., Gao, H., and Wood, E. F.: Evaluation of AMSR-E-derived soil moisture retrievals using ground-based and PSR airborne data during SMEX02, J Hydrometeorol, 6, 864-877, DOI: 10.1175/JHM463.1, 2005.

McCallum, A., Wagner, W., Schmullius, C., Shvidenko, A., Obersteiner, M., Fritz, S., and Nilsson, S.: Comparison of four global FAPAR datasets over Northern Eurasia for the year 2000, Remote Sensing of Environment, 114, 941-949, DOI: 10.1016/j.rse.2009.12.009, 2010.

Mcintyre, B. D., Flower, D. J., and Riha, S. J.: Temperature and soil-water status effects on radiation use and growth of pearl-millet in a semiarid environment, Agr. Forest. Meteorol., 66, 211-227, DOI: 10.1016/0168-1923(93)90072-P, 1993.

McKee, T. B. N., Doesken, J. and Kleist, J.: The relationship of drought frequency and duration to time scales, paper presented at Eighth Conference on Applied Climatology, Am. Meteorol. Soc., Anaheim, Calif., 1993.

McKinley, G. A., Fay, A. R., Takahashi, T., and Metzl, N.: Convergence of atmospheric and North Atlantic carbon dioxide trends on multidecadal timescales, Nat Geosci, 4, 606-610, DOI: 10.1038/Ngeo1193, 2011.

McVicar, T. R., Roderick, M. L., Donohue, R. J., and Van Niel, T. G.: Less bluster ahead? Ecohydrological implications of global trends of terrestrial near-surface wind speeds, Ecohydrology, 5, 381-388, DOI: 10.1002/eco.1298, 2012.

Meijer, W. J. M., van der Werf, H. M. G., Mathijssen, E. W. J. M., and Vandenbrink, P. W. M.: Constraints to dry-matter production in fiber hemp (Cannabis-Sativa L), Eur. J. Agron., 4, 109-117, 1995.

Mendham, N. J., Shipway, P. A., and Scott, R. K.: The effects of delayed sowing and weather on growth, development and yield of winter oil-seed rape (brassica-napus), J. Agr. Sci., 96, 389-416, 1981.

Mercado, L. M., Bellouin, N., Sitch, S., Boucher, O., Huntingford, C., Wild, M., and Cox, P. M.: Impact of changes in diffuse radiation on the global land carbon sink, Nature, 458, 1014-1017, DOI: 10.1038/Nature07949, 2009.

Meyers, T. P., and Hollinger, S. E.: An assessment of storage terms in the surface energy balance of maize and soybean, Agr. Forest. Meteorol., 125, 105-115, DOI: 10.1016/j.agrformet.2004.03.001, 2004.

Meyers, T. P., Luke, W. T., and Meisinger, J. J.: Fluxes of ammonia and sulfate over maize using relaxed eddy accumulation, Agr. Forest. Meteorol., 136, 203-213, DOI: 10.1016/j.agrformet.2004.10.005, 2006.

Miralles, D. G., Crow, W. T., and Cosh, M. H.: Estimating spatial sampling errors in coarse-scale soil moisture estimates derived from point-scale observations, J Hydrometeorol, 11, 1423-1429, DOI: 10.1175/2010jhm1285.1, 2010.

Mishra, A. K., and Desai, V.: Drought forecasting using stochastic models, Stoch Env Res Risk A, 19, 326-339, DOI: 10.1007/s00477-005-0238-4, 2005.

Monfreda, C., Ramankutty, N., and Foley, J. A.: Farming the planet: 2. Geographic distribution of crop areas, yields, physiological types, and net primary production in the year 2000, Global Biogeochem Cy, 22, GB1022, DOI: 10.1029/2007gb002947, 2008.

Monteith, J. L.: Solar-radiation and productivity in tropical ecosystems, J Appl Ecol, 9, 747-766, 1972.

Monteith, J. L., and Moss, C. J.: Climate and the Efficiency of Crop Production in Britain [and Discussion], Philosophical Transactions of the Royal Society of London. B, Biological Sciences, 281, 277-294, DOI: 10.1098/rstb.1977.0140, 1977.

Moors, E. J., Jacobs, C., Jans, W., Supit, I., Kutsch, W. L., Bernhofer, C., Beziat, P., Buchmann, N., Carrara, A., Ceschia, E., Elbers, J., Eugster, W., Kruijt, B., Loubet, B., Magliulo, E., Moureaux, C., Olioso, A., Saunders, M., and Soegaard, H.: , Agriculture Ecosystems & Environment, 139, 325-335, DOI: 10.1016/j.agee.2010.04.013, 2010.

Morrison, M. J., and Stewart, D. W.: Radiation-use efficiency in summer rape, Agron. J., 87, 1139-1142, 1995.

Morton, D. C., DeFries, R. S., Shimabukuro, Y. E., Anderson, L. O., Arai, E., Espirito-Santo, F. D., Freitas, R., and Morisette, J.: Cropland expansion changes deforestation dynamics in the southern Brazilian Amazon, Proc. Natl. Acad. Sci. USA, 103, 14637-14641, doi:10.1073/pnas.0606377103, 2006.

Muchow, R. C., Robertson, M. J., and Pengelly, B. C.: Radiation-use efficiency of soybean, mungbean and cowpea under different environmental-conditions, Field Crop. Res., 32, 1-16, 1993.

Muchow, R. C., Evensen, C. I., Osgood, R. V., and Robertson, M. J.: Yield accumulation in irrigated sugarcane .2. Utilization of intercepted radiation, Agron. J., 89, 646-652, 1997.

Muurinen, S., and Peltonen-Sainio, P.: Radiation-use efficiency of modern and old spring cereal cultivars and its response to nitrogen in northern growing conditions, Field Crop. Res., 96, 363-373, 2006.

Myneni, R. B., Keeling, C. D., Tucker, C. J., Asrar, G., and Nemani, R. R.: Increased plant growth in the northern high latitudes from 1981 to 1991, Nature, 386, 698-702, DOI: 10.1038/386698a0, 1997.

Myneni, R. B., Dong, J., Tucker, C. J., Kaufmann, R. K., Kauppi, P. E., Liski, J., Zhou, L., Alexeyev, V., and Hughes, M. K.: A large carbon sink in the woody biomass of Northern forests, P Natl Acad Sci USA, 98, 14784-14789, DOI: 10.1073/pnas.261555198, 2001.

Myneni, R. B., Hoffman, S., Knyazikhin, Y., Privette, J. L., Glassy, J., Tian, Y., Wang, Y., Song, X., Zhang, Y., Smith, G. R., Lotsch, A., Friedl, M., Morisette, J. T., Votava, P., Nemani, R. R., and Running, S. W.: Global products of vegetation leaf area and fraction absorbed PAR from year one of MODIS data, Remote Sensing of Environment, 83, 214-231, DOI: 0.1016/S0034-4257(02)00074-3, 2002.

Nam, N. H., Subbarao, G. V., Chauhan, Y. S., and Johansen, C.: Importance of canopy attributes in determining dry matter accumulation of pigeonpea under contrasting moisture regimes, Crop Sci., 38, 955-961, 1998.

Nemani, R. R., Keeling, C. D., Hashimoto, H., Jolly, W. M., Piper, S. C., Tucker, C. J., Myneni, R. B., and Running, S. W.: Climate-driven increases in global terrestrial net primary production from 1982 to 1999, Science, 300, 1560-1563, DOI: 10.1126/science.1082750, 2003.

Nicholson, S. E., Davenport, M. L., and Malo, A. R.: A comparison of the vegetation response to rainfall in the Sahel and East-Africa, using Normalized Difference Vegetation Index from Noaa AVHRR, Climatic Change, 17, 209-241, DOI: 10.1007/BF00138369, 1990.

Niyogi, D., Chang, H. I., Saxena, V. K., Holt, T., Alapaty, K., Booker, F., Chen, F., Davis, K. J., Holben, B., Matsui, T., Meyers, T., Oechel, W. C., Pielke, R. A., Wells, R., Wilson, K., and Xue, Y. K.: Direct observations of the effects of aerosol loading on net ecosystem CO_2 exchanges over different landscapes, Geophys Res Lett, 31, L20506, DOI: 10.1029/2004gl020915, 2004.

Njoku, E. G., Wilson, W. J., Yueh, S. H., Dinardo, S. J., Li, F. K., Jackson, T. J., Lakshmi, V., and Bolten, J.: Observations of soil moisture using a passive and active low-frequency microwave airborne sensor during SGP99, Ieee T Geosci Remote, 40, 2659-2673, DOI: 10.1109/Tgrs.2002.807008, 2002.

Oak Ridge National Laboratory Distributed Active Archive Center, and DAAC), O.: MODIS subsetted land products, Collection 5. Available on-line [http: //daac.ornl.gov/MODIS/modis.html] from ORNL DAAC, Oak Ridge, Tennessee, U.S.A. Accessed Month 8, 2010.

Opoku-Ameyaw, K., and Harris, P. M.: Intercropping potatoes in early spring in a temperate climate. 2. Radiation utilization, Potato Res., 44, 63-74, 2001.

Owe, M., de Jeu, R., and Holmes, T.: Multisensor historical climatology of satellite-derived global land surface moisture, J Geophys Res-Earth, 113, F01002, DOI: 10.1029/2007jf000769, 2008.

Pagani, M., Liu, Z. H., LaRiviere, J., and Ravelo, A. C.: High Earth-system climate sensitivity determined from Pliocene carbon dioxide concentrations, Nat Geosci, 3, 27-30, DOI: 10.1038/ngeo724, 2010.

Palmer, W. C.: Meteorological drought, Research Paper NO.45, U.S. Dept. of Commerce, 58, 1965.

Pan, Y. D., Birdsey, R. A., Fang, J. Y., Houghton, R., Kauppi, P. E., Kurz, W. A., Phillips, O. L., Shvidenko, A., Lewis, S. L., Canadell, J. G., Ciais, P., Jackson, R. B., Pacala, S. W., McGuire, A. D., Piao, S. L., Rautiainen, A., Sitch, S., and Hayes, D.: A large and persistent carbon sink in the world's forests, Science, 333, 988-993, DOI: 10.1126/science.1201609, 2011.

Parinussa, R. M., Meesters, A. G. C. A., Liu, Y. Y., Dorigo, W., Wagner, W., and de Jeu, R. A. M.: Error estimates for near-real-time satellite soil moisture as derived from the land parameter retrieval model, Ieee Geosci Remote S, 8, 779-783, DOI: 10.1109/LGRS.2011.2114872, 2011.

Parmentier, F. J. W., van der Molen, M. K., van Huissteden, J., Karsanaev, S. A., Kononov, A. V., Suzdalov, D. A., Maximov, T. C., and Dolman, A. J.: Longer growing seasons do not increase net carbon uptake in the northeastern Siberian tundra, J Geophys Res-Biogeo, 116, G04013, DOI: 10.1029/2011jg001653, 2011.

Parr, J. F., and Sullivan, L. A.: Phytolith occluded carbon and silica variability in wheat cultivars, Plant Soil, 342, 165-171, DOI: 10.1007/s11104-010-0680-z, 2011.

Phillips, O. L., Aragao, L. E. O. C., Lewis, S. L., Fisher, J. B., Lloyd, J., Lopez-Gonzalez, G., Malhi, Y., Monteagudo, A., Peacock, J., Quesada, C. A., van der Heijden, G., Almeida, S., Amaral, I., Arroyo, L., Aymard, G., Baker, T. R., Banki, O., Blanc, L., Bonal, D., Brando, P., Chave, J., de Oliveira, A. C. A., Cardozo, N. D., Czimczik, C. I., Feldpausch, T. R., Freitas, M. A., Gloor, E., Higuchi, N., Jimenez, E., Lloyd, G., Meir, P., Mendoza, C., Morel, A., Neill, D. A., Nepstad, D., Patino, S., Penuela, M. C., Prieto, A., Ramirez, F., Schwarz, M., Silva, J., Silveira, M., Thomas, A. S., ter Steege, H., Stropp, J., Vasquez, R., Zelazowski, P., Davila, E. A., Andelman, S., Andrade, A., Chao, K. J., Erwin, T., Di Fiore, A., Honorio, E., Keeling, H., Killeen, T. J., Laurance, W. F., Cruz, A. P., Pitman, N. C. A., Vargas, P. N., Ramirez-Angulo, H., Rudas, A., Salamao, R., Silva, N., Terborgh, J., and Torres-Lezama, A.: Drought sensitivity of the Amazon Rainforest, Science, 323, 1344-1347, DOI: 10.1126/science.1164033, 2009.

Piao, S. L., Ciais, P., Friedlingstein, P., Peylin, P., Reichstein, M., Luyssaert, S., Margolis, H., Fang, J. Y., Barr, A., Chen, A. P., Grelle, A., Hollinger, D. Y., Laurila, T., Lindroth, A., Richardson, A. D., and Vesala, T.: Net carbon dioxide losses of northern ecosystems in response to autumn warming, Nature, 451, 49-52, DOI: 10.1038/Nature06444, 2008.

Piao, S., Sitch, S., Ciais, P., Friedlingstein, P., Peylin, P., Wang, X., Ahlström, A., Anav, A., Canadell, J. G., Cong, N., Huntingford, C., Jung, M., Levis, S., Levy, P. E., Li, J., Lin, X., Lomas, M. R., Lu, M., Luo, Y., Ma, Y., Myneni, R. B., Poulter, B., Sun, Z., Wang, T., Viovy, N., Zaehle, S., and Zeng, N.: Evaluation of terrestrial carbon cycle models for their response to climate variability and to CO_2 trends, Global Change Biol, 19, 2117-2132, DOI: 10.1111/gcb.12187, 2013.

Piao, S. L., Wang, X. H., Ciais, P., Zhu, B., Wang, T., and Liu, J.: Changes in satellite-derived vegetation growth trend in temperate and boreal Eurasia from 1982 to 2006, Global Change Biol, 17, 3228-3239, DOI: 10.1111/j.1365-2486.2011.02419.x, 2011.

Pinter, P. J., Kimball, B. A., Mauney, J. R., Hendrey, G. R., Lewin, K. F., and Nagy, J.: Effects of free-air carbon-dioxide enrichment on par absorption and conversion efficiency by cotton, Agr. Forest. Meteorol., 70, 209-230, 1994.

Pook, E. W., Gill, A. M., and Moore, P. H. R.: Long-term variation of litter fall, canopy leaf area and flowering in a Eucalyptus maculata forest on the south coast of New South Wales. Australian Journal of Botany, 45(5), 737–755, DOI: 10.1071/BT95063, 1997.

Porporato, A., and Rodriguez-Iturbe, I.: Ecohydrology - a challenging multidisciplinary research perspective, Hydrolog Sci J, 47, 811-821, DOI: 10.1080/02626660209492985, 2002.

Portmann, F. T., Siebert, S., and Doll, P.: MIRCA2000-Global monthly irrigated and rainfed crop areas around the year 2000: A new high-resolution data set for agricultural and hydrological modelling, Global Biogeochem. Cy., 24, GB1011, DOI: 10.1029/2008GB003435, 2010.

Potter, C., Klooster, S., and Genovese, V.: Net primary production of terrestrial ecosystems from 2000 to 2009, Climatic Change, 115, 365-378, DOI: 10.1007/s10584-012-0460-2, 2012.

Potter, C., Gross, P., Genovese, V., and Smith, M. L.: Net primary productivity of forest stands in New Hampshire estimated from Landsat and MODIS satellite data, Carbon Balance Manage, 2, 1-11, DOI: 10.1186/1750-0680-2-9, 2007.

Potter, C., Klooster, S., Myneni, R., Genovese, V., Tan, P. N., and Kumar, V.: Continental-scale comparisons of terrestrial carbon sinks estimated from satellite data and ecosystem modeling 1982–1998, Global Planet Change, 39, 201-213, DOI: 10.1016/j.gloplacha.2003.07.001, 2003.

Potter, C. S., Randerson, J. T., Field, C. B., Matson, P. A., Vitousek, P. M., Mooney, H. A., and Klooster, S. A.: Terrestrial ecosystem production - a process model-based on global satellite and surface data, Global Biogeochem Cy, 7, 811-841, DOI: 10.1029/93GB02725, 1993.

Prince, S. D., and Goward, S. N.: Global primary production: A remote sensing approach, J Biogeogr, 22, 815-835, DOI: 10.2307/2845983, 1995.

Ramankutty, N., and Foley, J. A.: Estimating historical changes in global land cover: Croplands from 1700 to 1992, Global Biogeochem Cy, 13, 997-1027, 10.1029/1999GB900046, 1999.

Ramankutty, N., Evan, A. T., Monfreda, C., and Foley, J. A.: Farming the planet: 1. Geographic distribution of global agricultural lands in the year 2000, Global Biogeochem Cy, 22, GB1003, DOI: 10.1029/2007gb002952, 2008.

Rebel, K. T., de Jeu, R. A. M., Ciais, P., Viovy, N., Piao, S. L., Kiely, G., and Dolman, A. J.: A global analysis of soil moisture derived from satellite observations and a land surface model, Hydrol Earth Syst Sc, 16, 833-847, DOI: 10.5194/hess-16-833-2012, 2012.

Reichstein, M., Falge, E., Baldocchi, D., Papale, D., Aubinet, M., Berbigier, P., Bernhofer, C., Buchmann, N., Gilmanov, T., Granier, A., Grunwald, T., Havrankova, K., Ilvesniemi, H., Janous, D., Knohl, A., Laurila, T., Lohila, A., Loustau, D., Matteucci, G., Meyers, T., Miglietta, F., Ourcival, J. M., Pumpanen, J., Rambal, S., Rotenberg, E., Sanz, M., Tenhunen, J., Seufert, G., Vaccari, F., Vesala, T., Yakir, D., and Valentini, R.: On the separation of net ecosystem exchange into assimilation and ecosystem respiration: review and improved algorithm, Global Change Biol, 11, 1424-1439, DOI: 10.1111/j.1365-2486.2005.001002.x, 2005.

Reichstein, M., Ciais, P., Papale, D., Valentini, R., Running, S., Viovy, N., Cramer, W., Granier, A., Ogee, J., Allard, V., Aubinet, M., Bernhofer, C., Buchmann, N., Carrara, A., Grunwald, T., Heimann, M., Heinesch, B., Knohl, A., Kutsch, W., Loustau, D., Manca, G., Matteucci, G., Miglietta, F., Ourcival, J. M., Pilegaard, K., Pumpanen, J., Rambal, S., Schaphoff, S., Seufert, G., Soussana, J. F., Sanz, M. J., Vesala, T., and Zhao, M.: Reduction of ecosystem productivity and respiration during the European summer 2003 climate anomaly: a joint flux tower, remote sensing and modelling analysis, Global Change Biol, 13, 634-651, DOI: 10.1111/j.1365-2486.2006.01224.x, 2007a.

Reichstein, M., Papale, D., Valentini, R., Aubinet, M., Bernhofer, C., Knohl, A., Laurila, T., Lindroth, A., Moors, E., Pilegaard, K., and Seufert, G.: Determinants of terrestrial ecosystem carbon balance inferred from European eddy covariance flux sites, Geophys Res Lett, 34, L01402, DOI: 10.1029/2006gl027880, 2007b.

Reichstein, M., Bahn, M., Ciais, P., Frank, D., Mahecha, M. D., Seneviratne, S. I., Zscheischler, J., Beer, C., Buchmann, N., Frank, D. C., Papale, D., Rammig, A., Smith, P., Thonicke, K., van der Velde, M., Vicca, S., Walz, A., and Wattenbach, M.: Climate extremes and the carbon cycle, Nature, 500, 287-295, DOI: 10.1038/Nature12350, 2013.

Rhee, J., Im, J., and Carbone, G. J.: Monitoring agricultural drought for arid and humid regions using multi-sensor remote sensing data, Remote Sensing of Environment, 114, 2875-2887, DOI: 10.1016/j.rse.2010.07.005, 2010.

Richard, Y., and Poccard, I.: A statistical study of NDVI sensitivity to seasonal and interannual rainfall variations in Southern Africa, Int J Remote Sens, 19, 2907-2920, DOI: 10.1080/014311698214343, 1998.

Rizzalli, R. H., Villalobos, F. J., and Orgaz, F.: Radiation interception, radiation-use efficiency and dry matter partitioning in garlic (Allium sativum L.), Eur. J. Agron., 18, 33-43, 2002.

Rodriguez-Iturbe, I.: Ecohydrology: A hydrologic perspective of climate-soil-vegetation dynamics, Water Resour Res, 36, 3-9, DOI: 10.1029/1999WR900210, 2000.

Rosenthal, W. D., and Gerik, T. J.: Radiation use efficiency among cotton cultivars, Agron. J., 83, 655-658, 1991.

Rosenthal, W. D., Gerik, T. J., and Wade, L. J.: Radiation-use efficiency among grain-sorghum cultivars and plant densities, Agron. J., 85, 703-705, 1993.

Ruimy, A., Saugier, B., and Dedieu, G.: Methodology for the estimation of terrestrial net primary production from remotely sensed data, J Geophys Res-Atmos, 99, 5263-5283, DOI: 10.1029/93JD03221, 1994.

Ruimy, A., Dedieu, G., and Saugier, B.: TURC: A diagnostic model of continental gross primary productivity and net primary productivity, Global Biogeochem Cy, 10, 269-285, DOI: 10.1029/96GB00349, 1996.

Ruimy, A., Kergoat, L., Bondeau, A. and Intercomparison, ThE. P. OF. ThE. P. NpP. M.: Comparing global models of terrestrial net primary productivity (NPP): analysis of differences in light absorption and light-use efficiency. Global Change Biology, 5: 56–64. DOI: 10.1046/j.1365-2486.1999.00007.x, 1999.

Running, S. W., Baldocchi, D. D., Turner, D. P., Gower, S. T., Bakwin, P. S., and Hibbard, K. A.: A global terrestrial monitoring network integrating tower fluxes, flask sampling, ecosystem modeling and EOS satellite data, Remote Sensing of Environment, 70, 108-127, DOI: 10.1016/S0034-4257(99)00061-9, 1999.

Running, S. W., Nemani, R. R., Heinsch, F. A., Zhao, M. S., Reeves, M., and Hashimoto, H.: A continuous satellite-derived measure of global terrestrial primary production, Bioscience, 54, 547-560, DOI: 10.1641/0006-3568(2004)054[0547: ACSMOG]2.0.CO;2, 2004.

Running, S. W., Thornton, P., Nemani, E. R., Glassy, J. M.: Global terrestrial gross and net primary productivity from the Earth Observing System. In: Sala O. E., Jackson R. B., Mooney H. A., Howarth R. W., (eds) Methods in ecosystem science. Springer, New York, 44–57, 2000.

Russell, G., Jarvis, P. G., and Monteith, J. L.: Absorption of radiation by canopies and stand growth, in: Plant Canopies: Their Growth, Form and Function, edited by: Russell, G., Marshall, B., and Jarvis, P. G., Cambridge University Press, 21-39, 1989.

Ruiz, R. A., and Bertero, H. D.: Light interception and radiation use efficiency in temperate quinoa (Chenopodium quinoa Willd.) cultivars, Eur. J. Agron., 29, 144-152, 2008.

Ryu, Y., Baldocchi, D. D., Kobayashi, H., van Ingen, C., Li, J., Black, T. A., Beringer, J., van Gorsel, E., Knohl, A., Law, B. E., and Roupsard, O.: Integration of MODIS land and atmosphere products with a coupled-process model to estimate gross primary productivity and evapotranspiration from 1 km to global scales, Global Biogeochem Cy, 25, Gb4017, DOI: 10.1029/2011gb004053, 2011.

Samanta, A., Costa, M. H., Nunes, E. L., Vieira, S. A., Xu, L., and Myneni, R. B.: Comment on "Drought-induced reduction in global terrestrial net primary production from 2000 through 2009", Science, 333, DOI: 10.1126/science.1199048, 2011.

Sarmiento, J. L., Gloor, M., Gruber, N., Beaulieu, C., Jacobson, A. R., Fletcher, S. E. M., Pacala, S., and Rodgers, K.: Trends and regional distributions of land and ocean carbon sinks, Biogeosciences, 7, 2351-2367, DOI: 10.5194/bg-7-2351-2010, 2010.

Saugier, B., Roy, J., and Mooney, H. A.: Estimations of global terrestrial productivity: converging toward a single number? In: Roy J, Saugier B, and Mooney HA (Eds). Terrestrial global productivity pp. 543-557, New York: Academic Press, 2001.

Schlesinger, W.H.: Biogeochemistry, an Analysis of Global Change. New York, USA, Academic Press, 1991.

Schmid, H. P.: Footprint modeling for vegetation atmosphere exchange studies: a review and perspective, Agr Forest Meteorol, 113, 159-183, Pii S0168-1923(02)00107-7, DOI: 10.1016/S0168-1923(02)00107-7, 2002.

Schneider, B., and Schneider, R.: Palaeoclimate: Global warmth with little extra CO_2, Nat Geosci, 3, 6-7, DOI: 10.1038/ngeo736, 2010.

Schulze, E. D., Luyssaert, S., Ciais, P., Freibauer, A., Janssens, I. A., Soussana, J. F., Smith, P., Grace, J., Levin, I., Thiruchittampalam, B., Heimann, M., Dolman, A. J., Valentini, R., Bousquet, P., Peylin, P., Peters, W., Rodenbeck, C., Etiope, G., Vuichard, N., Wattenbach, M., Nabuurs, G. J., Poussi, Z., Nieschulze, J., Gash, J. H., and Team, C.: Importance of methane and nitrous oxide for Europe's terrestrial greenhouse-gas balance, Nat Geosci, 2, 842-850, DOI: 10.1038/ngeo686, 2009.

Schuster, U., and Watson, A. J.: A variable and decreasing sink for atmospheric CO_2 in the North Atlantic, J Geophys Res-Oceans, 112, C11006, DOI: 10.1029/2006jc003941, 2007.

Scipal, K., Holmes, T., de Jeu, R., Naeimi, V., and Wagner, W.: A possible solution for the problem of estimating the error structure of global soil moisture data sets, Geophys Res Lett, 35, DOI: 10.1029/2008GL035599, 2008.

Scott, R.K., and Jaggard, K. W.: Crop physiology and agronomy. In The Sugar Beet Crop: Science into Practice (Eds D. A. Cooke & R. K. Scott), pp. 178-237.London: Chapman and Hall. 1993.

Sellers, P. J.: Canopy Reflectance, Photosynthesis and Transpiration, Int J Remote Sens, 6, 1335-1372, DOI: 10.1080/01431168508948283, 1985.

Shah, S. F. A., McKenzie, B. A., Gaunt, R. E., Marshall, J. W., and Frampton, C. M.: Effect of production environments on radiation interception and radiation use efficiency of potato (Solanum tuberosum) grown in Canterbury, New Zealand, New Zeal J. Crop. Hort., 32, 113-119, 2004.

Sheffield, J., Wood, E. F., and Roderick, M. L.: Little change in global drought over the past 60 years, Nature, 491, 435–438, DOI: 10.1038/nature11575, 2012.

Sigman, D. M., Hain, M. P., and Haug, G. H.: The polar ocean and glacial cycles in atmospheric CO_2 concentration, Nature, 466, 47-55, DOI: 10.1038/nature09149, 2010.

Sinclair, T. R., and Horie, T.: Leaf Nitrogen, Photosynthesis, and Crop Radiation Use Efficiency - a Review, Crop Sci, 29, 90-98, DOI: 10.2135/cropsci1989.0011183X002900010023x, 1989.

Sitch, S., Huntingford, C., Gedney, N., Levy, P. E., Lomas, M., Piao, S. L., Betts, R., Ciais, P., Cox, P., Friedlingstein, P., Jones, C. D., Prentice, I. C., and Woodward, F. I.: Evaluation of the terrestrial carbon cycle, future plant geography and climate-carbon cycle feedbacks using five Dynamic Global Vegetation Models (DGVMs), Global Change Biol, 14, 2015-2039, DOI: 10.1111/j.1365-2486.2008.01626.x, 2008.

Sjöström, M., Zhao, M., Archibald, S., Arneth, A., Cappelaere, B., Falk, U., de Grandcourt, A., Hanan, N., Kergoat, L., Kutsch, W., Merbold, L., Mougin, E., Nickless, A., Nouvellon, Y., Scholes, R. J., Veenendaal, E. M., and Ardö, J.: Evaluation of MODIS gross primary productivity for Africa using eddy covariance data, Remote Sensing of Environment, 131, 275-286, DOI: 10.1016/j.rse.2012.12.023, 2013.

Smith, P., Martino, D., Cai, Z., Gwary, D., Janzen, H., Kumar, P., McCarl, B., Ogle, S., O'Mara, F., Rice, C., Scholes, B., Sirotenko, O., Howden, M., McAllister, T., Pan, G., Romanenkov, V., Schneider, U., Towprayoon, S., Wattenbach, M., and Smith, J.: Greenhouse gas mitigation in agriculture, Philos T R Soc B, 363, 789-813, DOI: 10.1098/rstb.2007.2184, 2008.

Southgate, R., and Masters, P.: Fluctuations of rodent populations in response to rainfall and fire in a central Australian hummock grassland dominated by Plectrachne schinzii, Wildlife Res, 23, 289-303, DOI: 10.1071/WR9960289, 1996.

Squire, G. R.: The physiology of tropical crop production, C.A.B. International, Wallingford, U.K. , 1990.

Steingrobe, B., Schmid, H., Gutser, R., and Claassen, N.: Root production and root mortality of winter wheat grown on sandy and loamy soils in different farming systems, Biol. Fert. Soils, 33, 331-339, DOI: 10.1007/s003740000334, 2001.

Stephenson, N. L.: Climatic control of vegetation distribution - the role of the water-balance, Am Nat, 135, 649-670, 1990.

Stocker, T. et al., Working group I contribution to the IPCC fifth assessment report (AR5), climate change 2013: the physical science basis, 2013.

Suntharalingam, P., Kettle, A. J., Montzka, S. M., and Jacob, D. J.: Global 3-D model analysis of the seasonal cycle of atmospheric carbonyl sulfide: Implications for terrestrial vegetation uptake, Geophys Res Lett, 35, L19801, DOI: 10.1029/2008GL034332, 2008.

Takahashi, T., Sutherland, S. C., Wanninkhof, R., Sweeney, C., Feely, R. A., Chipman, D. W., Hales, B., Friederich, G., Chavez, F., Sabine, C., Watson, A., Bakker, D. C. E., Schuster, U., Metzl, N., Yoshikawa-Inoue, H., Ishii, M., Midorikawa, T., Nojiri, Y., Kortzinger, A., Steinhoff, T., Hoppema, M., Olafsson, J., Arnarson, T. S., Tilbrook, B., Johannessen, T., Olsen, A., Bellerby, R., Wong, C. S., Delille, B., Bates, N. R., and de Baar, H. J. W.: Climatological mean and decadal change in surface ocean pCO_2, and net sea-air CO_2 flux over the global oceans (vol 56, pg 554, 2009), Deep-Sea Res Pt I, 56, 2075-2076, DOI: 10.1016/j.dsr.2009.07.007, 2009.

Taylor, C. M., de Jeu, R. A. M., Guichard, F., Harris, P. P., and Dorigo, W. A.: Afternoon rain more likely over drier soils, Nature, 489, 423-426, DOI: 10.1038/nature11377, 2012.

Taylor, K. E.: Summarizing multiple aspects of model performance in a single diagram., J Geophys Res-Atmos, 106, 7183-7192, DOI: 10.1029/2000JD900719, 2001.

Toms, J. D., and Lesperance, M. L.: Piecewise regression: A tool for identifying ecological thresholds, Ecology, 84, 2034-2041, 2003.

Trapani, N., Hall, A. J., Sadras, V. O., and Vilella, F.: Ontogenic changes in radiation use efficiency of sunflower (helianthus-annuus l) crops, Field Crop. Res., 29, 301-316, 1992.

Trenberth, K. E., et al. (2007), Observations: Surface and atmospheric climate change, in Climate Change 2007: The Physical Science Basis, Contribution of Working Group 1 to the Fourth Assessment Report of the Intergovernmental Panel on Climate Change, edited by S. Solomon et al., pp. 235–336, Cambridge Univ. Press, Cambridge, U. K.

Tucker, C. J., Fung, I. Y., Keeling, C. D., and Gammon, R. H.: Relationship between atmospheric CO_2 variations and a satellite-derived vegetation index, Nature, 319, 195-199, 1986.

Tucker, C. J., Pinzon, J. E., Brown, M. E., Slayback, D. A., Pak, E. W., Mahoney, R., Vermote, E. F., and El Saleous, N.: An extended AVHRR 8-km NDVI dataset compatible with MODIS and SPOT vegetation NDVI data, Int J Remote Sens, 26, 4485-4498, DOI: 10.1080/01431160500168686, 2005.

Tucker, C. J.: Red and photographic infrared linear combinations for monitoring vegetation, Remote Sensing of Environment, 8, 127-150, DOI: 10.1016/0034-4257(79)90013-0, 1979.

Turner, D. P., Ritts, W. D., Cohen, W. B., Gower, S. T., Running, S. W., Zhao, M., Costa, M. H., Kirschbaum, A. A., Ham, J. M., Saleska, S. R., and Ahl, D. E.: Evaluation of MODIS NPP and GPP products across multiple biomes, Remote Sensing of Environment, 102, 282-292, DOI: 10.1016/j.rse.2006.02.017, 2006.

Unsworth, M. H., Lesser, V. M., and Heagle, A. S.: Radiation interception and the growth of soybeans exposed to ozone in open-top field chambers, J. Appl. Ecol., 21, 1059-1077, 1984.

van der Molen, M. K., Dolman, A. J., Ciais, P., Eglin, T., Gobron, N., Law, B. E., Meir, P., Peters, W., Phillips, O. L., Reichstein, M., Chen, T., Dekker, S. C., Doubkova, M., Friedl, M. A., Jung, M., van den Hurk, B. J. J. M., de Jeu, R. A. M., Kruijt, B., Ohta, T., Rebel, K. T., Plummer, S., Seneviratne, S. I., Sitch, S., Teuling, A. J., van der Werf, G. R., and Wang, G.: Drought and ecosystem carbon cycling, Agr Forest Meteorol, 151, 765-773, DOI: 10.1016/j.agrformet.2011.01.018, 2011.

van der Werf, G. R., Randerson, J. T., Collatz, G. J., Giglio, L., Kasibhatla, P. S., Arellano, A. F., Olsen, S. C., and Kasischke, E. S.: Continental-scale partitioning of fire emissions during the 1997 to 2001 El Nino/La Nina period, Science, 303, 73-76, DOI: 10.1126/science.1090753, 2004.

van der Werf, G. R., Randerson, J. T., Giglio, L., Collatz, G. J., Mu, M., Kasibhatla, P. S., Morton, D. C., DeFries, R. S., Jin, Y., and van Leeuwen, T. T.: Global fire emissions and the contribution of deforestation, savanna, forest, agricultural, and peat fires (1997-2009), Atmos Chem Phys, 10, 11707-11735, DOI: 10.5194/acp-10-11707-2010, 2010.

Varlet-Grancher, C., Chartier, M., Lemaire, G., Gosse, G., Bonhomme, R., Cruz, P., Castal, F., and Lenoble, S.: Productivity of sweet sorghum compared to Sudan-grass and sorghum Sudan grass hybrids: Radiationinterception and biomass accumulation under non limiting water and nitrogen conditions. In: Grassi, G.,Collina, A., Zibetta, H. (eds) Proceedings 6th EC Conf, Biomass for Energy Industry and Environment, Elsevier Applied Science, Oxford, pp 265-267, 1992.

Verdon-Kidd, D. C., and Kiem, A. S.: Nature and causes of protracted droughts in southeast Australia: Comparison between the Federation, WWII, and Big Dry droughts, Geophys Res Lett, 36, DOI: 10.1029/2009GL041067, 2009.

Verma, S. B., Dobermann, A., Cassman, K. G., Walters, D. T., Knops, J. M., Arkebauer, T. J., Suyker, A. E., Burba, G. G., Amos, B., Yang, H. S., Ginting, D., Hubbard, K. G., Gitelson, A. A., and Walter-Shea, E. A.: Annual carbon dioxide exchange in irrigated and rainfed maize-based agroecosystems, Agr. Forest. Meteorol., 131, 77-96, 2005.

Vicente-Serrano, S. M., Begueria, S., and Lopez-Moreno, J. I.: A multiscalar drought index sensitive to global warming: the standardized precipitation evapotranspiration index, J Climate, 23, 1696-1718, DOI: 10.1175/2009jcli2909.1, 2010.

Vicente-Serrano, S. M., Gouveia, C., Camarero, J. J., Begueria, S., Trigo, R., Lopez-Moreno, J. I., Azorin-Molina, C., Pasho, E., Lorenzo-Lacruz, J., Revuelto, J., Moran-Tejeda, E., and Sanchez-Lorenzo, A.: Response of vegetation to drought time-scales across global land biomes, P. Natl. Acad. Sci. USA, 110, 52-57, 2013.

Vieira, M. I., de Melo-Abreu, J. P., Ferreira, M. E., and Monteiro, A. A.: Dry matter and area partitioning, radiation interception and radiation-use efficiency in open-field bell pepper, Sci Hortic-Amsterdam, 121, 404-409, 2009.

Vuichard, N., Ciais, P., Belelli, L., Smith, P., and Valentini, R.: Carbon sequestration due to the abandonment of agriculture in the former USSR since 1990, Global Biogeochem. Cy., 22, GB4018, DOI: 10.1029/2008GB003212, 2008.

Wagner, W., Lemoine, G., and Rott, H.: A method for estimating soil moisture from ERS scatterometer and soil data, Remote Sensing of Environment, 70, 191-207, DOI: 10.1016/S0034-4257(99)00036-X, 1999.

Wagner, W., Scipal, K., Pathe, C., Gerten, D., Lucht, W., and Rudolf, B.: Evaluation of the agreement between the first global remotely sensed soil moisture data with model and precipitation data, J Geophys Res-Atmos, 108, 4611, DOI: 10.1029/2003jd003663, 2003.

Wang, J., Rich, P. M., and Price, K. P.: Temporal responses of NDVI to precipitation and temperature in the central Great Plains, USA, Int J Remote Sens, 24, 2345-2364, DOI: 10.1080/01431160210154812, 2003.

Wang, G., Garcia, D., Liu, Y., de Jeu, R., and Johannes Dolman, A.: A three-dimensional gap filling method for large geophysical datasets: Application to global satellite soil moisture observations, Environ Modell Softw, 30, 139-142, DOI: 10.1016/j.envsoft.2011.10.015, 2012a.

Wang, X., Ma, M., Li, X., Song, Y., Tan, J., Huang, G., Zhang, Z., Zhao, T., Feng, J., Ma, Z., Wei, W., and Bai, Y.: Validation of MODIS-GPP product at 10 flux sites in northern China, Int J Remote Sens, 34, 587-599, DOI: 10.1080/01431161.2012.715774, 2012b.

Waring, R. H., Landsberg, J. J., and Williams, M.: Net primary production of forests: a constant fraction of gross primary production?, Tree Physiol, 18, 129-134, DOI: 10.1093/treephys/18.2.129, 1998.

Wei, Y. P., Langford, J., Willett, I. R., Barlow, S., and Lyle, C.: Is irrigated agriculture in the Murray Darling Basin well prepared to deal with reductions in water availability? Global Environ Chang, 21, 906-916, DOI: 10.1016/j.gloenvcha.2011.04.004, 2011.

Welp, L. R., Keeling, R. F., Meijer, H. A. J., Bollenbacher, A. F., Piper, S. C., Yoshimura, K., Francey, R. J., Allison, C. E., and Wahlen, M.: Interannual variability in the oxygen isotopes of atmospheric CO_2 driven by El Nino, Nature, 477, 579-582, DOI: 10.1038/nature10421, 2011.

Wen, J., Su, Z. B., and Ma, Y. M.: Determination of land surface temperature and soil moisture from Tropical Rainfall Measuring Mission/Microwave Imager remote sensing data, J Geophys Res-Atmos, 108, 4038, DOI: 10.1029/2002jd002176, 2003.

West, T. O., Brandt, C. C., Baskaran, L. M., Hellwinckel, C. M., Mueller, R., Bernacchi, C. J., Bandaru, V., Yang, B., Wilson, B. S., Marland, G., Nelson, R. G., Ugarte, D. G. D., and Post, W. M.: Cropland carbon fluxes in the United States: increasing geospatial resolution of inventory-based carbon accounting, Ecol Appl, 20, 1074-1086, DOI: 10.1890/08-2352.1, 2010.

Whitman, C. E., Hatfield, J. L., and Reginato, R. J.: Effect of slope position on the microclimate, growth, and yield of barley, Agron. J., 77, 663-669, 1985.

Williams, R. J., Myers, B. A., Muller, W. J., Duff, G. A., and Eamus, D.: Leaf phenology of woody species in a North Australian tropical savanna, Ecology, 78, 2542-2558, DOI: 10.1890/0012-9658(1997)078[2542: LPOWSI]2.0.CO;2, 1997.

Xiao, X. M., Zhang, Q. Y., Hollinger, D., Aber, J., and Moore, B.: Modeling gross primary production of an evergreen needleleaf forest using modis and climate data, Ecol Appl, 15, 954-969, DOI: 10.1890/04-0470, DOI: 10.1016/j.rse.2004.03.010, 2005.

Yuan, W. P., Liu, S. G., Yu, G. R., Bonnefond, J. M., Chen, J. Q., Davis, K., Desai, A. R., Goldstein, A. H., Gianelle, D., Rossi, F., Suyker, A. E., and Verma, S. B.: Global estimates of evapotranspiration and gross primary production based on MODIS and global meteorology data, Remote Sensing of Environment, 114, 1416-1431, DOI: 10.1016/j.rse.2010.01.022, 2010.

Zeng, N., Mariotti, A., and Wetzel, P.: Terrestrial mechanisms of interannual CO_2 variability, Global Biogeochem Cy, 19, GB1016, DOI: 10.1029/2004GB002273, 2005.

Zhang, L., Wylie, B., Loveland, T., Fosnight, E., Tieszen, L. L., Ji, L., and Gilmanov, T.: Evaluation and comparison of gross primary production estimates for the Northern Great Plains grasslands, Remote Sensing of Environment, 106, 173-189, DOI: 10.1016/j.rse.2006.08.012 , 2007.

Zhang, Y. B., Tang, Q. Y., Zou, Y. B., Li, D. Q., Qin, J. Q., Yang, S. H., Chen, L. J., Xia, B., and Peng, S. B.: Yield potential and radiation use efficiency of "super" hybrid rice grown under subtropical conditions, Field Crop. Res., 114, 91-98, 2009.

Zhang, Y. C., Rossow, W. B., Lacis, A. A., Oinas, V., and Mishchenko, M. I.: Calculation of radiative fluxes from the surface to top of atmosphere based on ISCCP and other global data sets: Refinements of the radiative transfer model and the input data, J Geophys Res-Atmos, 109, D19105, DOI: 10.1029/2003jd004457, 2004.

Zhang, Y. Q., Yu, Q., Jiang, J., and Tang, Y. H.: Calibration of Terra/MODIS gross primary production over an irrigated cropland on the North China Plain and an alpine meadow on the Tibetan Plateau, Global Change Biol, 14, 757-767, DOI: 10.1111/j.1365-2486.2008.01538.x, 2008.

Zhao, M. S., Heinsch, F. A., Nemani, R. R., and Running, S. W.: Improvements of the MODIS terrestrial gross and net primary production global data set, Remote Sensing of Environment, 95, 164-176, DOI: 10.1016/j.rse.2004.12.011, 2005.

Zhao, M., Running, S. W., and Nemani, R. R.: Sensitivity of Moderate Resolution Imaging Spectroradiometer (MODIS) terrestrial primary production to the accuracy of meteorological reanalyses, J Geophys Res-Biogeo, 111, G01002, DOI: 10.1029/2004JG000004, 2006.

Zhao, M. S., and Running, S. W.: Drought-induced reduction in global terrestrial net primary production from 2000 through 2009, Science, 329, 940-943, DOI: 10.1126/science.1192666, 2010.

Publications

Journals (peer-reviewed)

Chen, T., van der Werf, G. R., Gobron, N., Moors, E. J., and Dolman, A. J.: Global cropland monthly Gross Primary Production in the year 2000, Biogeosciences Discuss., 11, 3465-3488, DOI:10.5194/bgd-11-3465-2014, 2014.

Chen, T., de Jeu, R. A. M., Liu, Y. Y., van der Werf, G. R., and Dolman, A. J.: Using satellite based soilmoisture to quantify thewater driven variability in NDVI: A case study over mainland Australia, Remote Sensing of Environment, 140, 330-338, DOI: 10.1016/j.rse.2013.08.022, 2014.

Chen, T., van der Werf, G. R., de Jeu, R. A. M., Wang, G., and Dolman, A. J.: A global analysis of the impact of drought on net primary productivity, Hydrol. Earth Syst. Sci., 17, 3885-3894, DOI: 10.5194/hess-17-3885-2013, 2013.

Chen, T., van der Werf, G. R., Dolman, A. J., and Groenendijk, M.: Evaluation of cropland maximum light use efficiency using eddy flux measurements in North America and Europe, Geophys Res Lett, 38, L14707, DOI: 10.1029/2011gl047533, 2011.

Dolman, A. J., Shvidenko, A., Schepaschenko, D., Ciais, P., Tchebakova, N., **Chen, T**., van der Molen, M. K., Belelli Marchesini, L., Maximov, T. C., Maksyutov, S., and Schulze, E. D.: An estimate of the terrestrial carbon budget of Russia using inventory-based, eddy covariance and inversion methods, Biogeosciences, 9, 5323-5340, DOI: 10.5194/bg-9-5323-2012, 2012.

Dong, Q., Chen, X., and **Chen, T**.: Characteristics and Changes of Extreme Precipitation in the Yellow–Huaihe and Yangtze–Huaihe Rivers Basins, China, J Climate, 24, 3781-3795, DOI: 10.1175/2010JCLI3653.1, 2011.

van der Molen, M. K., Dolman, A. J., Ciais, P., Eglin, T., Gobron, N., Law, B. E., Meir, P., Peters, W., Phillips, O. L., Reichstein, M., **Chen, T**., Dekker, S. C., Doubková, M., Friedl, M. A., Jung, M., van den Hurk, B. J. J. M., de Jeu, R. A. M., Kruijt, B., Ohta, T., Rebel, K. T., Plummer, S., Seneviratne, S. I., Sitch, S., Teuling, A. J., van der Werf, G. R., and Wang, G.: Drought and ecosystem carbon cycling, Agr Forest Meteorol, 151, 765-773, DOI: 10.1016/j.agrformet.2011.01.018, 2011.